IDENTIFICATION OF SELECTED EXPERIMENTAL DATA ON THERMAL STRESSES

B. E. Gatewood and James S. O'Connor

Changed to U2 3/12/1973

FOREWORD

This report was prepared by the Department of Aeronautical and Astronautical Engineering, The Ohio State University, Columbus, Ohio, under Contract AF 33(615)-5074. Dr. B. E. Gatewood was Technical Director of the study. The contract was initiated under Project 1467, "Structural Analysis Method", Task 146702, "Thermoelastic Stress Analysis Methods". The work was administered under the direction of the Structures Division, Air Force Flight Dynamics Laboratory, Research and Technology Division, Mr. Gene E. Maddux, Project Engineer (FDTR).

This report covers work conducted during the period 15 May 1966 to 15 September 1967.

This technical report has been reviewed and is approved.

FRANCIS J. JANIK, JR.
Chief, Theoretical Mechanics Branch
Structures Division

ABSTRACT

This report identifies experimental data on thermal stresses contained in selected reports in the literature. For each selected report, a summary of selected tests, geometry of test specimens, restraints, material properties, temperature distributions, experimental strain and deflection data, and comparisons to theory are given or are identified as to location by figure number or table number in the original published report. Also, the bibliographical listing and evaluation of test data on thermal stress testing given in Technical Report AFFDL-TR-66-67, "Development of Experimental Testing Programs to Verify Thermal Stress Analysis," is brought up to date in an appendix to the present report.

TABLE OF CONTENTS

TABLE OF CONTENTS (Continued)

TABLE OF CONTENTS (Continued)

LIST OF ILLUSTRATIONS

LIST OF ILLUSTRATIONS (Continued)

LIST OF TABLES

INTRODUCTION

A bibliography on experimental data on thermal stresses is given in Ref. 1. Each report listed in Ref. 1 was assigned a number and was evaluated as to structural type and usefulness of the data by means of tables in Ref. 1. The purpose of the present report is to select the best data from the list in Ref. 1 and to identify the data in such a way that it can be readily compared to theoretical calculated results.

Each selected report is identified by its number and title in Ref. 1, together with the identification of tables in Ref. 1 that describe and evaluate it. For each selected report, the following items are given:

1. Identification in Ref. 1
2. Brief summary of tests selected from report
3. Geometry of test specimens
4. Restraints of test specimens
5. Material properties
6. Temperature distributions
7. Experimental data
8. Theoretical comparisons given in report
9. Comments

The data is identified in the selected tests by means of the figure, table, and page numbers in the original report. For shorter tests, copies of the data from the original report is given.

The selected reports are numbered consecutively as S1, S2, etc. A brief title, not necessarily the original title, is assigned each selected report or report group.

REFERENCE

1. Gatewood, B. E., A. R. Glaser, and B. H. Ulrich, Jr., "Development of Experimental Testing Programs to Verify Thermal Stress Analysis," AFFDL-TR-66-67, The Ohio State University Research Foundation, Columbus, Ohio 43212, June, 1966.

S1. THERMAL STRESSES IN A FLAT PLATE

1. Reference 21-32, Table 2-7, Table 2-16 of Ref. 1. Heldenfels, R. R. and W. M. Roberts "Experimental and Theoretical Determination of Thermal Stresses in a Flate Plate," NACA-TN 2769, 1952.

2. Summary of Tests

Test of 24-inch by 36-inch rectangular plate with tent-like temperature distribution in short direction--two dimensional stresses.

3. Geometry

See Fig. 4, page 3, for geometry.

4. Unrestrained

5. Material Properties

Material is 75S-T6. Ratio of E_{temp}/E_{room} is plotted against temperature in Fig. 2, page 4. Suggest using room values of $E = 10.2(10^6)$ psi, $\alpha = 13(10^{-6})$, $\nu = 0.3$.

6. Temperature Distributions

Temperature distribution is shown in Fig. 6, page 5.

7. Experimental Data

Experimental data for σ_x transverse and longitudinal are in Figs. 7a and 7b, pages 6,7. σ_y transverse and longitudinal are in Figs. 9a and 9b, pages 10, 11. τ_{xy} transverse and longitudinal are in Figs. 8a and 8b, pages 8, 9.

8. Theoretical Results

Theoretical results are compared to test results in Figs. 7a, 7b, 8a, 8b, 9a, and 9b.

9. Comments

This report contains experimental and theoretical stress distributions for an unrestrained plate subjected to a tent-like temperature distribution. Three tests were made. After the strains were measured and the stresses calculated, the stresses were adjusted to a temperature difference of 150°F between the center line and longitudinal edges of the plate assuming that the stresses were a linear function of the temperature difference. This adjustment was made to provide a common basis for comparing the three tests which were made at different temperature differences.

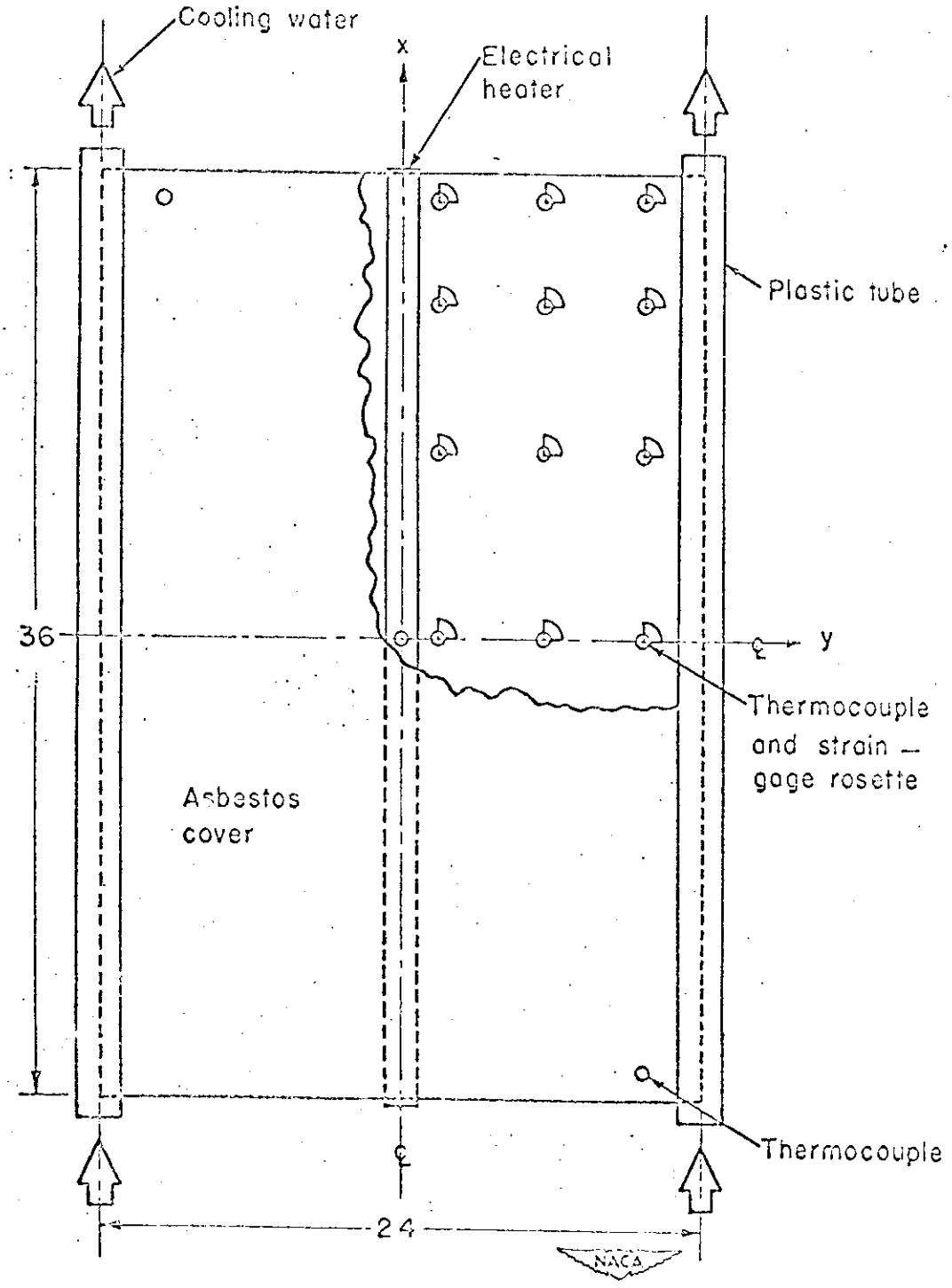

Figure 4. - Sketch of thermal-stress test specimen.

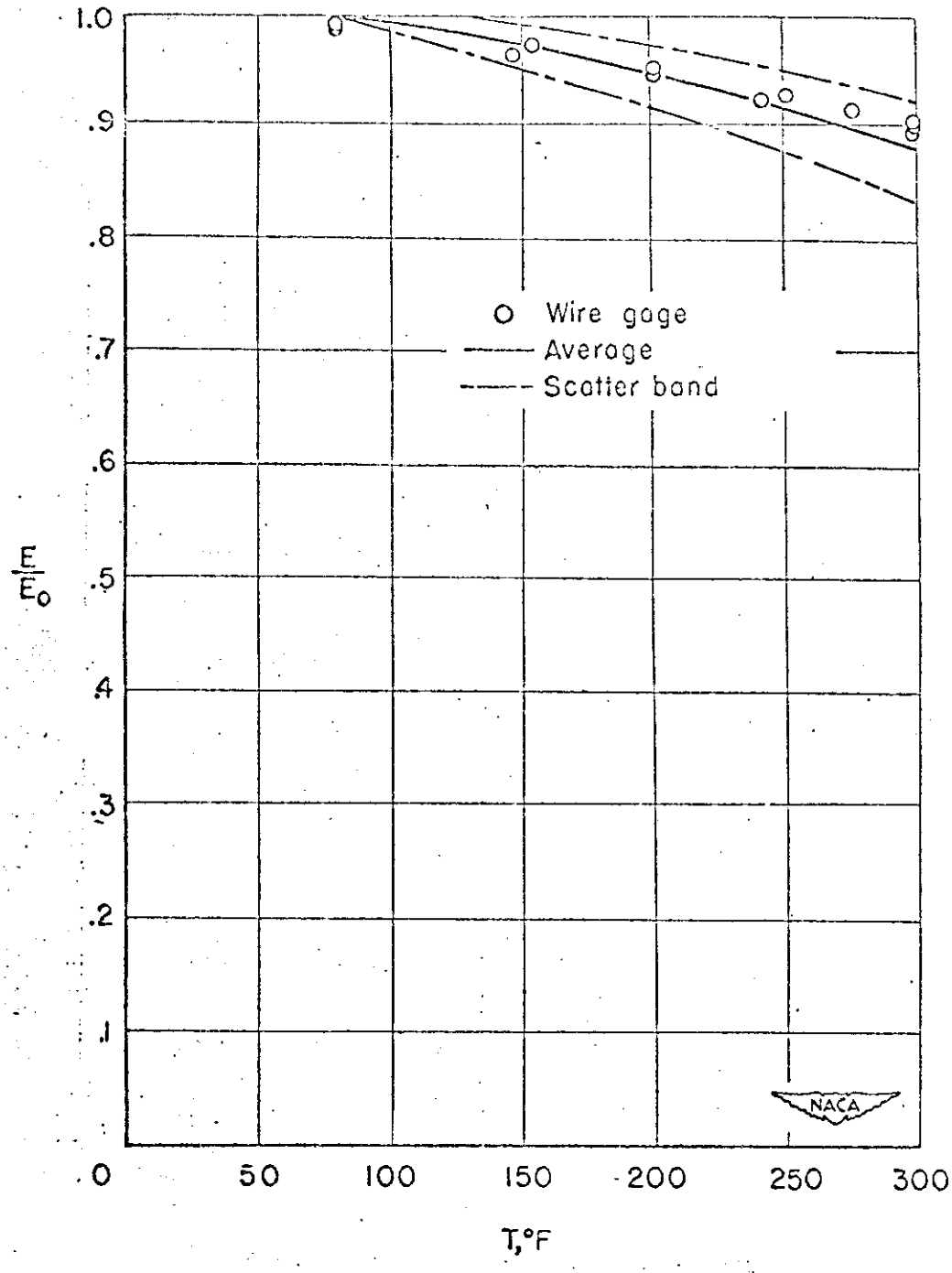

Figure 2.- Ratio of modulus of elasticity at elevated temperature to that at room temperature for 75S-T6 aluminum alloy.

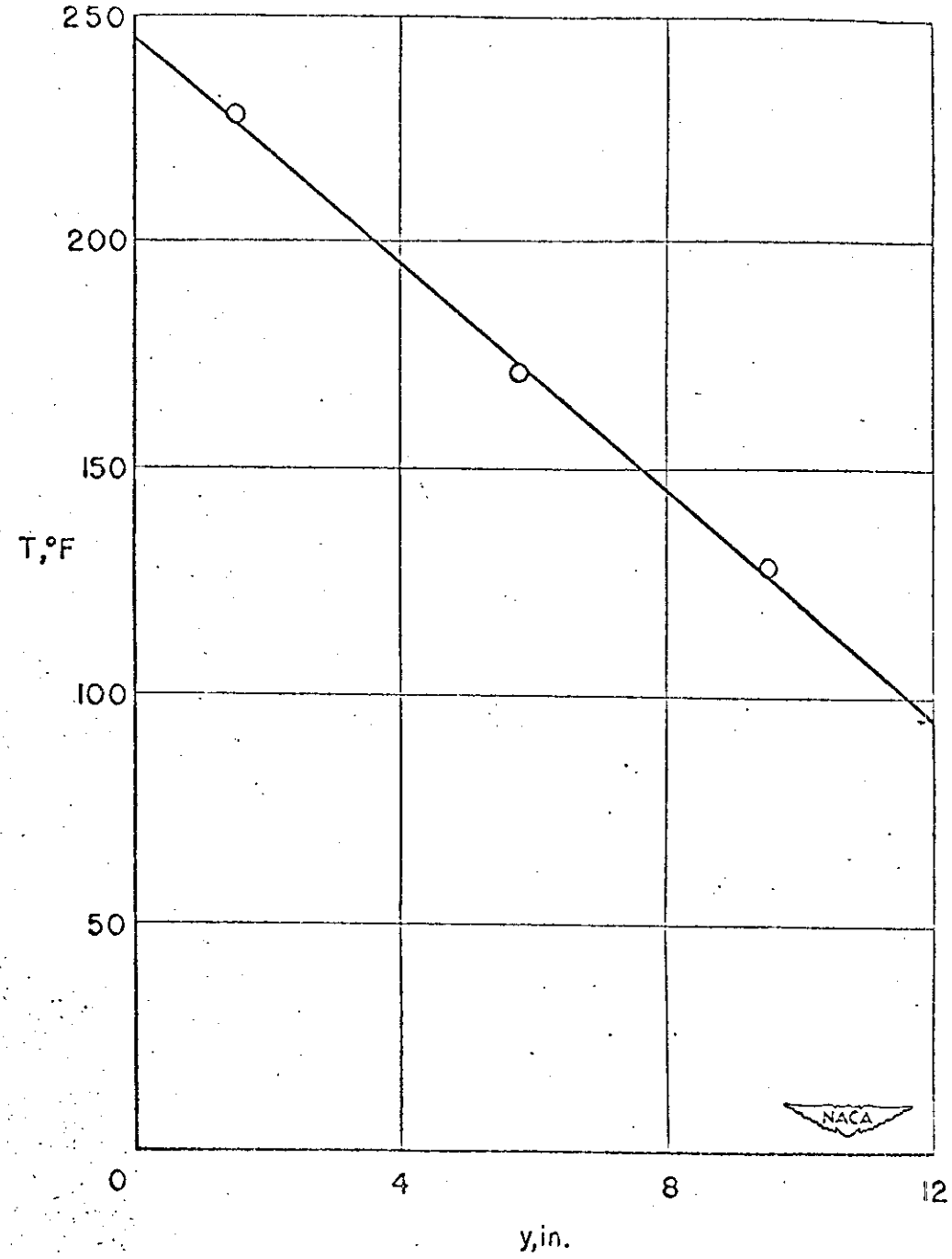

Figure 6.- Transverse temperature distribution.

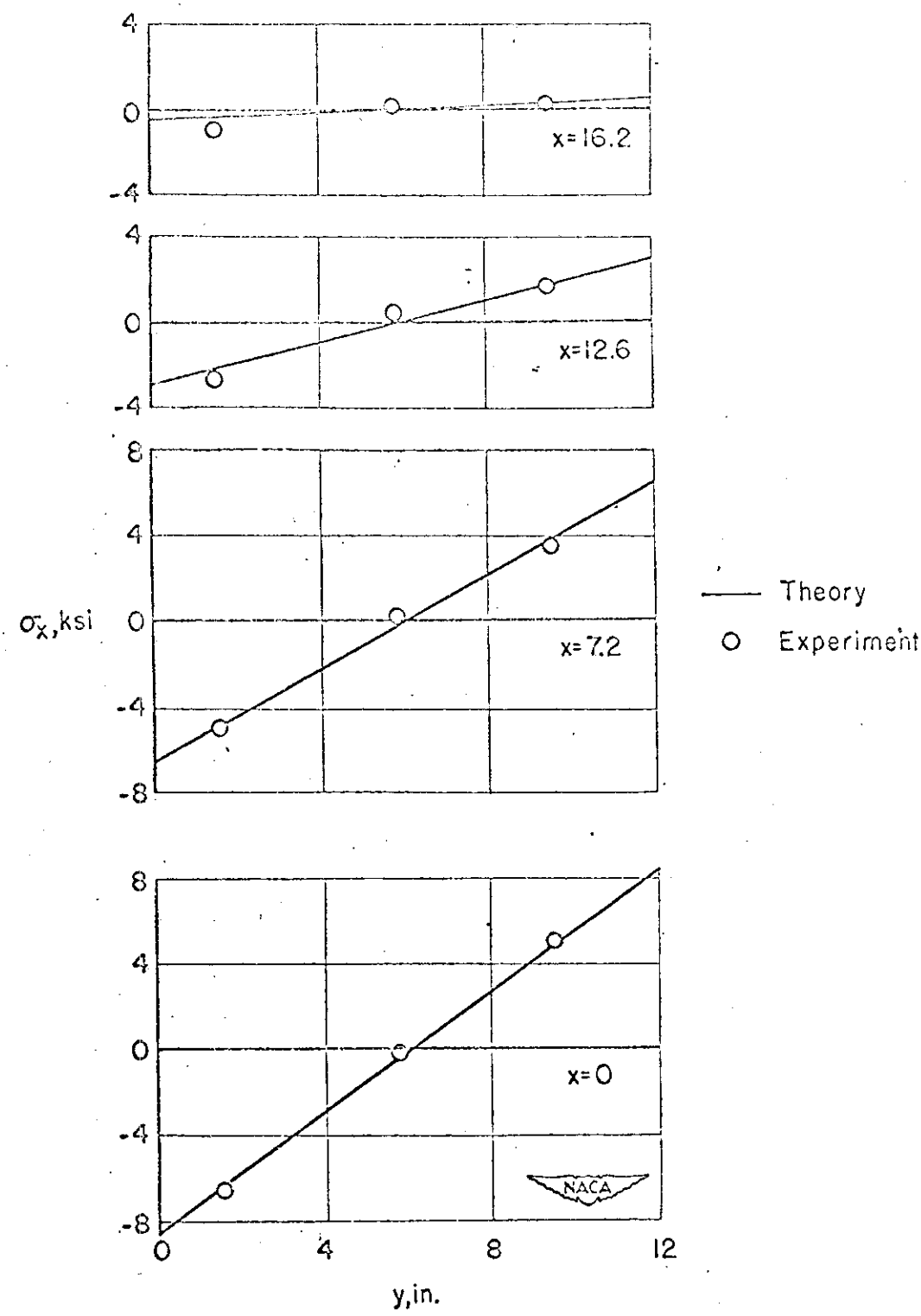

(a) Transverse distribution.

Figure 7. - Longitudinal direct stresses induced in test specimen by the temperature distribution of Fig. 6.

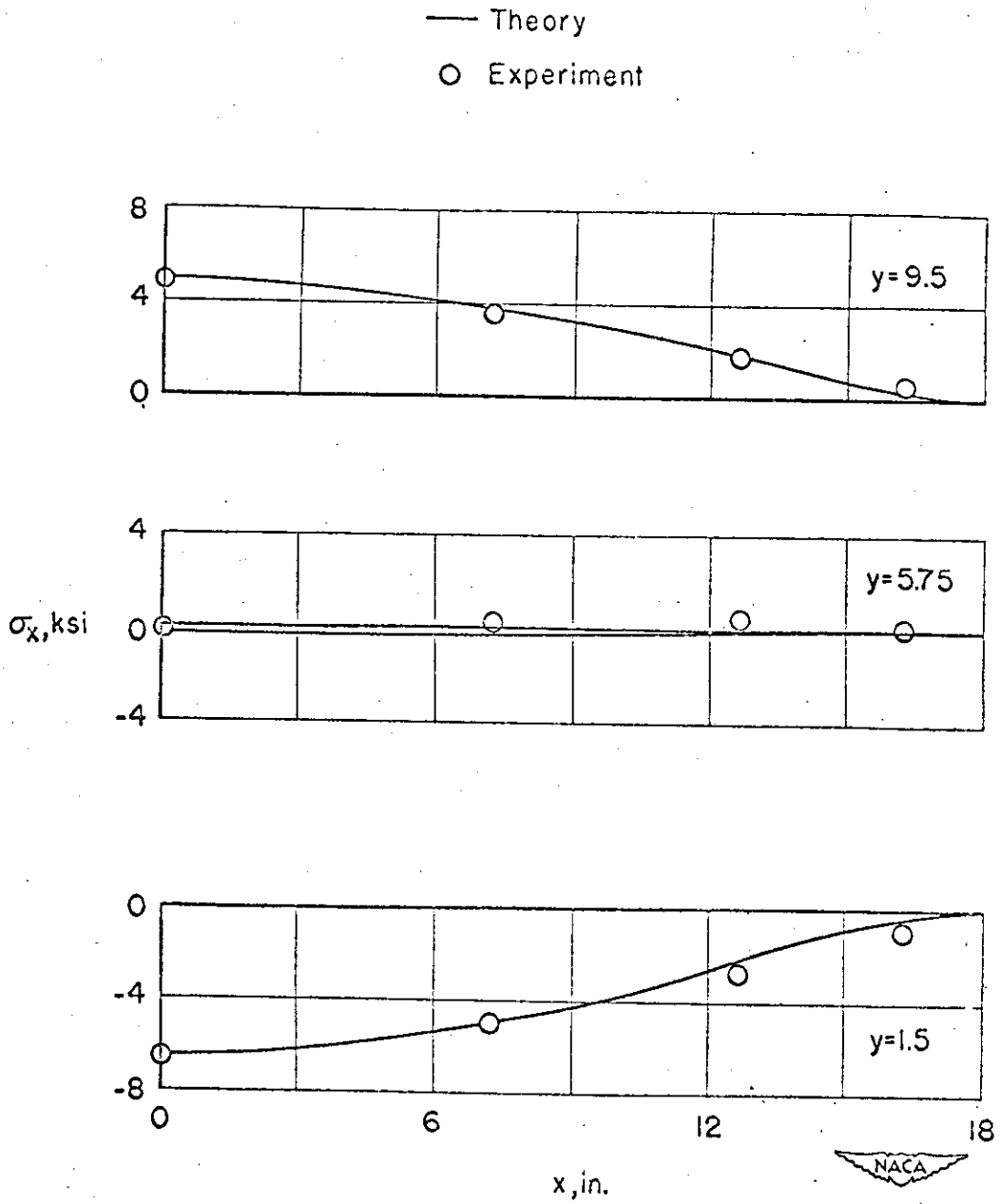

(b) Longitudinal distribution

Figure 7.- Concluded

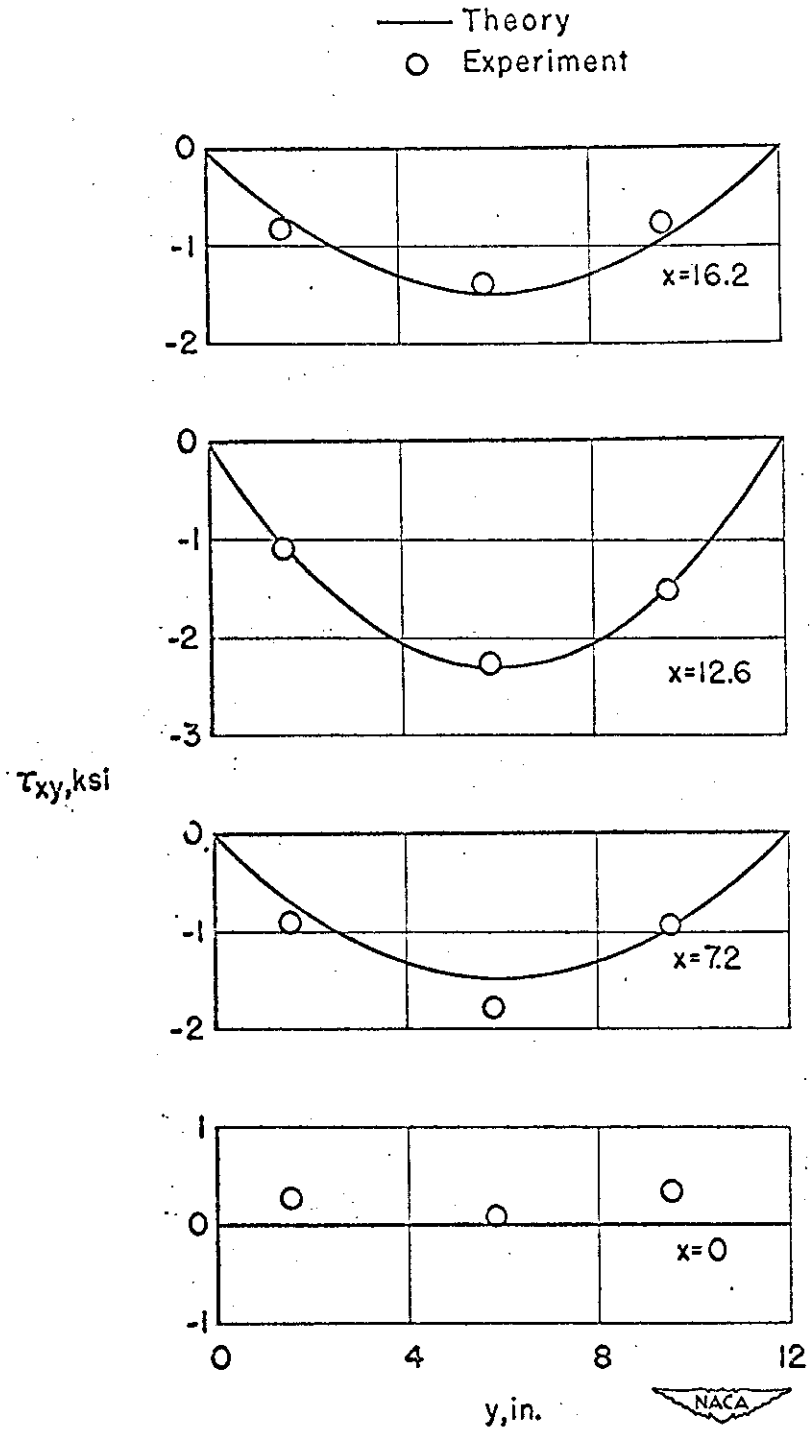

(a) Transverse distribution

Figure 8. - Shear stresses induced in test specimen by the temperature distribution of Fig. 6.

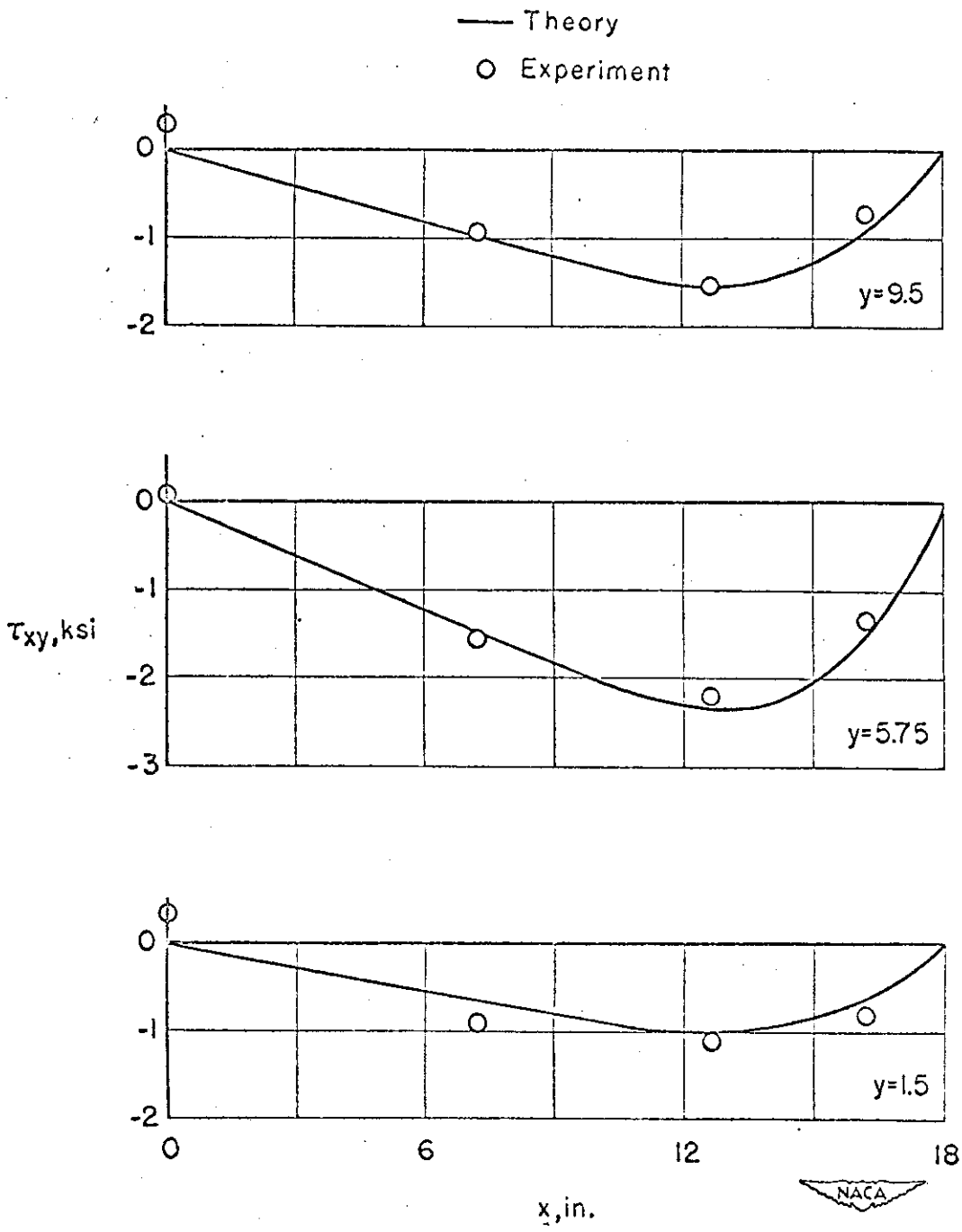

(b) Longitudinal distribution

Figure 8. - Concluded.

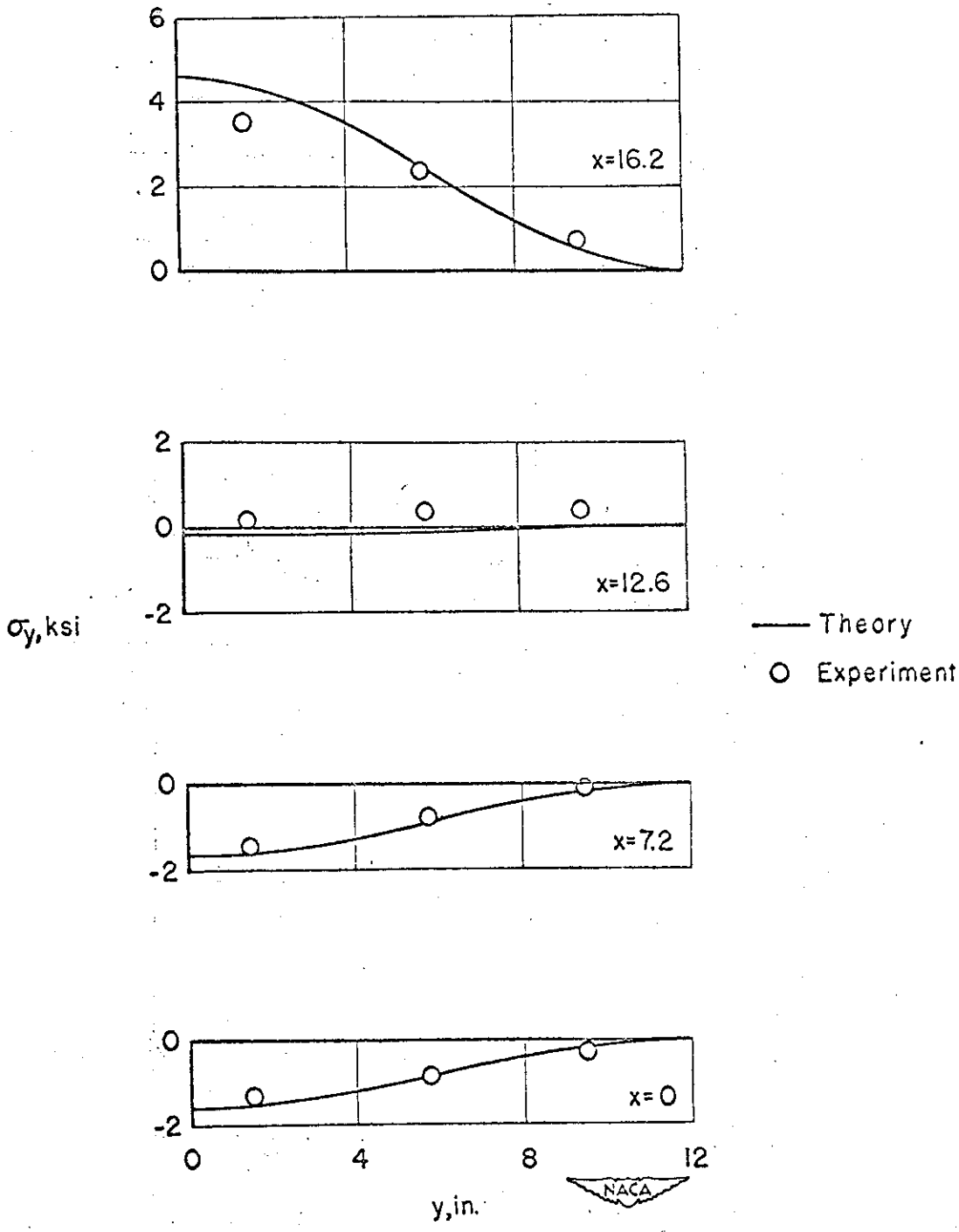

(a) Transverse distribution.

Figure 9. - Transverse direct stresses induced in test specimen by the temperature distribution of Fig. 6.

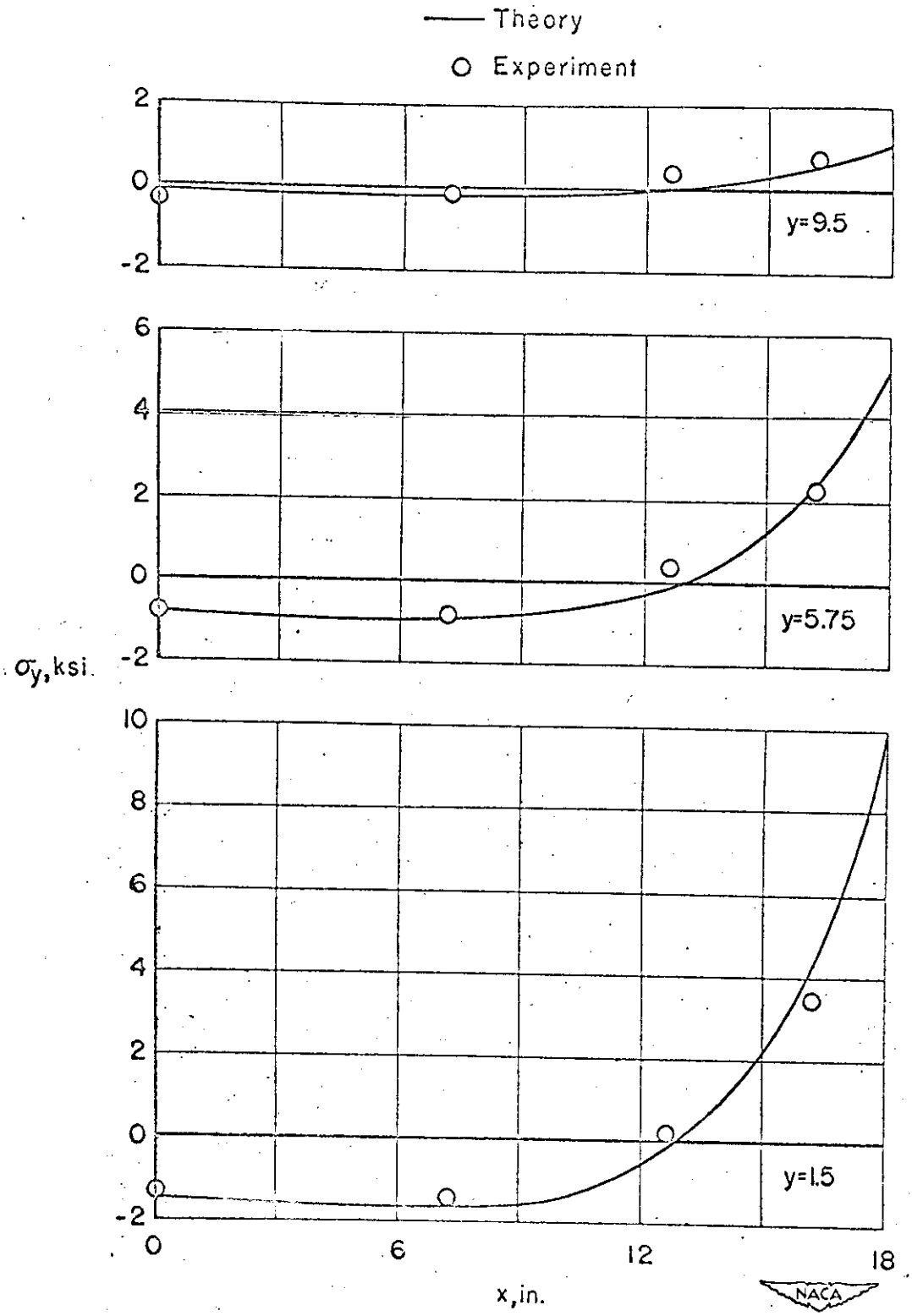

(b) Longitudinal distribution

Figure 9.- Concluded

The experimental points shown in Figs. 7 to 9 are the average of the three tests; separate points are not shown for each test since in most cases they are too close together to be easily distinguishable. The actual temperature distribution, given by the test points in Fig. 6 varied slightly from a straight line, but they are within a few degrees. No measureable temperature variation was recorded through the thickness of the plate. Initial imperfections in the plate which would cause out-of-plane deformations were compensated for by mounting the plate in a jig designed to provide the required restraint without extraneous stresses. Readings of strain gages on opposite sides of the plate were averaged before stress calculations were made.

S2. ONE-DIMENSIONAL COMBINED THERMAL AND APPLIED STRESSES IN LONG FLAT PLATES

1. Reference 31-5, Table 2-9, Table 2-16, of Ref. 1 "Analytical and Experimental Investigation of Stress Distributions in Long Flat Plates Subjected to Longitudinal Loads and Transverse Temperature Gradients," WADC Technical Rep't. 55-350, September, 1956.

2. Summary of Tests Selected

Test No.	Description
2551	symmetrical temperature distribution, no applied load (elastic)
2554	unsymmetrical temperature distribution, no applied load (elastic)
2679 seq 400,	linear temperature distribution with applied tension load (elastic)
2684 seq 500,	linear temperature distribution with applied tension load (inelastic)
469-497	room-temperature buckling, with applied compression (pre and post buckling)
698-727	300°F uniform temperature with applied compression (pre-and post-buckling)

The large number of tables and figures for data have not been included herein. It is expected that a copy of the original report will be used to obtain the identified data.

3. Geometry

The geometry for all tests is shown in Fig. 1, page 14.

4. Unrestrained

5. Material Properties

See tables and figures in original report as identified in Table S2. The material test coupon is shown in Fig. 2, original report.

6. Temperature Distribution

2551 - Fig. D-4; Tables 1 and 9

2554 - Fig. D-4; Tables 2 and 9

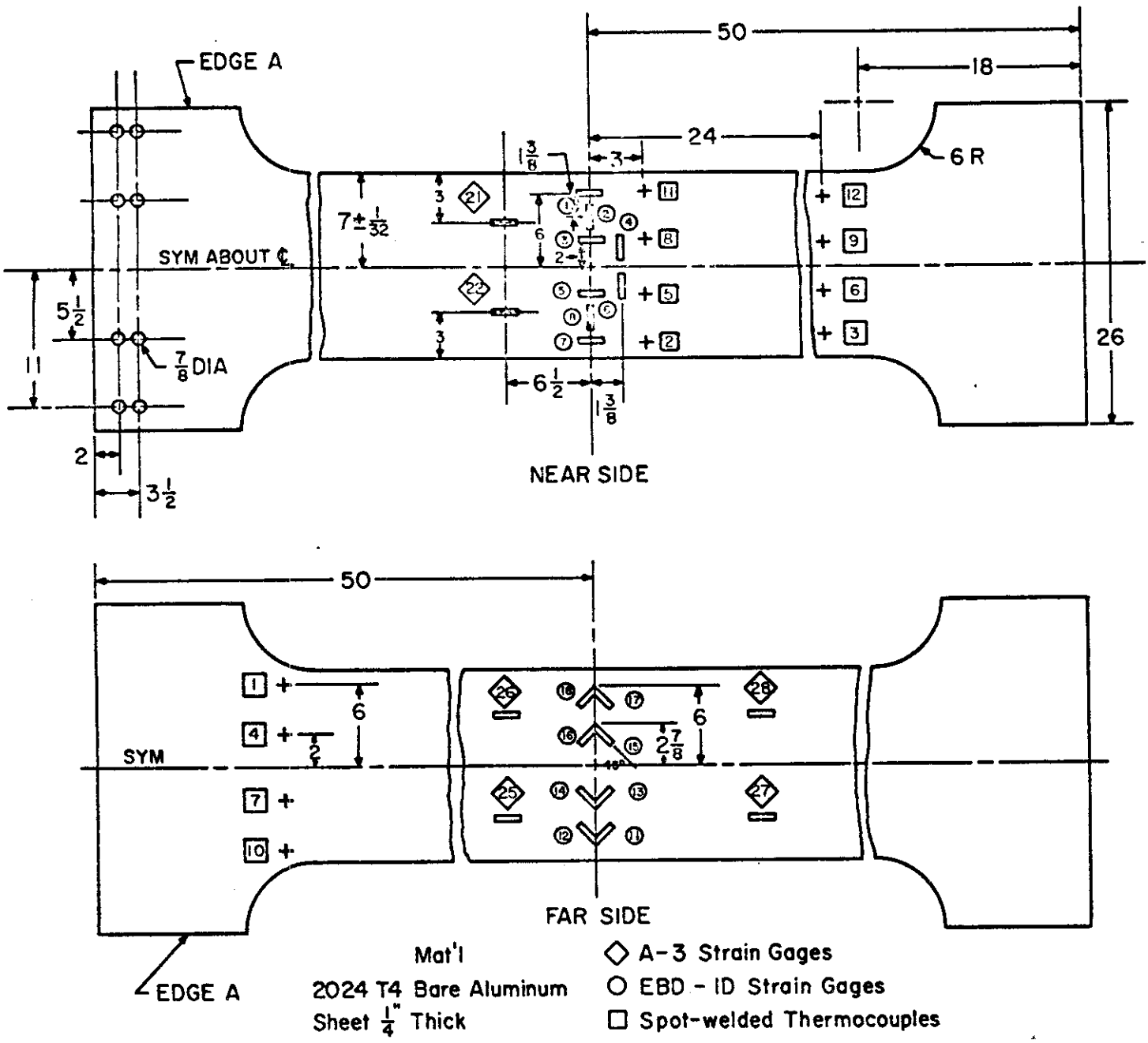

Figure 1. - Test specimen for S2.

Table S2 - Material Properties

	E_t		E_c		Es/E		α		ν
Test No.	Table No.	Fig. No.	Table No.	Fig. No.	Table No.	Fig. No.	Table No.	Fig. No.	Fig. No.
2551	1 & 9	D-27	--	--	--	--	1	17	--
2554	2 & 9	D-27	--	--	--	--	2	17	--
2679 seq 400	4 & 11	D-27	--	--	--	--	4	17	--
2684 seq 500	11	--	--	--	11	19	--	17	--
469-497	--	--	16	--	--	--	--	17	D-29
698-727	--	--	16	D-28	--	--	--	17	D-29

2679 seq 400 - Fig. D-8; Tables 4 and 11

2684 seq 500 Fig. D-8; Tables 6 and 11

469-497 - uniform, room temperature

698-727 - uniform, 300°F

Applied Loads

2551 - none

2554 - none

2679 - 107, 833 lb

2684 - 183,793 lb

469-497 - variable load

698-727 - variable load

7. Test Results

2551 - Fig. D-1 and Table 9, strain distribution
Table 9, Fig. 9, stress distribution

2554 - Fig. D-1 and Table 9, strain distribution
Table 9, Fig. 10, stress distribution

2679 seq 400 - Fig. D-11, load-induced longitudinal strain distribution

Table 11, strain distribution
Fig. D-9, vertical deflection at transverse center line
Fig. 12, Table 11, stress distribution

2684 seq 500 - Fig. D-11, load-induced longitudinal strain distribution

Table 11, strain distribution
Fig. D-9, vertical deflection at transverse center line
Fig. 13, Table 11, stress distribution

469-497 - Fig. D-14, 21, Table 13, lateral deflection
Fig. D-15, 24,25, Table 13, longitudinal strain
Fig. 27 - stress distribution below buckling

698-727 - Fig. D-20, Fig. 23, Table 15, lateral deflection
Fig. 25, 26, D-21, Table 18, longitudinal strain
Fig. 23, stress distribution below buckling

8. Theoretical Comparisons

2551 - Table 1, 7, Fig. 9, stress distribution
Table 1, strain distribution

2554 - Table 2;7, Fig. 10, stress distribution
Table 2, strain distribution

2679 seq 400 - Table 4, 8b, Fig. 12, stress distribution
Table 4, strain distribution

2684 seq 500 - Table 6, 8b, Fig. 14, stress distribution
Table 6, Fig. 14, strain distribution

469-497 - Table 13, 16, Fig. 21, lateral deflection
Table 16, post-buckling stress
Fig. 27, pre-buckling stress distribution
Table 16, Fig. 24, 25, longitudinal strain

698-727 - Table 15, 16, Fig. 23, lateral deflection
Table 16, post-buckling stress
Fig. 28, pre-buckling stress distribution
Table 16, 26, longitudinal strain

9. Comments

About 21 tests are given in the report. Six have been selected and identified above. The six selected appear to provide useful data for correlation with theoretical calculations.

S3. ONE-DIMENSIONAL COMBINED THERMAL AND AXIAL LOADING AND CREEP IN LONG FLAT PLATES

1. Reference 31-7, Table 2-9 and Table 2-16 of Ref. 1, Huang, P. C. and Van Der Maas, C. J., "Combined Effects of Axial Load, Thermal Stress, and Creep in Flat Plates," WADC Technical Report 57-442, March, 1958 and "Large-Deflection Analysis of Buckled Plates under Thermal Effects," WADC Technical Report 57-442 Supplement 1, (Martin Company RR-8), January, 1959.

2. Summary of Tests

A. Tension Test - linear temperature gradient. The temperature varies from approximately 100°F at the edges to 451°F at the center. The specimen is tested in tension at a constant strain rate of 0.04 in./in.-min. up to a total strain of 0.017 in./in.

B. Compression Tests - The transverse temperature gradients are approximately linear from the edges to the longitudinal center line temperature of 400°F. All specimens were tested at a constant strain rate of 0.01 in./in.-min. up to post-buckling failure. Supported by knife edges 1/2 in. from edges. End pins connected to loading jacks.

Test 1. Edge temperature of 203°F. Data readings were taken for loads varying from 23,963 lb to 103,759 lb.

Test 2. Edge temperature of 139°F. Loads vary from 18,203 lb to 93,004 lb.

Test 3. Edge temperature of 88°F. Loads vary from 14,288 lb to 81,371 lb.

C. Tension/Compression - The transverse temperature gradient is approximately linear from 139°F at the edges to 406°F at the center. The speciment is loaded in tension at a constant strain rate of 0.021 in./in.-min. up to a total strain of 0.09 in./in. (inelastic) subsequent to unloading, it is loaded in compression at a constant strain rate of 0.007 in./in.-min. beyond the critical compression load.

D. Tension Creep - The transverse temperature gradient is approximately linear with a longitudinal center line temperature of 465°F.

Test 1. Edge temperature 306°F, sustained tension load of 117,000 lb for 49 hours 13 min.

Test 2. Edge temperature 322°F, sustained tension load of 134,245 lb for 40 hours and 22 min. (test terminated by creep rupture).

3. Geometry

The geometry is the same as that as in Selected Experimental Data on Thermal Stresses No. S2 above.

4. Unrestrained

5. Material Properties

A. Tension Test

E_t vs T - Fig. 31, Table 19

$\epsilon_{0.2\%}/\epsilon_{0.2\%RT}$ vs T - Fig. 32, Table 22

E_{sec}/E vs $\epsilon/\epsilon_{0.2\%}$ - Fig. 33a

α vs T - Fig. 37 (Taken from literature, not determined experimentally)

B. Compression Test

E_c/E_{RT} vs T - Fig. 34, Table 20, or Fig. 2 of Supplement 1

Poisson's Ratio vs T - Fig. 35, Table 21 or Fig. 3 of Supplement 1

C. Tension/Compression Test

E/E_{RT} vs T - Fig. 31, Table 19

$\epsilon_{0.2\%}/\epsilon_{0.2\%RT}$ vs T - Fig. 32, Table 22

E_{sec}/E vs $\epsilon/\epsilon_{0.2\%}$ - Fig. 33b

E_c/E_{RT} vs T - Fig. 34, Table 20

Poisson's Ratio vs T - Fig. 35, Table 21

D. Tension Creep Test

Test 1. E/E_{RT} vs T - Fig. 31, Table 19

E_{sec}/E vs $\epsilon/\epsilon_{0.2\%}$ - Fig. 33c

Test 2. E/E_{RT} vs T - Fig. 31, Table 19

E_{sec}/E vs $\epsilon/\epsilon_{0.2\%}$ - Fig. 33d

6. Temperature Distributions

A. Tension Test - Fig. 5

B. Compression Test

Tests 1, 2, 3 - Fig. 15 or Fig. 1 of Supplement 1

C. Tension/Compression - Fig. 19

D. Tension Creep Test

Tests 1 and 2 - Fig. 25

7, 8. Experimental Data and Theoretical Comparisons

A. Tension Test

1. Load vs strain associated with stress above longitudinal center line - Fig. 6

2. Load vs strain associated with stress below longitudinal center line - Fig. 7

3. Load vs total strain - Fig. 8

4. Comparison of elastic and plastic stress and strain distributions - Fig. 12

5. Distribution of strain associated with stress - Fig. 9

6. Distribution of total strain - Fig. 10

7. Stress distribution - Fig. 11

8. Stress and strain distributions - Table 8

B. Compression Tests

1. Longitudinal distribution of lateral deflections - Fig. 16 or Table 1 of Supplement 1

2. Transverse distribution of lateral deflections - Fig. 17

3. Lateral deflections (both directions)
Test 1. Table 15
Test 2. Table 16
Test 3. Table 17

4. Summary of critical compression stresses - Table 1

5. Distributions of strain associated with stress, total strain, and stress across the specimen - Fig. 18

6. Load vs strain associated with stress for individual gages
   Test 1. Fig. 59
   Test 2. Fig. 60
   Test 3. Fig. 61

7. Load vs strain associated with stresses below longitudinal center line
   Test 1. Fig. 72
   Test 2. Fig. 73
   Test 3. Fig. 74

8. Load vs total strain - Fig. 75

9. Stress and strain distributions
   Test 1. Table 9 or Table 2 of Supplement 1
   Test 2. Table 10 or Table 3 of Supplement 1
   Test 3. Table 11 or Table 4 of Supplement 1

10. Transverse stress distributions
    Test 1. Fig. 4 of Supplement 1
    Test 2. Fig. 5 of Supplement 1
    Test 3. Fig. 6 of Supplement 1

C. Tension/Compression Test

1. Longitudinal distributions of lateral deflections - Fig. 20

2. Lateral deflections (both directions) - Table 18

3. Transverse distribution of lateral deflections - Fig. 21

4. Distribution of strain associated with stress - Fig. 22

5. Distribution of total strain - Fig. 23

6. Stress distribution - Fig. 24

7. Load vs strain associated with stress for individual gages - Fig. 62

8. Load vs strain associated with stress below longitudinal center line - Fig. 77

9. Load vs total strain - Fig. 78

10. Stress and strain distributions - Table 12

D. Tension Creep Test

1. Creep curves - Fig. 26

2. Creep readings from strain gages, Test 1 - Fig. 27

3. Distribution of strain associated with stress, Test 1, Fig. 23

4. Distribution of total strain, Test 1 - Fig. 29

5. Stress distribution, Test 1 - Fig. 30

6. Strains, Test 1 - Table 13

7. Strains, Test 2 - Table 14

9. Comments

All tests in the reports have been selected.

S4. COMBINED THERMAL AND APPLIED STRESSES
IN PLATES WITH CUTOUT

1. Reference 21-38, Table 2-7 and Table 2-16 of Ref. 1, Huang, P. C. and Van Der Maas, C. J. "Theoretical and Experimental Studies of the Stresses and Strains around Cutouts in Loaded, Unevenly Heated Plates," WADC Technical Report 59-2, March, 1959.

2. Summary of Tests

A. Test No. 6-068-1

This test is conducted at room temperature. The specimen is loaded at a constant strain rate of 0.0175 in./in.-min. up to a maximum strain of 0.0205 in./in. at the net section. (25,750 lb tension)

B. Test No. 6-400-1

The specimen is heated to 400°F at the longitudinal center line and cooled to 103°F at the longitudinal edges, and loaded with a tension load of 60,000 lb at a strain rate of 0.0191 in./in.-min. (maximum strain is 0.0152 in./in. at net section). Also conducted for zero load.

C. Test No. 6-450-2

The specimen is heated to 450°F at the longitudinal center line and cooled to 206°F at the longitudinal edges. It is loaded to failure at approximately a constant strain rate of 0.012 in./in.-min. at the net section. Also conducted for zero load.

3. Geometry

The geometry is shown in Fig. 20 and the strain gage locations in Fig. 21.

4. Unrestrained

5. Material Properties

Variation of Tension Modulus of Elasticity with Temperature Fig. 36, Table 8 (Obtained from coupon test) Variation of Poisson's Ratio (Tension) with Temperature Fig. 37, Table 9 (Obtained from coupon test) Variation of Thermal Coefficient of Expansion with Temperature Fig. 33 (Obtained from literature)

6. Temperature Distribution

Test No. 6-068-1 - room temperature

Test No. 6-400-1 - Fig. 7, Table 4, Fig. 63a, 63b

Test No. 6-450-2 - Fig. 15, Table 4, Fig. 73a, 73b

7, 8. Experimental and Theoretical Results

Test No. 6-068-1

1. Variation of longitudinal strain - Fig. 4
2. Variation of transverse strain - Fig. 5
3. Strain vs load for various times and strain gages, Table 5
4. Load vs time - Fig. 54
5. Load vs longitudinal strain $y = 5.72$ in. - Fig. 55a
6. Load vs longitudinal strain $y = 5.72$ in. - Fig. 55b
7. Load vs longitudinal strain $y = 4.47$ in. - Fig. 56
8. Load vs longitudinal strain $y = 3.22$ in. - Fig. 57
9. Load vs longitudinal strain $7 = 1.00$ in. - Fig. 58
10. Load vs transverse strain $x = 7$ in. - Fig. 59
11. Load vs transverse strain $x = 5$ in. - Fig. 60
12. Load vs transverse strain $x = 3$ in. - Fig. 61
13. Load vs transverse strain $x = 1$ in. - Fig. 62

Test No. 6-400-1

1. Variation of longitudinal strain (zero load) - Fig. 11
2. Variation of longitudinal strain (60,000-lb load) - Fig. 12
3. Variation of transverse strain (zero load) - Fig. 13
4. Variation of transverse strain (60,000-lb load) - Fig. 14
5. Experimental data - Table 6
6. Load vs longitudinal strain $y = 5.72$ in. - Fig. 65a
7. Load vs longitudinal strain $y = 5.72$ in. - Fig. 65b
8. Load vs longitudinal strain $y = 4.47$ in. - Fig. 66
9. Load vs longitudinal strain $y = 3.22$ in. - Fig. 67

10. Load vs longitudinal strain y = 1.00 in. - Fig. 68a
11. Load vs longitudinal strain y = 1.00 in. - Fig. 68b
12. Load vs transverse strain x = 7 in. - Fig. 69
13. Load vs transverse strain x = 5 in. - Fig. 70
14. Load vs transverse strain x = 3 in. - Fig. 71
15. Load vs transverse strain x = 1 in. - Fig. 72

Test No. 6-450-2

1. Variation of longitudinal strain (zero load) - Fig. 16
2. Variation of longitudinal strain (60,000-lb load) - Fig. 17
3. Variation of transverse strain (zero load) - Fig. 18
4. Variation of transverse strain (60,000-lb load) - Fig. 19
5. Experimental data - Table 7
6. Load vs time - Fig. 74
7. Load vs longitudinal strain y = 5.72 in. - Fig. 75a
8. Load vs longitudinal strain y = 5.72 in. - Fig. 75b
9. Load vs longitudinal strain y = 4.47 in. - Fig. 76
10. Load vs longitudinal strain y = 3.22 in. - Fig. 77a
11. Load vs longitudinal strain y = 3.22 in. - Fig. 77b
12. Load vs longitudinal strain y = 1.00 in. - Fig. 78a
13. Load vs longitudinal strain y = 1.00 in. - Fig. 78b
14. Load vs transverse strain x = 7 in. - Fig. 79
15. Load vs transverse strain x = 5 in. - Fig. 80
16. Load vs transverse strain x = 3 in. - Fig. 81
17. Load vs transverse strain x = 1 in. - Fig. 82

S5. COMBINED TWO-DIMENSIONAL TEMPERATURE DISTRIBUTION AND APPLIED LOADING OF A LONG FLAT PLATE IN THE ELASTIC AND INELASTIC REGIONS

1. "Elasto-Plastic Analysis of Structures under Load and Two-Dimensional Temperature Distribution," Edwards, R. J., P. C. Huang et al., ASD-TR 61-667, Vol. I, April, 1962; Vol. II, April, 1962; Reference 21-46, Tables VII and XVI of Reference 1, Vol. III, Reference 21-52, Tables VII and XVI of Reference 1.

2. Summary of Tests

Test 1 - Tent distribution--thermal only. Specimen 510
Test 2 - Tent distribution--thermal only. Specimen 520
Test 3 - Recessed distribution--thermal only. Specimen 510
Test 4 - Recessed distribution--thermal only. Specimen 520
Test 5 - Box-type distribution--thermal only. Specimen 510
Test 6 - Box-type distribution--thermal only. Specimen 520
Test 7 - Tent distribution--thermal + applied load. Specimen 510
Test 8 - Tent distribution--thermal + applied load. Specimen 520

Specimen 520 is subjected to higher temperature gradients than Specimen 510.

3. Geometry

The geometry is the same as that of the S2, S3, and S4 reports in the series. Location of strain gages and thermal couples for specimen 510 is shown in Fig. 1 of Vol. I. The instrumentation of specimen 520 is shown in Figs. 2 and 3 of Vol. I.

4. Unrestrained

5. Material Properties (all tests)

A. Variation of Poisson's Ratio with Temperature, Fig. 12, Vol. I.

B. Modulus of Elasticity vs Temperature, Fig. 13, Vol. I; Fig. 33, Vol. III.

C. Nondimensional Stress Strain Curve, Fig. 14, Vol. I; Fig. 34, Vol. III.

D. Spectral-Stress Strain Curves, Fig. 15, Vol. I; Fig. 35, Vol. III.

E. Thermal Coefficient of Expansion, Fig. 31, Vol. III.

6. Temperature Distributions

Nominal distributions for all tests shown in Fig. 4, Vol. I; and Fig. 4, Vol. III.

Test 1 - Fig. 8, Vol. I; Table 2, Vol. II.
Test 2 - Fig. 10, Vol. I; Table 4, Vol. II.
Test 3 - Fig. 8, Vol. I; Table 2, Vol. II.
Test 4 - Fig. 10, Vol. I; Table 4, Vol. II.
Test 5 - Fig. 8, Vol. I; Table 2, Vol. II.
Test 6 - Fig. 10, Vol. I; Table 4, Vol. II.
Test 7 - Fig. 8, Vol. I; Table 2, Vol. II.
Test 8 - Fig. 10, Vol. I; Table 4, Vol. II.

Applied Loads

Test 7 - Fig. 9, Vol. I; Figs. 1-25, Vol. II (Load vs Strain);
Fig. 26. Vol. II (Load vs Time).
Test 8 - Fig. 11, Vol. I; Figs. 27-32, Vol. II (Load vs Strain);
Fig. 33, Vol. II (Load vs Time).

7,8. Experimental and Theoretical Results
(e = experimental)
(t = theoretical)

Test 1
Thermal Strain - Fig. 16, Vol. I (e & t); Table 1, Vol. II (e). Thermal Stress - Fig. 17, Vol. I (e & t).

Test 2
Thermal Strain - Fig. 20, Vol. I (e & t); Table 3, Vol. II (e). Thermal Stress- Fig. 21, Vol, I (e & t).

Test 3
Thermal Strain - Fig. 18, Vol. I (e & t); Table 1, Vol. II (e). Thermal Stress - Fig. 19, Vol. I (e & t).

Test 4
Thermal Strain - Fig. 22, Vol. I (e & t); Table 3, Vol. II (e). Thermal Stress - Fig. 23, Vol I (e & t).

Test 5
Thermal Strain - Fig. 29, Vol. I (e & t); Table 1, Vol. II (e).

Test 6
Thermal Strain - Table 3, Vol. II (e).

Test 7
Stress and Strain distributions - Figs. 24-27, Vol. I (e & t); Table 1, Vol. II (e). Vertical and Diagonal Strain - Fig. 30, Vol. I (e & t).

Test 8

Stress and Strain distributions - Fig. 28, Vol. I (e & t); Table 2, Vol. II (e).

9. Comments

All tests in the report have been selected.

S6. TIME-DEPENDENT INELASTIC BENDING UNDER ARBITRARY TEMPERATURE DISTRIBUTION AND LOADS

1. (a)"Time-Dependent, Elasto-Plastic Bending Analysis for Structures under Arbitrary-Load-Temperature Environments," Van Der Maas, C. J., Huang, P. C., Volumes I & II, WADD-TR-60-541; Reference 21-39, Tables VII and XVI of Ref. 1.

(b)"Transient Structural Performance under an Intermittent Load-Temperature-Time Environment," Huang, P. C., USAF Symposium on Aerothermoelasticity, Dayton, Ohio, Oct. 30 - Nov. 1, 1961; ASD-TR-61-645, 1961; pp. 918-961; Reference 21-44, Tables VII and XVI of Reference 1.

2. (a) Specimen 100--Constant load, varying temperature distributions; followed by varying load, constant temperature distribution.

(b) Specimen 200--Varying loads and varying transverse temperature distributions.

3. Geometry

The geometry is the same as that of the S2, S3, S4, and S5 reports in this series. Location of strain gages and thermocouples is shown in Fig. 3 of Ref. 21-39.*

4. Unrestrained

5. Material Properties

Modulus of Elasticity vs Temp.--Fig. 9; Table 1.
Nondimensional Stress-Strain Curve--Fig. 10.
Spectral Stress-Strain Curve--Fig. 11.
Spectral Creep Curve (200°F)--Fig. 12a.
Spectral Creep Curve (300°F)--Fig. 12b.
Spectral Creep Curve (350°F)--Fig. 12c.
Spectral Creep Curve (400°F)--Fig. 12d.
Spectral Creep Curve (450°F)--Fig. 12e.
Thermal Expansion (Strain vs Temp.)--Fig. 13.
Thermal Coefficient of Expansion--Fig. 14.

6. Temperature and Load Spectra

Specimen 100--Fig. 2(planned)
Specimen 200--Figs. 6-7, Table 12, Figs. 49-52, Fig. 1 of 21-44.

*Unless noted the figures are from Ref. 21-39.

7, 8. Experimental and Theoretical Results
(e = experimental; t = theoretical)

Specimen 200
Total strain vs time--Fig. 15 (e & t); Figs. 54-57 (e).
Typical total strain disbributions--Fig. 16 (e & t).
Average total strain vs time--Figs. 58-59 (e).
Experimental strain data--Table 13.
Strain vs time--Fig. 2 of 21-44 (e & t).

9. Comments

The data from test 100 were not reduced because of doubtful reliability of strain-gage readings. For test 200, strain-gage instrumentation and techniques were refined to give "moderately satisfactory" results.

S7. JOINTS UNDER THERMAL AND APPLIED LOADS

1. "Thermo-mechanical analysis of structural joint study," Lobbett, J. W. and E. A. Robb, WADD TR 61-151, January, 1962. Reference 21-83, Tables XII and XVI of Ref. 1.

2. Three types of joints, brazed (type A), bolted (type B), and spotwelded (type C) were tested under various thermal and applied loads. A summary of the tests conducted is given in Table 20 of Ref. 21-83.*

3. Geometry

The geometry of type A, B, and C joints is given in Fig. 87.

4. Unrestrained

5. Material Properties

Joint material was PH 15-7 Mo stainless steel cond. TH 1050; bolts were NAS 144; all properties were obtained from MIL Handbook-5, March, 1959.

6. Temperature Distributions

Temperature gradients are given in Table 20.

7. Test Results

(a)Brazed Joints
Sheet stress vs joint deflection (test and analytic results) Fig. 97.

(b)Bolted Joint
(1)Ultimate test results--Table 23.
(2)Ultimate load vs temperature for 0.040", 0.071", and 0.100" ga. plates (uniform temperature)--Fig. 94.
(3)Ultimate deflection vs temp. for 0.040", 0.071", and 0.100" ga. plates (uniform temperature)--Fig. 95.
(4)Load deflection curves (comparison bolted vs spotwelded joints) 1000°F with 150° thickness gradient--Fig. 96.

(c)Spotwelded Joint
(1)Ultimate tensile strength vs temperature--Fig. 89.
(2)Comparison of joint strength (Ultimate tensile vs temperature) with and without temperature gradient--Fig. 90.
(3)Load deflection curves for six temperature tests cases --Fig. 91.
(4)Strain rate vs temperature for uniform and nonuniform temperature cases--Fig. 92.
(5)Joint recovery load vs deflection(permanent set)--Fig. 93.

*Unless noted, Figure Numbers are from Ref. 21-83.

(6)Load deflection curves (comparison of bolted vs spotwelded joints) 1000°F with 150° thickness gradient--Fig. 96.

S8. THERMAL DEFLECTION BEHAVIOR OF CORRUGATED MULTI-WEB WING STRUCTURE

1. "Thermal Effects on Static Aeroelastic Stability Control." Quinn, James F., D. Turrentine and R. Gallagher. WADD TR 60-229, Nov. 1959; Ref. 21-81 of Ref. 1 and Tables I, II, and XVI.

2. Summary of Tests

Deflection tests of a low aspect ratio, multi-web, square planform wing section under selected temperature gradients.

3. Geometry

Figs. 1 and 2; Thermocouple and strain gage locations, Figs. 16 and 17.

4. Unrestrained

All tests using model number 3 were unrestrained. The model was converted to a thermally restrained model (designated 3A) by replacing leading and trailing edge members with solid, conventional spars. The tests were repeated using model number 3A.

5. Material Properties

Modulus of Elasticity vs Temperature--Fig. 7.
Coefficient of Thermal Expansion vs Temperature--Fig. 8.

6. Temperature Distributions

Model 3--Fig. 19, Table XVII (Tests I thru V).
Model 3A--Fig. 20, Table XVIII (Tests I thru V).

7. Test Results

A. Model number 3, Deflection Influence Coefficients, Unheated Test, Table III.

B. Model number 3, Deflection Influence Coefficients, Test I, Table IV.

C. Model number 3, Deflection Influence Coefficients, Test II, Table V.

D. Model number 3, Deflection Influence Coefficients, Test III, Table VI.

E. Model number 3, Deflection Influence Coefficients, Test IV, Table VII.

F. Model number 3, Deflection Influence Coefficients, Test V, Table VIII.

G. Model number 3, Deflections under Uniform Load Table IX.

H. Model number 3A, Deflection Influence Coefficients, Unheated Test, Table X.

I. Model number 3A, Deflection Influence Conefficients, Test I, Table XI.

J. Model number 3A, Deflection Influence Coefficients, Test II, Table XII.

K. Model number 3A, Deflection Influence Coefficients, Test III, Table XIII.

L. Model number 3A, Deflection Influence Coefficients, Test IV, Table XIV.

M. Model number 3A, Deflection Influence Coefficients, Test V, Table XV.

N. Model number 3A, Deflection under Uniform Load, Table XVI.

O. Strain Gage Measurements, Model number 3, Table XIX.

P. Strain Gage Measurements, Model number 3A, Table XX.

Q. Warpage Measurements, Model number 3 and 3A, Table XXI.

Point supports were used along semispan line.

S9. UNRESTRAINED LONG PLATES WITH SPANWISE TEMPERATURE GRADIENTS

1. "Thermal Stresses Due to Large Spanwise Temperature Gradients in Long Thin Plates," Gatewood, B. E.; R. G. Dale, A. R. Glaser, ARL 63-4 Jan., 1963, Ref. 31-2 of Ref. 1, Tables VII and XVI.

2. Summary of Tests

Test of long rectangular plate with spanwise temperature gradients.

3. Geometry

Fig. 1, Thermocouple and Strain Gage Locations, Fig. 13.

4. Unrestrained

5. Material Properties

None (2024-T3 bare aluminum alloy)

6. Temperature Distributions

Test 1, Fig. 14.
Test 2, Fig. 15.
Test 3, Fig. 16.
Test 4, Fig. 17.
Shortwave Case, Figs. 18 and 27.

7, 8. Test Results

A. Strain distribution in x-direction @ x/L = 0.25, Fig. 21.

B. Strain distribution in x-direction @ x/L = 0.75, Fig. 22.

C. Strain distribution in y-direction @ x/L = 0.25, Fig. 23.

D. Strain distribution in y-direction @ x/L = 0.25, Test 4, Fig. 24.

E. Strain distribution in x-direction @ x/L = 0.75, Test 4, Fig. 25.

F. Strain distribution in x-direction @ x/L = 0.25, Test 4, Fig. 26.

G. Tabular Presentation of Measured Data for Short Wave Case Fig. 34.

S10. UNRESTRAINED LONG PLATES WITH TWO DIMENSIONAL TEMPERATURE DISTRIBUTION

1. "Thermal Stresses Due to Large Spanwise and Chordwise Temperature Gradients in Long Thin Plate," Glaser, A. R.; R. G. Dale, B. E. Gatewood, ARL 63-236, December, 1963, Ref. 31-3 of Ref. 1, Tables VII and XVI.

2. Summary of Tests

Test of unrestrained long thin rectangular plates with two dimensional temperature gradients.

3. Geometry

Fig. 1, Thermocouple and Strain Gage Locations, Figs. 35 and 36.

4. Unrestrained

5. Material Properties

None (2024-T3 bare aluminum alloy)

6. Temperature Distributions

Test 1, Fig. 20.
Test 2, Fig. 21.
Test 3, Fig. 22.
Test 4, Fig. 23.
Test 5, Fig. 24.
3.5 inch heated length, Figs. 32 and 33.

7, 8. Test Results

A. Strain Distribution along $\eta = 0$ (in x-direction), $\lambda = 1.777$, Fig. 26, (Tests 1-5).

B. Strain Distribution along $\eta = 0$ (in y-direction), $\lambda = 1.777$, Fig. 27, (Tests 1-5).

C. Strain Distribution along $\eta = \pm 1$ (in x-direction), $\lambda = 1.777$, Fig. 28, (Tests 1-5).

D. Strain Distribution along $\psi = 0$ (in x-direction), $\lambda = 1.777$, Fig. 29, (Tests 1-5).

E. Table of Recorded Strains obtained with 3.5 inch heated length.

S11. TORSIONAL EFFECTS OF TEMPERATURE ON A FLAT PLATE

1. Reference 21-80, Table I, Table XVI, of Reference 1. Blackstock, W. J., "Some Effects of Thermal Stresses on Stiffness Reduction of Plane, Constant-Thickness Rectangular and Delta Specimens," WADC-TR-58-686, AD 208 154.

2. A Study of Torsional Stiffness Changes of an 18" x 28" x $\frac{1}{4}$" Rectangular Steel Specimen, and of an 18" x 18" x $\frac{1}{4}$" Constant Thickness Delta Specimen.

3. See Figure 19, of Ref. 21-80, for Geometry.

4. Plates are supported at one end as cantilevers.

5. The report does not list material properties. The material of the test specimen was described only as "mild steel."

6. Temperature distributions are shown in:

Fig. 1, "A Representative Temperature Distribution,"

Fig. 11, "Experimental Temperature Distribution for the Delta Shaped Specimen,"

Fig. 14, "Temperature Distribution for Nonsymmetrical Heating of Rectangular Specimen, θ = 10 Per cent,"

Fig. 15, "Temperature Distribution for Nonsymmetrical Heating of Rectangular Specimen, θ = 20 Per cent."

7. Experimental data is given in:

Fig. 4, "Experimental Load vs Twist Characteristics at Room Temperature."

Fig. 5, "Experimental Twist vs Temperature Excess with no External Loads."

Fig. 8, "Experimental First Torsional Frequency Ratio vs Temperature Excess."

8. Theoretical comparisons are given in:

Fig. 16, "Predicted Moment vs Twist for Various Values of Initial Twist."

S12. THERMAL STRESS-STRAIN DISTRIBUTION IN AN ANISOTROPIC MATERIAL

1. Reference 21-45, Table VII, Table XVI of Ref. 1. Suzuki, B. H., "Thermal Stress-Strain Distribution in a Tranversely Anisotropic Material during Transient Heating," Inst. of Engrg. Res., University of California, Berkeley, Calif., March 30, 1962, TR-HE-150-196.

2. Test of 6" x 4" x 1/8" and 6" x 4" x $\frac{1}{4}$" Pyrolytic Graphite Plates with Transient Heating.

3. Test specimens were 6" x 4" x 1/8" and 6" x 4" x $\frac{1}{4}$" flat plate. See Fig. 1 for coordinate axes and Fig. 3 for detail of test section assembly.

4. Unrestrained

5. For material properties, refer to Fig. 22, Fig. 23, Fig. 24, and Fig. 25 of Ref. 21-45 and to, Kotlensky, W. V. and H. E. Martens, "Tensile Properties of Pyrolytic Graphite to 5000°F," JPL. Tech. Rept. 32-71, March 10, 1961.

6. Temperature Distributions

Fig. 8A-Fig. 8E, "Temperature Rise at Various Depths in a $\frac{1}{4}$-inch Thick Pyrolytic Graphite Plate at Distances of $\frac{1}{2}$, 1-1/8, 1-7/8, 3-3/8, and 5-3/8 inches from the Leading Edge."

Fig. 9A-Fig. 9E, "Temperature Rise at Various Depths in a $\frac{1}{4}$-inch Thick Pyrolytic Graphite Plate at Distances of 1/3, 1-1/8, 1-7/8, 3-3/8, and 5-3/8 Inches from the Leading Edge."

Fig. 10, "Temperature Distribution at Various Times Through 1/8-inch Thick Pyrolytic Graphite Plate 5-3/8 Inches from Leading Edge."

Fig. 11, "Temperature Distribution at Various Times Through $\frac{1}{4}$-inch Thick Pyrolytic Graphite Plate 5-3/8 Inches from Leading Edge."

Fig. 12A-Fig. 12E, "Temperature Distribution Along Length of 1/8-inch Thick Pyrolytic Graphite Plate at Various Depths after 5, 10, 15, 20, and 30 Seconds of Heating."

Fig. 13A-Fig. 13G, "Temperature Distribution Along Length of $\frac{1}{4}$-inch Thick Pyrolytic Graphite Plate at Various Depths after 10, 20, 30, 40, 50, 60, and 70 Seconds of Heating."

7, 8. Test Data and Comparisons

Fig. 14, "Comparison of Experimental Data with Calculated Strains at Unheated Surface of 1/8-Inch Thick Pyrolytic Graphite Plate."

Fig. 15, "Comparison of Experimental Data with Calculated Strains at Unheated Surface of $\frac{1}{4}$-Inch Thick Pyrolytic Graphite Plate."

Fig. 16, "Distribution of σ_1 Through 1/8-Inch Thick Plate after 20 Seconds of Heating."

Fig. 17, "Distribution of σ_1 Through $\frac{1}{4}$-Inch Thick Plate after 40 Seconds of Heating."

Fig. 18, "Variation of σ_1 at Heated Surface and Midplane of 1/8-Inch Thick Plate."

Fig. 19, "Variation of σ_1 at Heated Surface and Midplane of $\frac{1}{4}$-Inch Thick Plate."

Fig. 20, "Distribution of σ_3 Through $\frac{1}{4}$-Inch Thick Plate after 30 Seconds of Heating."

Fig. 21, "Distribution of σ_5 Through $\frac{1}{4}$-Inch Thick Plate after 40 Seconds of Heating."

9. Comments

Four or five tests were necessary before consistent data were obtained. Only the best data is given in the report, all of which is listed above.

S13. THERMAL STRESSES IN BOX BEAMS

1. Reference 21-6, Table I, Table XVI of Ref. 1, Kotanchik, J. N., Johnson, A. E. and Ross, R. D. "Rapid Radiant Heating Tests of Multiweb Beams," NACA TN 3474, September, 1955.

2. Tests of four multiweb box beams, two with ribs and two without, subject to radiant heating of one cover and no external loads.

3. Geometry

Figure 1 of subject report.

4. Unrestrained

5. Material Properties

2024-T4 aluminum alloy, see Heimerl, G. J. and Inge, J. E. "Tensile Properties of 7075-T6 and 2024-T4 Aluminum Alloy Sheet Heated at Uniform Temperature Rates under Constant Load," NACA TN 3462, 1955.

6. Temperature Distributions

Figure 4, "Temperature Distribution in Beam 1, Heating Rate, 90 BTU/Ft^2-Sec."

Figure 5, "Temperature Distribution in Beam 2, Heating Rate, 29 BTU/Ft^2-Sec."

Figure 6, "Temperature Distribution in Beam 3, Heating Rate, 77 BTU/Ft^2-Sec."

Figure 7, "Temperature Distribution in Beam 4, Heating Rate, 24 BTU/Ft^2-Sec."

7. Experimental Data

Figure 8, "Measured Longitudinal Strains in Webs during Heating."

Figure 9, "Time History of Strain at Center of Web, Beam 3."

Figure 11, "Typical Deformations after Heating."

Table 1, "Test Data and Results for Box Beams Subjected to Rapid Heating."

8. Comparisons of Test and Theory

See pages 4 and 5 of subject report.

9. Comments

Heat was applied up to buckling of cover plate.

S14. COMPRESSIVE STRENGTH OF A PLATE AT A STABILIZED ELEVATED TEMPERATURE

1. Reference 21-31, Table IX, Table XVI of Ref. 1, Heimerl, G. J. and Roberts, W. M., "Determination of Plate Compressive Strengths at Elevated Temperature," NACA Report 960, 1950.

2. Buckling tests of H-section plate assembles under stabilized temperature conditions up to 600°F.

3. Geometry

Refer to, Heimerl, G. J., "Determination of Plate Compressive Strengths," NACA TN 1480, 1947, Fig. 4, for Geometry of test sample.

4. Unrestrained

5. Material Properties

Material is 7075-T6 (75S-T6) aluminum alloy. Figure 7 gives the ratio of E/E_{rt} and Poisson's ratio at elevated temperatures.

6. Temperature Distributions

Stabilized elevated temperatures at 200°F, 400°F, and 600°F.

7, 8. Test Data and Comparisons

Table 1. Local-instability test results for extruded 75S-T6 H-sections

Figure 4. Compressive stress-strain curves

Figure 5. Secant and tangent modulus curves at 200°F, 400°F, 600°F

Figure 6. Yield stresses at various temperatures

Figure 8. Effect of exposure time on yield stress at 400°F

Figure 9. Relations between buckling stress, maximum stress, and yield stress at elevated temperatures

S15. EFFECT OF THERMAL STRESS ON PANEL FLUTTER

1. Reference 21-43, Table XII and Table XVI of Ref. 1, Dixon, S. C., Griffith, G. E., and Bohon, H. L., "Experimental Investigation at Mach 3.0 of the Effects of Thermal Stress and Buckling on the Flutter of Four-Bay Aluminum Alloy Panels with Length Width Ratios of 10," NASA TN D-921, October, 1961.

2. An investigation of skin stiffener panels consisting of four panels, each 2.6 inch x 26 inch, at dynamic pressures ranging from 1,500 psf to 5,000 psf at stagnation temperatures ranging from 300°F to 655°F.

3. Geometry

Figure 2. Instrumentation in Fig. 6.

4. Restraints

Partially restrained. Panels were allowed 0.05 inch of expansion on all sides. See Fig. 5 for mounting details.

5. Material Properties

The material is 2024-T3 aluminum alloy. No material properties are given in the report.

6. Temperature Distribution

Temperature distribution is given in Fig. 7.

7. Experimental Data

Table I, "Panel Flutter Data"

Figure 8, "Variation of Flutter Parameters during Test in which Flutter Started, Stopped, and Restarted."

Figure 9, "Effects of Aerodynamic Heating on Flutter of Partially Restrained Panels with Length Width Ratios of 10."

Figure 11a to 11j, "Sample Deflectometer Records."

8. Comparison of Test and Theory

No theoretical values for flutter are given.

S16. THERMAL CONDUCTANCE OF VARIOUS JOINTS

1. Reference 21-71, Barzelay, M. E., Tong, K. N., Hollo, G., "Thermal Conductance of Contacts in Aircraft Joints," NACA TN 3167, 1954.

2. Tests of various types of joints of both aluminum and stainless steel with a constant contact pressure. See Table I of subject report for a complete description of the tests.

3. Geometry

Description of test specimens is given in Table I.

4. Unrestrained

5. Material Properties

Materials used were type 75S-T6 (7075-T6) aluminum and type 416 stainless steel. For a complete description of material, see Table I.

6,7,8. Temperature Distributions and Thermal Conductance

The purpose of this report is to measure thermal conductance for various types of aircraft joints. The temperature distribution is the output data, which is used to calculate thermal-conductance parameters.

The results are given in:

Table II,	"Test Results on Thermal Conductance Measurements"
Fig. 7(a)-7(c),	"Interface Conductance versus Temperature Drop for Various Mean Interface Temperatures."
Fig. 8(a)-8(e),	"Variation of Interface Conductance with Mean Interface Temperature."
Fig. 9(a)-9(l),	"Temperature Distribution in Typical Riveted Specimens."
Fig. 10(a)-10(d),	"Heat Flow versus (T_1M - T_2M)"
Fig. 12,	"Logarithmic Plot of Variation in Interface Conductance with Interface Temperature."

9. Comments

This report does not concern itself with thermal strains or stresses. Only the joint conductance is within the scope of this report.

S17. ANALYSIS OF HEATED RING FRAME

1. Reference 21-22, Table V and Table XVI of Ref. 1, Gatewood, B. E., Gehring, E. R., "Inelastic Redundant Analysis and Test Data Comparison for a Heated Ring Frame," Journal of the Aerospace Sciences, March, 1962, 364.

2. Inelastic analysis of ring under combined loads and temperature and comparison to failure load.

3. Geometry

Figure 1 of subject report.

4. Unrestrained

5. Material Properties

See Peteros, G. A., "Static Test of a Frame Specimen Subjected to a Thermal Gradient for the Model X-15 Airplane (NAA Model NA-240)," North American Aviation, Inc. Report No. NA57-157, May 15, 1957.

6. Temperature Distribution

Figure 1 of subject report.

7. Experimental Data

Failure load from NA57-157 is 2350 pounds.

8. Comparison of Test and Theory

Theoretical results are in Fig. 2, "Moment Distribution Curve," and Fig. 3, "Allowable Load-Strain Curve."

9. Comments

This article develops a method for inelastic redundant analysis and applies it to a completed test. Detailed test data can be found in North American Aviation Report No. NA57-157, May 15, 1957.

S18. STATIC TESTS OF TWO LARGE DEFLECTION WING MODELS

1. Reference 21-17, Table II, Table XVI of Ref. 1, Cener, D., "Procedures for Including Temperature Effects in Structural Analysis of Elastic Wings-Static Tests of Two Large Deflection Wing Models," WADC TR57-754, Part III, 1960.

2. Deflection tests of two rectangular plan form wing models under various loads (uniform room temperature, but large amount of strain data for applied loads).

3. Geometry

Figure 2.1, Figure 2.2, and Figure 2.3.

4. Unrestrained

5. Material Properties

Material is 7075-T6 (75S-T6) aluminum. Reference: Miller J. A., "Stress-Strain and Elongation Graphs for Aluminum Alloy 75S-T6 Sheet," NACA TN 2805, April 1950.

6. Temperature Distributions

Uniform, room.

7. Experimental Data

Table 4.1, "Measured Deflections on Uniform Thickness Wing Model"

Table 4.2, "Measured Stresses on Uniform Thickness Wing Model"

Table 4.3, "Measured Stresses (Strain Rosette Gages) Uniform Thickness Wing Model"

Table 4.4, "Measured Deflections--Variable Thickness Wing Model"

Table 4.5, "Measured Stresses (Strain Gages)--Variable Thickness Wing Model"

Table 4.6, "Measured Stresses (Strain Rosette Gages)--Variable Thickness Wing Model"

Figure 4.1, "Location of Measured Deflections for Uniform and Variable Thickness Wing Model"

Figure 4.34, "Measured Stresses Aiding Leading Edge of Uniform and Variable Thcikness Wing Models--Load Level 1140 lb."

Figure 4.34, "Chordwise Stress Distribution--Uniform and Variable Thickness Wing Model, y = 1.83 inch, Load Level 1140 lb."

8. Comparison of Test and Theory

Experimental data is compared to theoretical calculations in Part IV of this report.

9. Comments

The main purpose of this ambient temperature analysis was to test the validity of the method described in Part II of the report.

S19. THREE-DIMENSIONAL PHOTOTHERMOELASTIC TECHNIQUE

1. Reference 21-19, Table VII and Table XVI of Ref. 1, Tramposch, H. and Gerard, G., "An Exploratory Study of Three-Dimensional Photothermoelasticity." Journal of Applied Mechanics, Vol. 28, No. 1, March, 1961, P. 35.

2. A series of exploratory tests of a new sandwich photothermalelastic material. The following known cases were examined:

a) Beam under simple bending - room temperature

b) Sphere under simple compression - room temperature

c) Thick-walled-cylinder-steady-state temperature distribution.

3. Geometry

Figure 2, cylinder dimensions are given in Table 2.

4. Unrestrained

5. Material Properties

Material is Hysol 6000-OP. Material Properties are given in Table 1.

6. Temperature Distribution

Figure 6.

7, 8. Experimental Data and Comparisons to Theory

Figure 1, "Correlation of Fringe Orders from Composite Beam and Single Beam."

Figure 2, "Fringe Patterns in Meridian Plane of a Sphere Compressed by Two Concentrated Forces."

Figure 3, "Correlation of Observed Fringe Orders with Photoelastic Results Obtained by Stress Freezing." (Sphere Test)

Figure 7, "Correlation of Experimental and Theoretical Results of a Cylinder and a Disk, both Exposed to the same Steady-State Temperature Distribution (ΔT_{max} = 49°F)."

9. Comments

Test results show that the sandwich models may be used effectively in three-dimensional problems.

S20. STRESS ANALYSIS OF HEATED COMPLEX SHAPES

1. Reference 21-47, Table VII and Table XVI of Ref. 1, Gallagher, R. H., Padlog, J., Bijlaard, P., "Stress Analysis of Heated Complex Shapes," American Rocket Society Journal, May, 1962, pp. 700-707.

2. (A) Test of a heated plate of nonuniform thickness

(B) Test of a uniaxially loaded plate with a centrally located hole under a time-dependent load-temperature sequence.

3. Geometry

Idealized geometry of the test specimen for Test A is shown in Fig. 6.

The geometry of the test specimen for Test B is shown in Fig. 8.

4. Unrestrained

5. Material Properties

For Test A, results are given in non-dimensional form and the material is not specified.

For Test B, the material is 2024-T4 aluminum plates. One-dimensional material properties were determined from tests performed on coupons of sheet stock. However, these properties were not published in this report.

6. Temperature Distributions

Temperature distribution for Test A is shown in Fig. 6.

The load-temperature history of the specimen in Test B is shown in Fig. 8.

7, 8. Test Data and Comparisons to Theory

Test A:

Figure 7, "Heated Plate Results."

Test B:

Figure 9, "Predicted Total Axial Strains for a Plate with a Centrally Located Hole."

Figure 11, "Stresses at Net Section."

Figure 12, "Total Plastic Strain versus Temperature."

9. Comments

This report presents an extension of the discrete elements method of structural analysis to include inelastic strains resulting from cyclic application of load and finite temperature differences. The method of analysis was then applied to two known test cases and the results were compared.

S21. STRAIN ACCUMULATION UNDER EQUIVALENT THERMAL CYCLING

1. Reference 21-28, Table IV and Table XVI of Ref. 1, Gatewood, B. E., Grothouse, A. D. and Von Hausen, W. D., "Experimental Data on Strain Accumulation under Equivalent Thermal Cycling," Journal of the Aerospace Sciences, Vol. 28, June, 1961, p. 502-503.

2. Test of strain accumulation under equivalent thermal cycling for a three element structure.

3. Geometry

See Figure 1.

4. Unrestrained

5. Material Properties

Material is 2024-T3 aluminum alloy. The test specimen was kept at room temperature to keep the material properties constant.

6. Temperature Distributions

The test specimen was cycled through an equivalent temperature change of 180°F by heating the center upper element. (See Fig. 1.)

7. Experimental Results

Figure 2, "Experimental Thermal Cycling--Strain Covergence to Elastic Shakedown."

Figure 3, "Allowable Stresses under Thermal Cycling with Axial Load-Experimental."

Figure 4, "Allowable Stresses under Thermal Cycling with Combined Axial Load and Bending Moment-Experimental."

8. Comparisons of Test and Theory

Test results compare favorably with calculations made by the method described in Gatewood, B. E., "The Problem of Strain Accumulation under Thermal Cycling," Journal of the Aerospace Sciences, Vol. 27, No. 6, pp. 461-462, June, 1960.

S22. INVESTIGATION OF THERMAL STRESSES BY THE MIORE' METHOD

1. Reference 21-25, Table VI and Table XVI of Ref. 1, Sciammarella, C. A., and Ross, B. E., "Thermal Stresses in Cylinders by the Miore' Method," Experimental Mechanics, Vol. 4, October, 1964, pp. 289-296.

2. Tests of the stress developed in a steel ring with a radial temperature distribution.

3. Geometry

Three test specimens were used with the following dimensions:

Specimen	OD	ID	OD/ID
Ring No. 1	5.50	2.35	2.34
Ring No. 2	5.50	3.00	1.83
Ring No. 3	5.50	4.04	1.36

Note: Dimensions are in inches.

4. Unrestrained

5. Material Properties

The material of the test specimens was steel. However, the results are given in nondimensional parameters which may be evaluated for any material.

6. Temperature Distributions

The theoretical and experimental temperature distribution is given in Fig. 1.

7. Experimental Results

Test data consists of temperature readings and photographs of the Miore' fringes of the specimens.

Temperature distributions for all specimens are shown in:

Figure 3, "Agreement between the Theoretical and Actual Radial Temperature Distribution in the Rings Tested."

Photographs of the Miore' fringes are shown in:

Figure 4, "Miore' Fringes Formed by Thermal Stresses in Steel Ring No. 1."

Figure 5, "Miore' Fringes Formed by Thermal Stresses in Steel Ring No. 2."

Figure 6, "Miore' Fringes Formed by Thermal Stresses in Steel Ring No. 3."

8. Comparisons of Test and Theory

Figure 7, "Theoretical Solution for Thermal Stresses in a Cylinder and Miore' Results. Ring No. 1."

Figure 8, "Theoretical Solution for Thermal Stresses in a Cylinder and Miore' Results. Ring No. 2."

Figure 9, "Theoretical Solution for Thermal Stresses in a Cylinder and Miore' Results. Ring No. 3."

Figure 10, "Variation of Maximum Thermal Stresses with Thickness of a Cylinder when several Points Are Plotted for a Given Ratio B/A. Results Correspond to Tests Conducted at Different Temperature Gradients."

Figure 11, "Variations of Maximum Thermal Stresses with Temperature for a Cylinder."

Figure 12, "Distribution of Strains and Temperature for One Radial Section of Ring No. 1."

S23. THERMAL STRESSES IN A FLAT PLATE

1. Reference 21-56, Table VIII and Table XVI of Ref. 1, Frisch, J., "Optical Strain Determination at Transient High Temperatures in Stainless Steel," Experimental Mechanics, Vol. 4, November, 1964, pp. 320-327.

2. Test of a 0.25 inch x 2.25 inch x 4.0 inch rectangular plate subjected to transient, three-dimensional temperature distribution.

3. Geometry

Geometry of the test specimen is shown in Fig. 1.

4. Unrestrained

5. Material Properties

Material is type 304 stainless steel. The properties are given in: Arne, C. L., "Optical Strain Measurements in Stainless Steel at Transient Temperatures up to 2000°F," University of California Eng. Project Report HE-150-204, December, 1962.

6. Temperature Distributions

The temperature distributions are given by Eqs. (2) through (6) in subject report.

7. Experimental Results

Figure 5, "Heat Flux into Specimen as a Function of Temperature at the Intersection of the X- and Y-Axes of Type 304 Stainless Steel."

Figure 6, "Experimental Optical Strain Measurements versus Time for Heated Type 304 Stainless Steel Plates."

Figure 7, "Experimental Temperature Measurements on Unheated Surface of Type 304 Stainless-Steel Plate (X = -25/32 inch, Y = 11/16 inch)."

Figure 10, "Calculated Stress Distribution through Specimen Thickness Based on Temperature Tz at X = 0, Y = 0 at 40 Seconds."

Figure 11, "Calculated Stress Distribution on Unheated Surface of Specimen Quadrant Based on Temperature Tx at Y = 0 at 40 Seconds."

Figure 12, "Calculated Stress Distribution on Unheated Surface of Specimen Quadrant Based on Temperature Ty at X = 0 at 40 Seconds."

Figure 13a, "Stress Distribution on Unheated Surface of Specimen Quadrant along Y-Axis at 40 Seconds."

Figure 14, "Net Strain on Unheated Surface Based on Stress Distribution versus Time for Type 304 Stainless-Steel Plate."

8. Comparisons between Theoretical and Experimental Results

Figure 8, "Comparison of Experimental and Calculated Strains versus Time for Type 304 Stainless-Steel Plate."

Figure 15, "Comparison of Total Calculates Strain and Strain Due to Free Thermal Expansion versus Time for Type 304 Stainless-Steel Plate."

9. Comments

The report primarily concerns itself with the techniques of strain measurement. It develops a method for extending the usefulness of the optical strain gage (Tuckerman Gage) to temperatures up to 2000°F.

S24. THERMAL STRESSES IN A COMPLEX WING SECTION

1. Reference 21-21, Table II, Table XVI of Ref. 1, Gallagher, R. H., Quinn, J. F., and Turrentine, D., "Techniques for Testing Thermally-affected Complex Structures." Experimental Mechanics, August, 1961, pp. 41-49 (WADC TR 58-378, December, 1959).

2. Deflection tests of multi-web wing sections under selected temperature gradients. The first model was a square planform wing section, the second model was a swept back planform wing section.

3. Geometry

Is shown in Figs. 1 and 3.

4. Unrestrained

5. Material Properties

Material--Type 301 stainless steel. The elastic modulus was determined from coupons of the test material for the various time-temperature histories, but the data was not published in the report.

6. Temperature Distributions

Temperature distributions are shown in Figs. 4 and 5.

7, 8. Experimental Data and Comparisons

Figure 11, "Analytical Stress versus Experimental Stress,"

Table 1, "Comparison of Elevated-Temperature Deflection Parameters with Room-Temperature Deflection Parameters--First Model,"

Table 2, "Comparison of Elevated Temperature Deflection Parameters with Room-Temperature Deflection Parameters--Second Model."

9. Comments

More experimental data are given in WADC TR 58-378 (December, 1959) by the same authors.

S25. ELEVATED TEMPERATURE TESTS OF BOX BEAM STRUCTURES

1. Reference 31-1, Table I, Table XVI of Ref. 1. Gehring, R. H., and R. L. Engle, "A Feasibility Study of Applied Load Ratios to Simulate Elevated Temperature Static Tests at Room Temperatures." NAA Report NA 62 H-973, May, 1963, pp. 2-48. Also, Reference 21-24 of Ref. 1.

2. Summary of Tests

Tests of box beam structures under various types of loadings. The test specimens were divided into three types:

Type A - Short Columns - 6 samples

Type B - Bending Beams - 16 samples

Type - Long Columns - 6 samples

Samples selected have two-dimensional temperature variations.

3. Geometry

The geometry of the samples is shown as follows:

Type A - Figure 5.3

Type B - Figure 5.1

Type C - Figure 5.2

Instrumentation of the samples is shown in Fig. 5.8.

4. Unrestrained

5. Material Properties

Material was 7075-T6 aluminum alloy.

Coupon Stress - Strain curves are given in Figs. A.1.1 through A.1.10.

A summary of coupon material data is given in Figs. 7.1 through 7.2.

Figures 7.12 and 7.13 give the variation in material porperties with temperature for specific values of the Larson-Miller Parameter.

6. Temperature Distributions

Cross-sectional temperature distributions are shown as follows:

Sample No.	Location
B-3 Through B-8	Fig. 6.12
A-3 Through A-6	Fig. 6.13
C-3 Through C-6	Fig. 6.14

7. Experimental Data

Test results are given in the following figures:

Sample No.	Location
B-3	Fig. A.3.2
B-4	Fig. A.2.3
B-5	Fig. A.2.4
B-6	Fig. A.2.5
B-7	Fig. A.2.6
B-8	Fig. A.2.7
A-3	Fig. A.2.11
A-4	Fig. A.2.12
A-5	Fig. A.2.13
A-6	Fig. A.2.14
C-3	Fig. A.2.16
C-4	Fig. A.2.17
C-5	Fig. A.2.18
C-6	Fig. A.2.19

8. Comparison of Test and Theory

Ultimate and yield test values are compared with analytical calculations in the following figures:

Sample No.	Location
B-3 Through B-8	Figs. 9.1 and 9.2
A-3 Through A-6	Fig. 9.3
C-3 Through C-6	Fig. 9.4

9. Comments

Only those test samples which underwent two-dimensional, cross-sectional temperature gradients have been selected. Considerable information is given in the original report on effects of temperature exposure during strain-gage curing on the material properties. Also, inelastic effects and buckling effects are included in the analysis and comparisons.

S26. BOX BEAMS UNDER COMBINED THERMAL AND DYNAMIC INPUTS

1. Reference 21-79, Table I, Table XVI of Ref. 1, Blackstock, W. J., "Structural Behavior of Box-Beams Under the Influence of Combined Thermal and Dynamic Inputs," WADC TR 58-685, December, 1958, ASTIA, AD208153.

2. Summary of Tests

A study of single-cell aluminum box beams subjected to both dynamic and thermal loads in the elastic range and the post-failure range.

3. Geometry

Geometry is given in Fig. 1.
Instrumentation is given in Fig. 6.

4. Cantilever Beam - Unrestrained

5. Material Properties

Room temperature material properties are given in Fig. 1. Figure 18 gives modulus of elasticity at elevated temperatures.

6. Temperature Distributions

Figure 9, "Representative Experimental Time History of Temperature at the Center of the Irradiated Skin."

Figure 10, "A Typical Experimental Temperature Distribution at Time of Peak Temperature at the Center of the Irradiated Skin."

7, 8. Experimental Data and Comparisons

Figure 14, "A Typical Experimental Strain-Distribution Time History."

Figure 15, "Typical Stress Distributions during the Transient-Heating Period."

Table 2, "Predicted Stress Distribution for a Thermal Intensity of 15 BTU/Ft^2-sec."

Table 3, "Predicted Stress Distribution for a Thermal Intensity of 15 BTU/Ft^2-sec. Applied Static Moment 480-Ft-Lb."

9. Comments

In this report, the interest in thermal stresses is concerned primarily with their influence in making the test specimen more susceptible to failure under external dynamic loading. Therefore, only a limited amount of thermal stress data are given in this report.

S27. THERMAL STRESS IN SOLID PROPELLANT GRAINS

1. Reference 21-90, Table IX, Table XVI of Ref. 1, Jones, J., J. E. Fitzgerald, and E. Francis, "Thermal Stress Investigation of Solid Propellant Grains, Vol. I, Theory and Experiment," LPC Report No. 578-F, May, 1963, ASTIA, AD 406338.

2. Summary of Tests

Tests of analog rocket motors with a length of 14 inches, outside diameter of 4 inches, and circular port diameters of 1.5 inches, 1.2 inches, 1.0 inch, and 0.866 inch.

3. Geometry

Figures 2-1 and 5-1 of original report.

4. Unrestrained

5. Material Properties

No material properties are given in this report. The bibliography lists these possible sources of material properties:

a. Ferry, J. D., 1961, ViscoElastic Properties of Polymers, John Wiley & Sons, Inc., New York, N. Y.

b. Treloar, L. R. G., 1958, The Physics of Rubber Elasticity, Oxford University Press, New York, N. Y.

c. Fitzgerald, J. E., et al. 1963 c, Final Report, MPO 556, "Structural Integrity of Propellant Grains," Lockheed Propulsion Company Redlands, California, LPD Report No. 478-F-1, AD406338.

6. Temperature Distributions

Figure 2-4, "Time Temperature Distribution in a Hollow Cylinder (Port Insulated) with Zero Initial Temperature and a Suddenly Applied Surface Temperature, T_o"

7. Experimental Data

Strain versus time for motors no.

(1) Fig. 5-3
(2) Fig. 5-4
(3) Fig. 5-5
(4) Fig. 5-6

Isothermic hoop strain versus temperature - Figure 5-7.

8. Comparison of Test and Theory

Only the failure points were predicted by the theory. The motors failed within 15% of the predicted temperature and within 3% of the predicted strain.

9. Comments

This report is concerned with total strain as a criterion of solid-propellant motor failure. It gives little attention to thermal stresses and does not present much useful data in this area.

S28. THERMAL STRESS IN A CIRCULAR PLATE

1. Reference 21-104, Table VII, Table XVI, Appendix A, Savchendo, V. I. and T. Sh. Chernis, "Obtaining Temperature Fields in Flat Models During Investigations by Photothermo-Elasticity Method," Zavodskaya Laboratoria, Vol. 29, No. 7, pp. 879-880, July 1963. Industrial Laboratory, Vol. 29, No.7, Dec., 1963. (Translation)

2. Summary of Tests

Test of a photelastic disc with a radius of 65 mm, with both open faces and insulated faces.

3. Geometry

See Fig. 1 for geometry.

4. Unrestrained

5. Material Properties

Material - ED-6 Epoxy Resin.
Material Properties are assumed constant with temperature.

6. Temperature Distributions

Temperature distributions are given in Fig. 2.

7, 8. Experimental and Theoretical Results

Theoretical and experimental results are compared in Fig. 3, "Distribution of Stresses σ_r and σ_θ along Radius."

S29. THERMAL STRESSES IN A DISC WITH EDGE RESTRAINTS

1. Reference 21-111, Table VII, Table XVI, Appendix A, Holland, M., "Thermal Stresses in a Thin Solid Disc." The Engineer, Vol. 221, Jan. 28, 1966, p. 165-168.

2. Summary of Tests

Tests of a thin circular homogeneous plate under radial temperature distribution with edge restraints.

3. Geometry

Figure 1.

4. Elastic Edge Restraints

5. Material Properties

No material properties are used. Test results are given in non-dimensional parameters.

6. Temperature Distribution

See Fig. 5.

7, 8. Test Data and Comparisons

Figure 6 - "Radial and Circumferential Stresses ($\tau_i - \tau_o$) Positive."

Figure 7 - "Radial and Circumferential Stresses ($\tau_i - \tau_o$) Negative."

Figure 8 - "Radial and Circumferential Stress Distribution ($\tau_i - \tau_o$) = 75°F."

S30. THERMAL STRESSES IN A PARTIALLY FILLED ANNULUS

1. Reference 21-99, Table VI and Table XVI, Appendix A. Emery, A. F., Barrett, C. F., and A. S. Kobayashi, "Temperature Distributions and Thermal Stresses in a Partially Filled Annulus." Experimental Mechanics, Vol. 6, No. 12, December, 1966.

2. Summary of Tests

Tests of the temperature distribution in a liquid filled annulus with various liquid levels. Also, test of radial crack effect on stress distribution.

3. Geometry

See Fig. 1.

4. Unrestrained

5. Material Properties

None - Test results are presented in non-dimensional parameters. Lucite and Hysol were used in the model for photothermoelastic measurements.

6. Temperature Distributions

Figure 1
Figure 5

7, 8. Analytical and Experimental Data

Figure 7 - "Maximum Shear-Stress Distribution; Liquid Level d = 0.5 in. Above Center. τ_m = 132 psi, τ_m = 1.13 Fringes"

Figure 8 - "Maximum Shear Stress Disbribution, Liquid Level d = 0.5 in. Below Center. τ_m = 105 psi, τ_m = 0.88 Fringes."

Analytical data for σ/τ_m versus a radial parameter is presented in Fig. 3.

Table 1, Stress Intensity Factor Determination

S31. RESIDUAL STRESSES IN WELDED PLATES

1. Reference 21-41, Table VII and Table XVI of Ref. 1, Rao, N. R. and L. Tall, "Residual Stresses in Welded Plates," Welding Journal, Vol. 40, No. 10, Oct. 1961, p. 468s-480s.

2. Summary of Tests

A series of tests conducted to determine residual stress in welded plates. Table 2 and Table 3 summarize the tests conducted on each specimen.

3. Geometry

All plates were rectangular. The plate sizes tested are shown in Table 1. Location of the weld line is shown in Fig. 7.

4. Edge Restraints - Unrestrained

5. Material Properties

Material used for all tests was ASTM-A7 Structural Steel. A summary of Coupon Tests is given in Table 5.

6. Temperature Distribution

The exact temperature distribution was not measured. The approximate temperature distribution is given in Fig. 2.

7. Experimental Data

Fig. 10, "Residual Stress Distribution, 4" x 1/4" plate.

Fig. 11, "Residual Stress Distribution, 6" x 1/4" plate.

Fig. 12, "Residual Stress Distribution, 6" x 3/8" and 6" x 1/2" Plates."

Fig. 13, "Residual Stress Distribution, 6" x 3/4" and 6" x 1" Plates."

Fig. 14, "Residual Stress Distribution, 8" x 1/2" Plate."

Fig. 15, "Residual Stress Distribution 10" x 1/2" Plate."

Fig. 16, "Residual Stress Distribution, 12" x 1/2" Plate."

Fig. 17, "Residual Stress Distribution, 12" x 3/8" Plate."

Fig. 18, "Residual Stress Distribution 16" x 1" Plate."

Fig. 19, "Residual Stress Distribution, 18" x 3/4" and 20" x 1/2" Plates."

Fig. 20, "Residual Stress Distribution, 6" x 1/2" and 8" x 1/2" Plates."

Fig. 21, "Residual Stress Distribution, 8" x 1/4" Plate."

Fig. 22, "Residual Stress Distribution, 10" x 1/2 Plate."

Fig. 23, "Residual Stress Distribution 12" x 3/4" and 12" x 1" Plates."

Fig. 24, "Residual Stress Distribution, 16" x 1/2", and 18" x 3/4" Plates."

Fig. 25, "Residual Stress Distribution 20" x 1/2" and 20" x 1" Plates."

Table 6, "Residual Stress Distribution in Center Welded Plates."

Table 7, "Residual Stress Distribution of Edge Welded Plates."

Table 8, "Average Experimental Values of Residual Stress Distribution in Welded Plates."

8. Comparisons of Theory and Test

No theoretical comparisons are given in this report.

9. Comments

The experimenters did not measure the experimental temperature distribution.

The time-dependent theoretical temperature distribution used in this report is that of Rosenthal.*

*Rosenthal, O., "Mathematical Theory of Heat Distribution during Welding and Cutting," Welding Journal, Vol. 20, No. 5, 1941, p. 220s-224s.

S32. CREEP IN A BEAM UNDER STRESSES PRODUCED BY A PURE BENDING MOMENT

1. Reference 21-1, Table I and Table XVI of Reference 1, Tapsel, H. J., and A. E. Johnson, "An Investigation of the Nature of Creep Under Stresses Produced by Pure Flexure," Journal of the Institute of Metals, No. 2, Vol. 57, 1935, p. 121.

2. Summary of Tests

Tests of a beam under a pure bending moment.

3. Geometry

The beam test specimen was a block 15" long x 7" deep x 2" wide.

4. Unrestrained

5. Material Properties

The material was commercially pure lead. The results of tensile tests conducted on coupons of the material are shown in Fig. 7 and Fig. 8. Stress vs. rate of strain for the material is shown in Fig. 12.

6. Temperature Distribution

Uniform Temperature.

7. Experimental Results

Fig. 2, "Mean Strain - Duration Curve Obtained by Modifying Scale of Curves for Individual Fibres."

Fig. 3, "Mean Strain-Duration Curve Obtained by Modifying Scale of Curves for Individual Fibres in Bending Test."

Fig. 4, "Strain Duration Curves for Various Fibres."

Fig. 5, "Strain - Duration Curves for Fibres in Tension."

Fig. 6, "Strain - Duration Curves for Fibres in Compression."

Fig. 9, "Stress Distribution for Bending Moment 13,340 in-lb."

Fig.10, "Stress Distribution for Bending Moment 17,152 in-lb."

Fig.11, "Redistribution of Stress in Beam when Creep Occurs."

8. Comparisons of Theory and Test

No comparisons between theoretical and experimental results are given.

9. Comments

Tests were conducted on lead at room temperature for experimental reasons. The behavior of any beam under flexure may be approximated entirely from the relations between tensile stress and the rate of strain.

S33. STRESS IN MULTICONNECTED FLAT CIRCULAR RINGS

1. Reference 21-100, Table VI and Table XVI of Appendix A. Rothstein, R. J., and W. F. Kirkwood, "Photothermoelastic Analysis of Stresses in Multiconnected Flat Circular Rings," Society for Experimental Stress Analysis-Proceedings, Vol. 21, No. 2, 1964, p. 237-243.

2. Summary of Tests

Tests of thermal stresses induced in several proposed designs of a multiconnected, flat, circular ring by a transient symmetrical temperature distribution.

3. Geometry

See Figure 6.

4. Restraints

The model was unrestrained in the radial direction. A spring with a spring constant of 10 lb/in was used to restrain the test specimen in the axial direction.

5. Material Properties

The material was ERL 2774.

Material Fringe Value (f) 70.5 lb/in/fringe

Thermal Coefficient of Expansion (α) 30 μin/in/^{o}F

Young's Modulus (E)	5.2 x 10^5 psi
Poissons Ratio (μ)	0.36

The properties were assumed constant over the entire temperature range.

6. Temperature Distribution

The experimental temperature distribution is given in Table 1.

7,8. Experimental Data and Comparisons to Theory

Fig. 5, "Stress Profiles - Ring 1."

Fig. 8, "Stress Profiles - Ring 2."

Fig. 9, "Stress Profiles - Ring 3, (ΔT = 221F^{o})."

Figure 10, "Stress Profiles - Ring 4, ($\Delta T = 221F^{O}$)."

9. Comments

The non-steady state situation examined gives smaller stress values than the steady state situation with the same temperature distribution, in this particular case. The test results show that the test procedure and model assembly construction can be applied to other thermal stress problems.

S34. COMBINED THERMAL AND STATIC LOADS ON A BOX BEAM

1. Reference 21-92, Table I and Table XVI of Ref. 1, Anderson, G. E. et. al., "Design Concepts for Minimum Weight High Performance Supersonic Aircraft Structures, Vol. I: Structural Design and Analysis, and Vol. III: Testing," ASD TDR 63-871, Vol. I, Sept. 1963; Vol. III, May, 1964.

2. Summary of Tests

Test of a box beam 52" wide, 15" deep, and 180" long under combined bending and thermal stresses. See Table 22, Vol. III for schedule of tests.

3. Geometry

See drawing Z-5775831 in Appendix 13 of Vol. I.

4. Unrestrained

5. Material Properties

See Vol. III, Figure 99.

6. Temperature Distribution

Fig. 109, Vol. III
Fig. 118, Vol. III
Fig. 119, Vol. III
Fig. 120, Vol. III
Fig. 121, Vol. III

7,8. Experimental Data and Comparisons to Theory

Vol. III, Figure 110, "Strain Gage Data - 1.67G, Heat to 300°F, Tank Empty."

Figure 112, "Strain Gage Data - 1.67G, Heat to 500°F, Tank Empty."

Figure 113, "Lower Surface Thermal Stress vs. Time-Heat to 500°F in 5 Minutes."

Figure 114, "Lower Surface Temperature, Thermal and Load Stress-Heat to 500°F, Tank Full."

Figure 115, "Lower Surface Thermal Stress and Temperature-Heat to 650°F, Tank Full."

Figure 116, "Upper Surface Temperature Heat to 650°F, Tank Empty."

Figure 117, "Wing Box Lower Surface Thermal Stress vs. Temperature Gradient."

The complete data printouts for Test No. 10, Test No. 33, and Test No. 62 (see Table 22, Vol. III) are included in Appendix III, Vol. III.

9. Comments

Only the thermal stress data has been included in this report.

S35. TESTS OF STRUCTURAL JOINTS

1. Reference 21-92, Table XIII and Table XVI of Reference 1, Anderson, G. E., et. al., "Design Concepts for Minimum Weight High Performance Supersonic Aircraft Structures Vol. I - Structural Design and Analysis, and Vol. III - Testing," ASD-TDR 63-871, Vol. I, Sept., 1963; Vol. III, May 1964.

2. Summary of Tests

Fatigue and tensile tests of joints with honeycomb cores. A summary of the tests is given in Table 15, Vol. I.

3. Geometry

Production drawing of the test samples are given in Appendix A, Vol. I. A summary of the test samples is given in Table 6, Vol. III.

4. Unrestrained

5. Material Properties

None given.

6. Temperature Distribution

Uniform elevated temperature.

7. Experimental Data

Vol. I, Table 15, "Summary of Phase II Joint Test Data."

Vol. III, Table 7, "Summary of Structural Joint Fatigue Test Results."

8. Comparison to Theory

None attempted.

9. Comments

The scope of this phase of the report is the mode of failure and the fatigue life of the structural joints. Only data on the ultimate stress of the joints was recorded.

S36. TESTS OF THIN WALLED CYLINDRICAL TUBES

1. Reference 21-100, Table VI and Table XVI of Appendix A. Frisch, J., and W. H. Geidt, "Thermal Stresses during Rapid Transient Heating." Final Report: Part II; "Thermal Strains in Tubes during Transient Heating to 2000°F," U. of California, Livermore Lawrence Radiation Lab., UCRL 13147, Feb. 1965.

2. Summary of Tests

Tests of cylindrical thin-walled tubes subjected to transient internal heating.

3. Geometry

Test specimens were thin walled cylindrical tubes

Specimen	Material	O. D.	Wall Thickness	Tube Length
1	304 Stainless Steel	1.00	0.035	8"
2	Tantalum	1.00	0.020	8"
3	Molybdenum	0.880	0.035	8"

4. Unrestrained

5. Material Properties

See Goldsmith, Hirschhorn, Waterman, "Thermophysical properties of solid materials," WADC TR 58-476, Revised Nov. 1960. Materials are type 304 stainless steel, tantalum, and molybdenum.

6. Temperature Distribution

Figure A- Axial Temperature Distribution

Figure 11- Axial Temperature Distribution

Figure 12- Circumferential Temperature Distribution

7,8. Experimental Data and Comparisons with Theory

Figure 8, "Thermal Dimetral Expansion Type 304 Stainless Steel Tube vs. Temperature and Time."

Figure 9, "Thermal Dimetral Expansion of Tantalum Tube vs. Temperature and Time."

Figure 10, "Thermal Dimetral Expansion of Molybdenum Tube vs. Temperature and Time."

9. Comments

The scope of the report was the accuracy of reluctance type displacement transducers at temperatures up to 2000°F. The data is presented in terms of total expansion of the tube diameter.

S37. EFFECT OF TEMPERATURE ON TORSIONAL STIFFNESS OF FINITE PLATES

1. Reference 21-123, Table I and Table XVI of Appendix A, Breuer, D. W., "Effects of Finite Displacement, Aspect Ratio, and Temperature on Torsional Stiffness of Cantilever Plates," Fourth U. S. National Congress of Applied Mechanics - Proceedings Vol. I, New York, 1962, p. 475-487.

2. Summary of Tests

Tests of the variation of torsional frequency with temperature and initial twist.

3. Geometry

See Fig. 1a.

The test samples had (a/b) ratios of 2,3,4,5,6,7, and 8. The thickness (t) was 1/8" for all specimens.

4. Unrestrained

5. Material Properties

The material was 2024-T3 aluminum alloy. The material properties were considered constant with temperature.

6. Temperature Distribution

Fig. 1b

Fig. 6 - Spanwise Temperature

Fig. 7 - Midspan Chordwise Temperature Variation

7,8. Experimental Data and Comparisons with Theory

Fig. 2, "Ratio of Buckling Temperature Differences."

Fig. 8, "Comparison of Experimental and Theoretical Torsional Frequencies (Room Temperature)."

Fig. 9, "Comparison of Theoretical and Experimental Buckling Temperatures (Flat Plate)."

Fig. 10, "Variation of Frequency Ratio and Tip Twist Temperature Ratio ((a/b) = 2)."

Fig. 11, "Variation of Frequency Ratio and Tip Twist with Temperature Ratio ((a/b) = 4)."

Fig. 12, "Variation of Frequency Ratio and Tip Twist with Temperature Ratio (a/b = 5)."

Fig. 13, "Variation of Frequency and Tip Twist with Temperature Ratio (a/b = 8)."

9. Comments

The scope of this report does not include measurement of the thermal stresses in the plate. However, it does include the effects of these thermal stresses upon the torsional frequency of the plate.

S38. TEST OF SKIN-STIFFENER PANELS UNDER THERMAL AND APPLIED LOADS

1. Reference 21-124, Table VII and Table XVI of Appendix A, Claus, J., H. Dillman and F. Sutch, "Manufacturing Methods for 'Hot Structures'" AMC Technical Report 60-7-795, Dec. 1960, Section I, Vol. I, AD250-054; Section I, Vol. III, AD251-498.

2. Summary of Tests

Tests of zee-edge and creased-edge skin panels under a heat-load program simulating re-entry conditions for a hypersonic boost-glide vehicle. Maximum external skin temperature is approximately 2000°F.

3. Geometry

See Figs. 372, 373, 374, and 375, and paragraph 2a on p. 714 of Vol. III.

4. Unrestrained

5. Material Properties

The materials used were the superalloys Rene' 41, Hastelloy X, and HS-25. Material properties are given in Section I, Vol. I, Appendix II, pages 123-147.

6. Temperature Distribution

Temperature distributions are shown in Table 84, "Heat-Load Panels Thermocouple Data," p. 726, Vol. III.

7. Experimental Data

Vol. III, Table 85, "Heat Load Skin Panels Pressure and Deflection Results"

Table 86, "Test to Failure-Heat-Load Panels"

Figure 381, "Pressure and Deflection Results - Rene' 41 Zee-Edge Panel-Test to Failure."

Figures 383 through 395 show modes of failure.

8. Comparisons to Theory

None attempted.

9. Comments

Only the heat-load panel tests have been selected for this report.

S39. TEST OF F8U-3 HORIZONTAL STABILIZER UNDER THERMAL AND APPLIED LOADS

1. Reference 21-125, Table XII and Table XVI of Appendix A, Gehring, R. W., C. H. Maines, E. Alter and J. A. Lumm, "Application of Applied Load-Ratio Static Test Simulation Techniques to Full-Scale Structures; Vol. I - Methods of Analysis and Digital Computer Programs; Vol. II - Material Properties Studies and Evaluation; Vol. III - Experimental Program; Vol. IV - Summary of Results, Conclusions and Recommendations." North American Aviation, Columbus, Ohio. Vol. I Dec. 31, 1965, Vol. II Jan. 15, 1966, Vol. IV Aug. 31, 1966. NAEC-ASL 1094.

2. Summary of Tests

Part I tests producing bending failures in outboard structure of stabilizer (Vol. III, page 8):

Test 1. Room temperature

Test 2. Elevated temperature surveys at 250°F symmetrical and unsymmetrical, 425°F symmetrical and unsymmetrical.

Test 3. 250°F, symmetrical

Test 4. 425°F, symmetrical

Test 5. 250°F, unsymmetrical

Test 6. 425°F, unsymmetrical

Part II tests producing failure in inboard splice-joint of stabilizer:

Test 7. Room temperature

Test 8. Temperature surveys for same temperature conditions as in Test 2.

Test 9. 250°F, symmetrical

Test 10. 425°F, symmetrical

Test 11. 250°F, unsymmetrical

Test 12. 425°F, unsymmetrical

3. Geometry

Vol. I, Figures 5.1-5.6, 5.10-5.12, Tables 5.1-5.3, 5.6-5.8; Vol. III, strain gages and thermocouples, Figs. 14, 15, 16; Vol IV, Fig. 4.1.

4. Restraints

Cantilever beam.

5. Material Properties

The materials used were 7079-T6 aluminum alloy, AZ31B-H24 magnesium alloy, and stainless steel. Data given in Vol. II.

Tensile Test Data

Aluminum (7079-T6)

Table 3.1 - Room temperature
Table 3.2 - 250°F
Table 3.3 - 300°F
Table 3.4 - 350°F
Table 3.5 - 400°F
Table 3.6 - 450°F
Table 3.7 - 500°F

Magnesium (AZ31B-H24)

Table 3.8 - Room temperature
Table 3.9 - 250°F
Table 3.10 - 300°F
Table 3.11 - 350°F
Table 3.12 - 400°F
Table 3.13 - 450°F

Fig. 3.8, "Tensile Yield Strength at Various Temperatures Versus Larson-Miller Parameter for Elevated Temperature Exposure, 7079-T6 Aluminum Alloy Bare Plate."

Fig. 3.9, "Tensile Ultimate Strength at Various Temperatures Versus Larson-Miller Parameter for Elevated Temperature Exposure, 7079-T6 Aluminum Alloy Bare Plate."

Fig. 4.1, "Tensile and Compressive Yield Strength at Temperature AZ31B-H24 Magnesium Alloy."

Fig. 4.2, "Tensile Ultimate Strength at Temperature, AZ31B-H24 Magnesium Alloy."

Fig. 4.3, "Modulus of Elasticity Values for Horizontal Stabilizer Materials."

Values for the stainless steel elements were taken from Mil-HDBK-5.

6. Temperature Distributions

Some typical temperature distributions are given in Vol. IV: Table 2.1 for part of Test 6, Tables 2.4-2.11 for Test 10.

Temperatures for test 3, 4, 5, 6 are given in Appendix B of this report.

7,8. Experimental Data and Comparisons to Theory

Volume IV., Fig. 4.2, Load Deformation Curve - Room Temperature

Fig. 4.3, Load Deformation Curve - 250°F, Symmetrical

Fig. 4.4, Load Deformation Curve - 250°F, Unsymmetrical

Fig. 4.5, Load Deformation Curve - 425°F, symmetrical

Fig. 4.6, Load Deformation Curve - 425°F, unsymmetrical

Fig. 4.7, Ultimate Bending Moment versus Span, Room temperature

Fig. 4.8, Ultimate Bending Moment versus Span, 250°F, symmetrical

Fig. 4.9, Ultimate Bending Moment versus Span, 250°F, unsymmetrical

Fig. 4.10, Ultimate Bending Moment versus Span, 425°F, symmetrical

Fig. 4.11, Ultimate Bending Moment versus Span, 425°F, unsymmetrical

Fig. 4.12, Comparison of Test and Calculated Deflections, Part I

Fig. 4.13, Comparison of Test and Calculated Deflections, Part I

Table 5.1, Cross Section Failure and Applied Load Ratio Comparison

Table 5.2, Per Cent Deviation of Analysis Results from Test Ultimate Load, Part I

Table 5.3, Bending Moment Comparison at Test Failure Station, Part I.

Table 5.4, Summary of Results, Part II

Table 6.1, Test-Analysis Summary for Example Procedure - Part I

Table 6.2, Test-Analysis Summary for Example Procedure. Part II.

9. Comments

Comparisons of test strain data and theoretical calculations in the subject report NAEC-ASL 1094 were made for combined load and temperation cases (see Figs. 4.3-4.6 in Vol. IV). Since the temperature was applied first and strain data was recorded in the tests at various loads, including approximately zero load, it is possible to make a comparison of theoretical and measured strains for the temperature alone on the stabilizer. As this was not done in the subject report, it has been added to this report as Appendix B.

See S25 above for another application of the theory used in the subject report NAEC-ASL 1094.

S40. THERMAL STRESSES IN FLAT RINGS BY THE MOIRÉ METHOD

1. Reference 21-128, Table VII and Table XVI of Appendix A, Sciammarella C. A., and D. Sturgeon, "Thermal Stresses at High Temperatures in Stainless Steel Rings by the Moiré Method," Experimental Mechanics, Vol. VI, No. V, May, 1966, p. 235-243.

2. Summary of Tests

An extension of the Moiré method of strain analysis to temperatures up to 1600°F.

3. Geometry

Specimen No.	Thickness	ID	OD
1	1.0"	2.50"	5.50"
2	1.0"	0.50"	5.50"

4. Unrestrained

5. Material Properties

Garofalo, F., Malenock, P. R., and Smith, G. V., "The Influence of Temperature on the Elastic Constants of some Commercial Steels," ASTM Symposium on Elastic Constants, STP No. 129, p. 11, 1952.

Haythorn, P. A., "Steel Metals for High Temperature Service," Iron Age, 162, p. 92, Sept. 23, 1948.

Fig. 11.

6. Temperature Distributions

Ring No. 1 - Fig. 7

Ring No. 2 - Fig. 8

7,8. Experimental Data and Comparisons to Theory

Fig. 12 - Thermal Strains in Ring No. 1.

Fig. 13 - Thermal Stresses in Ring No. 1.

Fig. 14 - Thermal Strains in Ring No. 2.

Fig. 15 - Thermal Stresses in Ring No. 2.

Fig. 16 - Thermal Stress in Ring No. 2 computed under the incompressibility assumption.

9. Comments

The report is an extension of earlier work dealing with methods and techniques of the Moiré method at elevated temperatures. The results show this method can give good data up to 1600°F. See S22 above.

APPENDIX A

SUPPLEMENT TO LITERATURE SURVEY AND EVALUATION SECTION IN AFFDL-TR-66-67

This appendix has been prepared to supplement Section II of Report AFFDL-TR-66-67, Gatewood B. E., A. R. Glazer, and B. H. Ulrich, "Development of Experimental Testing Programs to Verify Thermal Stress Analysis," The Ohio State University, June, 1966. The appendix continues the literature survey and evaluation of Section II by adding references surveyed since the publication of the original report. Only reports containing thermal stress experimental data are included in this appendix.

The numbering system used for the additional references is a continuation of that which was used in the original report. The first entry is number 21-99.

The tables in the appendix are continuations of the tables in paragraphs 2.3 and 2.4 of the original report. Tables II, IV, VIII, and X have no entries from the additional references and have been omitted from the appendix.

21- 99 Emery, A. F., C. F. Barrett, and A. S. Kobayashi, "Temperature Distributions and Thermal Stresses in Partially Filled Annulus," Experimental Mechanics, Vol. 6, No. 12, December, 1966.

21-100 Rothestein, R. J., and W. F. Kirkwood, "Photothermoelastic Analysis of Stresses in Multiconnected Flat Circular Rings," Society for Experimental Stress Analysis-Proceedings, Vol. 21, No. 2, 1964, p. 237-243.

21-101 Brown, D. A., "Evaluation of Thermal Stress Resistance in Potential Radome Materials, Final Report," Stanford Research Institute, Menlo Park, California, February 15, 1965, p. 46, AD 613009.

21-102 Ross, B., "An Analog Study of the Thermal Buckling Behavior of Thin Cylindrical Shells," Stanford University, California, April, 1965, AFOSR 65-1875.

21-103 Singer J., M. Anliker, S. Lederman," Thermal Stresses and Thermal Buckling," Polytechnic Institue of Brooklyn, April, 1957, WADC TR 57-69.

21-104 Savchenko, V. I., and T. Sh. Chernis, "Detaining Temperature Fields in Flat Models During Investigations by Photothermoelastic Methods," Zavodakaia Laboratoria, Vol. 29, July, 1963, p. 879-880. Industrial Laboratory, December, 1963, p. 941-943 (Translation).

21-105 Kloud, Jan, "Thermal Stresses on Rotor Blades of Internal Combustion Turbines." Zpravodaj Vzlu, Vol. 37, No. 1, 1963, p. 33-38 (in Czech with Summaries in English and Russian).

21-106 Hoff, N. J., and B. Ross, "A New Solution of the Buckling Problem of Thin Circular Shells Heated Along an Axial Strip." AFOSR 65-0005 (Contract AF 49(638)-1776), May, 1965.

21-107 Bendavid, D., and J. Singer, "Thermal Buckling of Conical Shells Heated Along a Generator," Stanford University, California, February, 1966, AFOSR 66-0649.

21-108 Buckens, F., "Dynamic Behavior of Shells Under Thermal Stresses," Louvain University, (Belgium), 1965, AFOSR 66-0898.

21-109 Frisch, J., and W. H. Geidt, "Thermal Stresses During Rapid Transient Heating, Part II; Thermal Strains in Tubes During Transient Heating to 2000°F." University of California Lawrence Radiation Laboratory, Livermore, UCRL 13147, Contract W-7405-Eng. 48), February, 1965.

21-110 Liu, C. T., "Temperature Stresses in the Two Phase Alloy Al-Si," Brown University, Providence, R. I., May, 1964, (Contract AT(30-1)-2394).

21-111 Holland, M., "Thermal Stresses in a Thin Solid Disc," The Engineer, Vol. 221, January 28, 1966, p. 165-168.

21-112 Przemieniecki, J. S., "Alleviation of Thermal Stresses in Bi-Metallic Spar Webs," Aircraft Engineering, Vol. 37, September, 1965, p. 267-272.

21-113 Messner, A. M., and D. R. Scheiessmann, "Transient Thermal Stresses in Solid Propellant Grains," Journal of Spacecraft and Rockets, Vol. 2, No. 4, July-August, 1965, p. 565-570.

21-114 Becker, H., "Effect of Poisson's Ratio on Thermal Stresses," Journal of Applied Physics, Vol. 34, October, 1963, p. 3151-3152.

21-115 Krause, R. B., and W. H. Mahaffey, "Correlation of Visco-elastic Behavior with Model Thermal Testing," AIAA Journal, Vol. 1, October, 1963, p. 2320-2324.

21-116 Sampson, R. C., "Three-Dimensional Photoelastic Method for Analysis of Differential Contraction Stresses," Experimental Mechanics, Vol. 3, October, 1963, p. 225-235.

21-117 Mielke, L. G., and T. F. MacLaughlin, "Thermal Stresses Arising in Gun Tubes During Repetitive Firing," Army Conference of Dynamic Behavior of Materials and Structures Proceedings, Springfield, Mass., September, 26-28, 1962.

21-118 Orlos, Z., and Z. Dylag, "Photoelastic Investigation of Stress Strain States Caused by Thermal Loads," Rozprawy Inzynierskie, Vol. II, No. 2, 1963, p. 335-349. (In Polish).

21-119 Durelli, A. J., and V. J. Parks, "Thermal Stresses at the Closed End of the Em-1 Vessel, Phase II, Final Report," Catholic University of America, Washington, D. C., April, 1963 (Restricted Distribution).

21-120 Nardo, S. V., and J. E. Flanerty, "Temperatures and Stresses in Thick Walled Cylinders and a Comparison with Wind Tunnel Experiments," Polytechnic Institute of Brooklyn, June, 1966, Report No. Pl Bal-926. (Restricted Distribution).

21-121 Zeman, J. L., "Ortlich und Zeitlich Zufalling Verteilte Temperator--und Spannungsfelder." Technische Hochschule, Vienna, Austria, May 4, 1965, AFOSR 66-0659. (In German).

21-122 Kobayashi, A., "Column Creep Buckling Subjected to Arbitrary Non-uniform Temperature Distribution Alongside the Column Length." Transactions of the Japan Society for Aeronautical and Space Sciences, Vol. 8, No. 13, 1965, p. 67-80.

21-123 Breuer, D. W., "Effects of Finite Displacement, Aspect Ratio, and Temperature on Torsional Stiffness of Cantilever Plates," Fourth U. S. National Congress of Applied Mechanics - Proceedings, Vol. I, New York, 1962, p. 475-487.

21-124 Claus, J., D. Meredith, F. Sutch, "Manufacturing Methods for 'Hot Structures'," AMC TR 60-7-795, December 1960, Section I, Vol. I, AD 250-054; Section I, Vol. II, AD 250-750; Section I, Vol. III, AD 251-498 (authors, J. Claus, H. Dillman, F. Sutch) Section II, AMC TR 62-7-795, August 1962, AD 284-188 (authors, J. Claus, W. Seip).

21-125 Gehring, R. W. and C. H. Maines, "Application of Applied Load Ratio Static Test Simulation Techniques to Full-Scale Structures," NAEC-ASL-1094, Vol. I, "Methods of Analysis and Digital Computer Programs." December 1965; Vol. IV, "Summary of Results, Conclusions, and Recommendations," August 1966; Vol. II, "Material Properties Studies and Evaluation," January 1966, authors R. W. Gehring and J. A. Lumm; Vol. III, "Experimental Program," February 1967, author, E. Alter.

21-126 Avery, L. R., G. S. Carayanis, and G. L. Michky, "Thermal Fatigue Tests of Restrained Combustor Cooling Tubes." Experimental Mechanics, Vol. VII, No. 6, June 1967.

21-127 Ross, B., N. J. Hoff, and W. H. Horton, "The Buckling Behavior of Uniformly Heated Thin Circular Cylindrical Shells." Experimental Mechanics, Vol. VI, No. 11, Nov. 1966.

21-128 Sciammarella, C. A., and D. Sturgeon, "Thermal Stresses at High Temperatures in Stainless-Steel Rings by the Moiré Method." Experimental Mechanics, Vol. VI, No. 5, May, 1966.

21-129 Goodier, N. J., and A. L. Florence, "Localized Thermal Stresses at Holes, Cavities, and Inclusions Disturbing Uniform Heat Flow. Thermal Crack Propagation." Stanford Research Ins., Menlo Park, Calif., 1964, AD 647-145.

The following tables identify the structural factors included in each paper in the above Bibliographical list.

TABLE I

A. BEAM CROSS-SECTION ANALYSIS

Reference or test--	21-112	21-123
1. Symmetrical	x	x
2. Unsymmetrical		
3. Thick walls, solid		s
4. Thin wall, open sections		
5. Thin wall, box beam	x	
6. Thin wall, multi-cell box	x	
7. Local buckling, effective areas		x
8. Axial load P_x		
9. Shear load P_z		
10. Moment M_y		
11. Shear load P_y		
12. Moment M_z		
13. Torsion moment M_x		
14. Temperature variation T( )	T(y,z)	T(z)
15. Temperature history T(t)		
16. Temperature cycling		
17. Temperature and load sequencing		
18. Mixed materials	x	
19. Variable elastic properties		
20. Inelastic		
21. Changing stress-strain curves		
22. Strain rate		
23. Creep		

TABLE III

C. BEAM-COLUMNS

Reference or test--	21-102
1. Symmetrical	
2. Unsymmetrical	
3. Thick walls, solid	
4. Thin wall, open section	
5. Thin wall, closed section	
6. Eccentric axial load P_x	x
7. Local buckling, effective areas	
8. Variable section area A(x)	
9. Determinate end restraints	x
10. Redundant end restraints	
11. Intermediate restraints	x
12. Axial load P_x	x
13. Shear P_z	
14. Moment M_y	
15. Shear P_y	x
16. Moment M_z	
17. Torsion moment M_x	
18. Temperature variation T( )	
19. Temperature transient T(t)	
20. Mixed materials	
21. Variable elastic properties	
22. Inelastic	
23. Torsional instability	
24. Creep	

TABLE V

E. TRUSSES AND FRAMES, BEAM MEMBERS

Reference or Test--	21-124	21-124 Part II
1. Two-dimensional	x	
2. Three-dimensional		x
3. Variable areas of members		
4. Local buckling, effective areas	x	
5. Column buckling of members		
6. Various joint restraints		
7. Temperature uniform change, some members	x	x
8. Temperature T(y,z), cross-section	T(u)	x
9. Temperature T(x), length		x
10. Temperature T(x,y,z)		x
11. Mixed materials		x
12. Variable elastic properties	x	
13. Inelastic members		

TABLE VI

F. BEAM-CYLINDERS, PLANE STRAIN

Reference or test--	21-99	21-100	21-101	21-109
1. Axisymmetrical	x	x	x	x
2. Unsymmetrical				
3. Solid or Thick walls	x	x	x	
4. Variable cross-section area				
5. Temperature T(y,z)	T(r)	T(r)	T(r)	T_u
6. Temperature T(x,y,z)				
7. Surface loads P_n, P_t				
8. Mixed materials				
9. Nonisotropic material				
10. Sandwich material				
11. Variable elastic properties				
12. Inelastic				

TABLE VII

G. PLATES-INPLANE LOADS, NO BUCKLING

Reference or test--	21-103	21-109	21-111	21-114	21-128
1. Constant thickness	x	x	x	x	x
2. Thickness variation t( )	t(y)				
3. Rectangular	x				
4. Circular		x	x	x	x
5. Planview variation s( )					
6. Perforated				x	x
7. Stiffeners					
8. Unrestrained	x	x		x	x
9. Edge restraints			x		
10. Edge loads					
11. Body forces					
12. Temperature variation T( )	T(y)	T(r)	T(r)	T(xy)	T(r)
13. Temperature transient T(t)					
14. Nonisotropic					
15. Sandwich					
16. Variable elastic properties					x
17. Inelastic					
18. Creep					

TABLE IX

I. PLATES, INPLANE AND BENDING

Reference or test--	21-103	21-105
1. Constant thickness	x	
2. Thickness variation t( )		t(xy)
3. Rectangular	x	
4. Circular		
5. Planview variation s( )		
6. Perforated		
7. Stiffeners		
8. Cantilever		x
9. Edge supports		
10. Edge moments		
11. Transverse loading P_z		x
12. Temperature variation T( )		T(xyz)
13. Temperature transient T(t)	x	
14. Nonisotropic		
15. Sandwich		
16. Variable elastic properties		
17. Inelastic		
18. Creep		
19. Body forces		
20. Buckling	x	
21. Large deflections		
22. Von Karman equations		

TABLE XI

K. AXISYMMETRIC SHELLS, NO BUCKLING

Reference or test--	21-113	21-115	21-116
1. Variable thickness 2. Plate element representation 3. Truss representation 4. Ring representation 5. Harmonic representation	x	x	x
6. Axisymmetrical loading 7. Unsymmetrical loading 8. Temperature (axisymmetric) 9. Temperature (unsymmetrical) 10. Nonisotropic	x x	 T_u	 T_u
11. Sandwich 12. Mixed materials 13. Composites 14. Variable elastic properties 15. Inelastic	x	x x	x

TABLE XII

L. STRUCTURAL ASSEMBLY, BEAMS AND PLATES

Reference or test--	21-125
1. Beam and plate element representation	x
2. Truss representation	
3. Local buckling, effective areas	x
4. Various restraints	
5. Cut-outs	
6. General loading	x
7. Temperature T(x,y,z)	x
8. Mixed materials	x
9. Nonisotropic	
10. Composites	
11. Variable elastic properties	x
12. Inelastic	x

TABLE XIII

M. JOINTS

Reference or test--	21-124
1. Concentrated tension load	x
2. Concentrated compression load	x
3. Thin sheet butt joint	
4. Thin sheet lap joint	
5. Shear joints	x
6. Diagonal tension, shear buckling	
7. Temperature T(x,y)	T(u)
8. Mixed materials	
9. Variable elastic properties	x
10. Inelastic	
11. Bolted	x
12. Riveted	
13. Welded	
14. Bonded	
15. Eccentric loading	x

TABLE XIV

N. SHELLS, BUCKLING INCLUDED (Fig. 4)

(not covered in this contract)

21-106
21-107
21-108

O. THREE-DIMENSIONAL SOLIDS (Fig. 5)

(not covered in this contract)

21-110

Each paper on experimental data is evaluated in a special Table XVI including factors involved in the testing.

TABLE XVI

EVALUATION OF TEST DATA

Reference No.--	21-99	21-100	21-101	21-102	21-103	21-103	21-104	21-105	21-106	21-107	21-108
1. Problem class	F	F	F	C	G	I	G	I	N	N	N
2. Table identification	VI	VI	VI	III	VII	IX	VII	IX	XIV	XIV	XIV
3. Specific structure								x			
4. Failure only			x			x		x	x	x	
5. Temperature measured	x	x				x	x		x	x	x
6. Deflections measured				x		x					
7. Frequencies measured											
8. Mode shapes measured											x
9. Strain gages											
10. Photo stress	x	x					x				
11. Extensiometers											
12. Optical strain measurement											
13. Creep, fatigue											
14. Time sequence recording		x				x					
15. Steady state recording	x		x				x		x	x	x
16. Thermal shock			x					x		x	
17. Correlation with theory good	x	x		x			x				
18. Correlation with theory poor											
19. Test accepted over theory	x	x		x			x		x	x	
20. Theory accepted over test						x					
21. Data useful to verify analysis	x	x				?	x				
22. Data not useful			x	x	x			x	x	x	x
23. Correlate data with Reference											

TABLE XVI (Cont'd)

Reference No.--	21-109	21-110*	21-111	21-112	21-113	21-114	21-115	21-116	21-123	21-124	21-124	21-124	21-124 Part II	21-125	21-128
1. Problem class	F	O	G	A	K	G	K	K	A	E	M	G	E	L	G
2. Table identification	VI	XIV	VII	I	XI	VII	XI	XI	I	V	XIII	VII	V	XII	VII
3. Specific structure				x			x	x		x	x		x	x	x
4. Failure only															
5. Temperature measured	x	x	x	x	x		x	x	x	x	x	x	x	x	x
6. Deflections measured							x		x		x	x	x	x	
7. Frequencies measured									x						
8. Mode shapes measured									x						
9. Strain gages	x		x		x								x**	x	
10. Photo stress					x	x		x							x
11. Extensiometers	x						x			x	x		x		
12. Optical strain measurement							x								
13. Creep, fatigue												x			
14. Time sequence recording	x			x	x		x	x		x	x		x	x	
15. Steady state recording		x	x		x	x			x	x		x			x
16. Thermal shock															
17. Correlation with theory good	x		x											x	x
18. Correlation with theory poor		x													
19. Test accepted over theory		x		x	x			x		x	x			x	x
20. Theory accepted over test	x														
21. Data useful to verify analysis	x		x				x		x			x		x	x
22. Data not useful		x		x	x	x	x	x		x	x		x		
23. Correlate data with Reference No.									11-1,21-80						

* X-ray diffraction stress analysis.

**Strain gages used only on room temp. tests.

APPENDIX B

COMPARISON OF THEORETICAL AND EXPERIMENTAL THERMAL STRAINS ON F8U-3 HORIZONTAL STABILIZER

In Ref. 21-125 listed in Appendix A and described in section S39, a good correlation between experimental and theoretical strains was obtained for combined applied and thermal loads on the F8U-3 horizontal stabilizer. Also, excellent correlation was obtained for the failure loads, the location and type of failure, and the deflections. Although strain data was obtained in the tests with temperature applied at zero load, no report of these results is given in the reference 21-125.

The Aeronautical Structures Laboratory of the Naval Aircraft Engineering Center, where the tests were conducted, has furnished the thermal strain data through North American Aviation, Columbus Division, for use of this project. Their release of the data is greatly appreciated.

Figure B-1 shows a plan view of the F8U-3 horizontal stabilizer. Experimental temperature and strain data was obtained at stations 91, 102, 113, and 124 for several temperature conditions (see S39). Load was applied at a former station 135 to apply moments in the test section. Figure B-2 shows a cross section of the stabilizer, typical of each of the four stations 91, 102, 113, and 124, including element and strain gage relative locations. Tables B-I, B-II, B-III, B-IV give the temperatures of the elements at each of the four stations for the four different temperature cases, 250°F symmetrical, 250°F unsymmetrical, 425°F symmetrical, and 425°F unsymmetrical.

The theoretical analysis in Ref. 21-125 was based on a symmetrical cross section, which is satisfactory under large loads. However, for the small strains from temperature alone, and for some unsymmetry in the chordwise temperature distribution, it appears that an unsymmetrical bending analysis is desirable. Table B-V shows a comparison of the strains for the 250°F symmetrical case at station 102 for the symmetrical and unsymmetrical theoretical analyses. At the small strains for this case, it is evident that there is a considerable effect due to the unsymmetry of the temperature in the chordwise direction. Thus, an unsymmetrical bending analysis has been used in the theoretical calculations of this discussion.

Also, there was a small load acting on the stabilizer at the time the thermal strain readings were taken. Table B-V shows the effect on the strain of the -20,097 inch pounds moment acting at station 102 for the temperature case in Table B-I. Although this moment is only about 4% of the failing moment at station 102, it is evident that it produces strains of the order of magnitude of the strains produced by the temperature. These small moments have been included in the calculations

of this discussion in order to have the same input data in the theory as in the test.

Figures B-3 through B-18 show the comparisons of the theoretical calculated strain with the experimental strains under the four temperature conditions at the four stations 91, 102, 113, 124.

Although these same strain gages have very good results at large moments and the same temperatures, it is evident from the figures that in some cases the scatter in the gages may be of the order of the thermal strains being measured. Since a 10°F change in aluminum alloy gives about 130 microinches/inch thermal expansion, and since there may be considerably more than 10°F between the gage temperature and the surface temperature, it would appear that very little correlation should exist between theory and test at small thermal strains in the region less than 1000 microinches/inch. The strain gages were mounted in the skin above the beam flanges (Fig. B-2). However, since the skin is at a different temperature from the beam flange, the strain gage results should probably be compared to the nearest skin theoretical values rather than the beam flange theoretical strains. Note the large difference between beam flange and skin theoretical strains in some cases. The theoretical strains at elements 1, 11, 12, 30 are much larger than at other elements and have not been plotted on the scales used in Figs. B-3 through B-18. Also, strain gage readings larger than the scales used are not shown. The cases in which the experimental and theoretical strains agree reasonably well (such as Figs. B-3a and B-4b) are probably as much a matter of chance as those cases with large disagreements (such as Figs. B-3b and B-6a).

TABLE B-I

TEMPERATURE DISTRIBUTION - 250° SYMMETRICAL, (°F)

Elt. No.	Sta. 91	Sta. 102	Sta. 113	Sta. 124
1	181	181	181	181
2	215	237	240	208
3	223	247	250	213
4	227	251	254	216
5	228	245	245	205
6	213	248	246	222
7	221	254	252	220
8	221	254	254	215
9	226	248	242	206
10	225	218	211	170
11	93	93	93	93
12	93	93	93	93
13	225	218	211	170
14	228	245	245	205
15	227	251	254	216
16	223	247	250	213
17	225	250	244	208
18	220	256	256	217
19	220	256	254	222
20	213	250	248	224
21	215	237	240	208
22	210	249	247	224
23	218	255	253	222
24	218	255	255	217
25	223	249	243	208
26	223	249	243	208
27	218	255	255	217
28	218	255	253	222
29	210	249	247	224
30	181	181	181	181

TABLE B-II

TEMPERATURE DISTRIBUTION - 250° UNSYMMETRICAL

Elt. No.	Sta. 91	Sta. 102	Sta. 113	Sta. 124
1	156	156	156	156
2	226	235	236	227
3	222	250	247	220
4	232	250	247	222
5	225	245	241	208
6	188	214	218	207
7	192	222	222	205
8	198	224	222	199
9	191	215	211	185
10	214	232	228	178
11	94	94	94	94
12	94	94	94	94
13	133	133	135	127
14	155	168	165	137
15	150	163	163	148
16	145	163	164	144
17	170	183	177	156
18	163	183	182	158
19	154	173	172	165
20	161	180	181	170
21	117	126	127	128
22	171	194	196	186
23	169	195	194	183
24	177	199	198	177
25	177	195	190	168
26	177	195	190	168
27	177	199	198	177
28	169	195	194	183
29	171	194	196	186
30	156	156	156	156

TABLE B-III

TEMPERATURE DISTRIBUTION - 425° SYMMETRICAL

Elt. No.	Sta. 91	Sta. 102	Sta. 113	Sta. 124
1	271	282	293	303
2	357	401	400	368
3	348	403	402	361
4	351	403	405	373
5	353	404	403	371
6	341	404	413	383
7	338	402	414	391
8	339	405	413	391
9	348	402	414	386
10	386	388	375	350
11	97	97	97	97
12	96	180	264	348
13	352	382	373	321
14	341	401	410	365
15	344	406	409	367
16	344	406	408	350
17	348	402	418	390
18	336	400	417	406
19	338	402	418	406
20	338	404	417	387
21	350	394	383	297
22	334	400	413	388
23	334	398	415	403
24	336	401	413	403
25	344	398	415	390
26	344	398	415	390
27	336	401	413	403
28	334	398	415	403
29	334	400	413	388
30	271	282	293	303

TABLE B-IV

TEMPERATURE DISTRIBUTION - 425° UNSYMMETRICAL

Elt. No.	Sta. 91	Sta. 102	Sta. 113	Sta. 124
1	185	206	225	246
2	360	413	427	423
3	380	438	445	400
4	430	457	448	383
5	412	450	444	387
6	309	380	398	355
7	323	380	389	352
8	370	399	402	357
9	345	385	395	341
10	369	415	428	341
11	103	103	103	103
12	103	103	103	103
13	200	212	210	190
14	242	280	279	232
15	234	270	270	242
16	232	273	273	240
17	269	302	302	275
18	255	289	289	268
19	239	250	265	272
20	248	292	296	283
21	167	198	204	190
22	273	330	340	314
23	273	306	327	310
24	304	335	343	311
25	300	336	345	305
26	300	336	345	305
27	304	335	343	311
28	273	306	327	310
29	273	330	340	314
30	185	206	225	246

TABLE B-V

COMPARISON OF ANALYTICAL STRAINS AT STA. 102 - 250°
SYMMETRICAL TEMPERATURE DISTRIBUTION

Elt. No.	Symmetrical Cross-Section Analysis	Unsymmetrical Cross-Section Analysis	Unsymmetrical Analysis with -20,097 in.lb Moment
1	1200	1749	1692
2	- 197	29	- 204
3	- 23	22	- 274
4	- 75	- 86	- 413
5	2	- 63	- 357
6	- 36	39	- 162
7	- 114	- 94	- 369
8	- 114	- 153	- 427
9	- 36	- 131	- 318
10	87	- 16	- 203
11	1979	1690	1640
12	1980	1691	1742
13	89	- 14	172
14	5	- 60	232
15	- 72	- 82	245
16	- 20	25	323
17	- 60	- 155	31
18	- 137	- 176	98
19	- 137	- 117	157
20	- 59	15	216
21	- 194	32	266
22	- 48	26	- 88
23	- 126	- 106	- 252
24	- 126	- 165	- 311
25	- 48	- 143	- 254
26	- 47	- 142	- 31
27	- 125	- 163	- 17
28	- 125	- 105	40
29	- 47	27	142
30	1201	1750	1807

Strain in microinches/inch

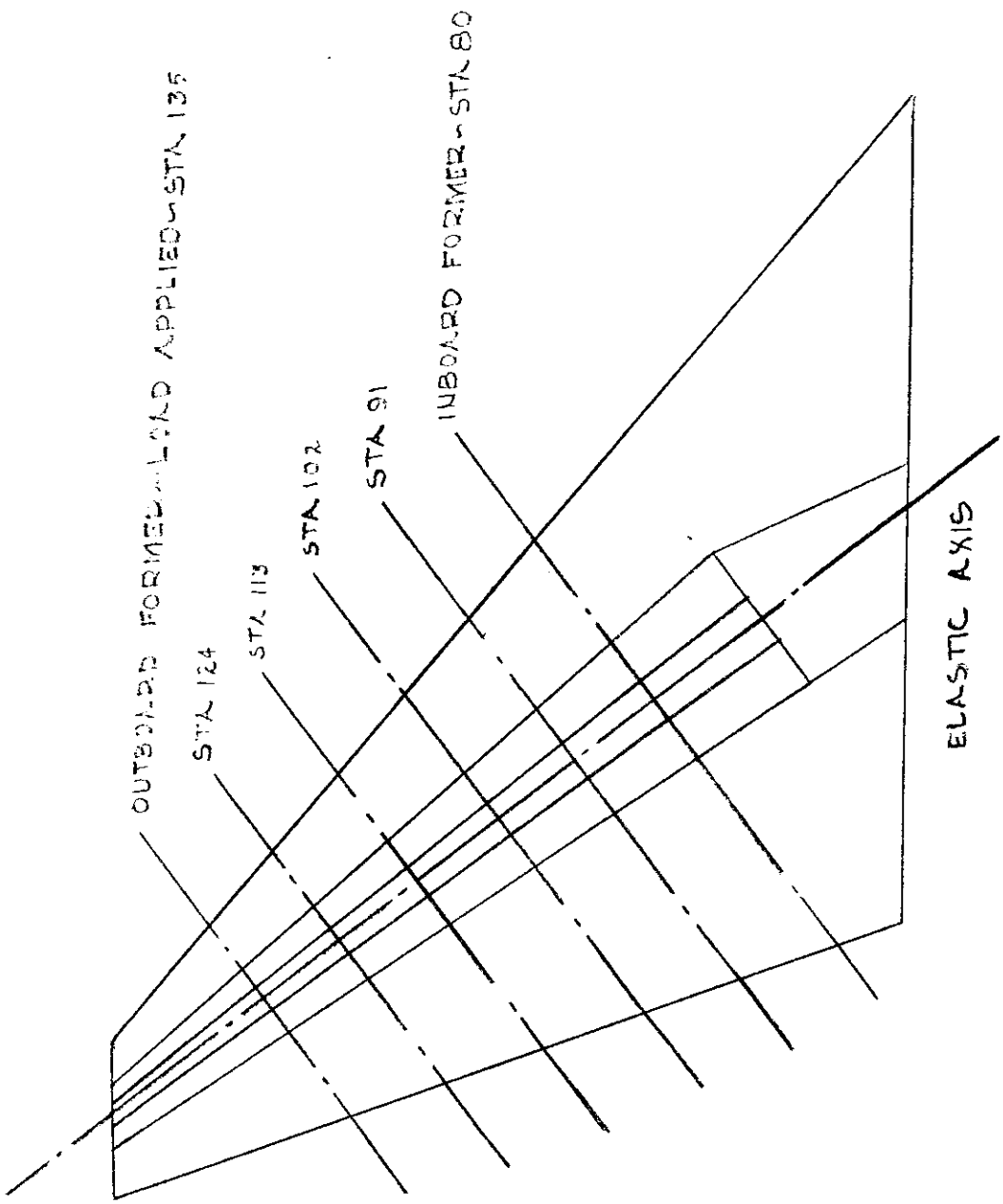

Figure B-1. - Planview F8U-3 horizontal stabilizer

Element Description

(1) & (30) Stainless steel leading edge

(2), (10), (13), & (21) Magnesium alloy forward and aft box skins

(3), (4), (5), (14), (15), & (16) 7079-T6 aluminum alloy main box skins

(6), (7), (8), (9), (17), (18), (19), & (20) 7079-T6 aluminum alloy beam flanges

(11) & (12) 7075-T6 aluminum alloy trailing edge honeycomb facings

(22), (23), (24), (25), (26), (27), (28), & (29) 7079-T6 aluminum alloy beam webs

(1A) (2A) (3A) (4A) Upper Skin Strain Gages

(1B) (2B) (3B) (4B) Lower Skin Strain Gages

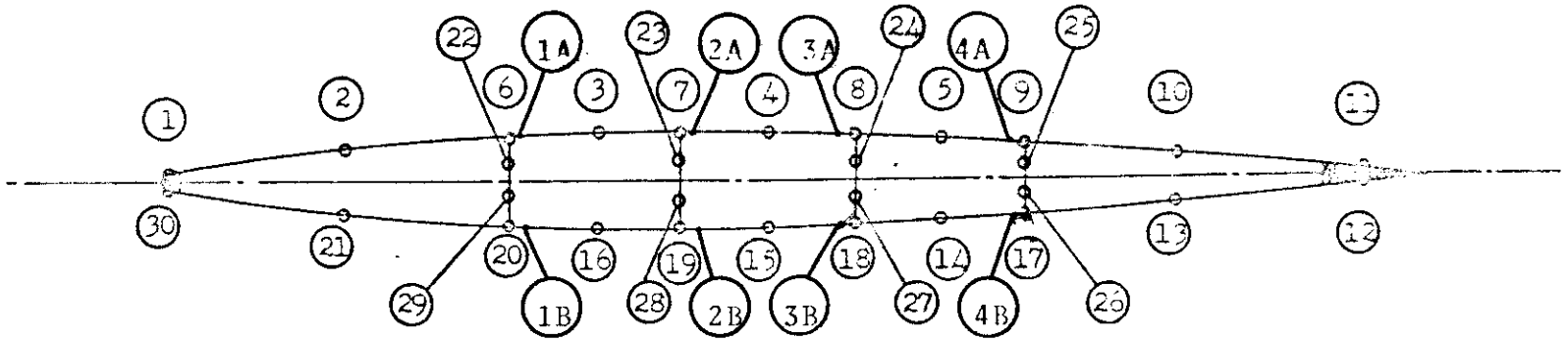

Figure B-2. - Cross-section of stabilizer

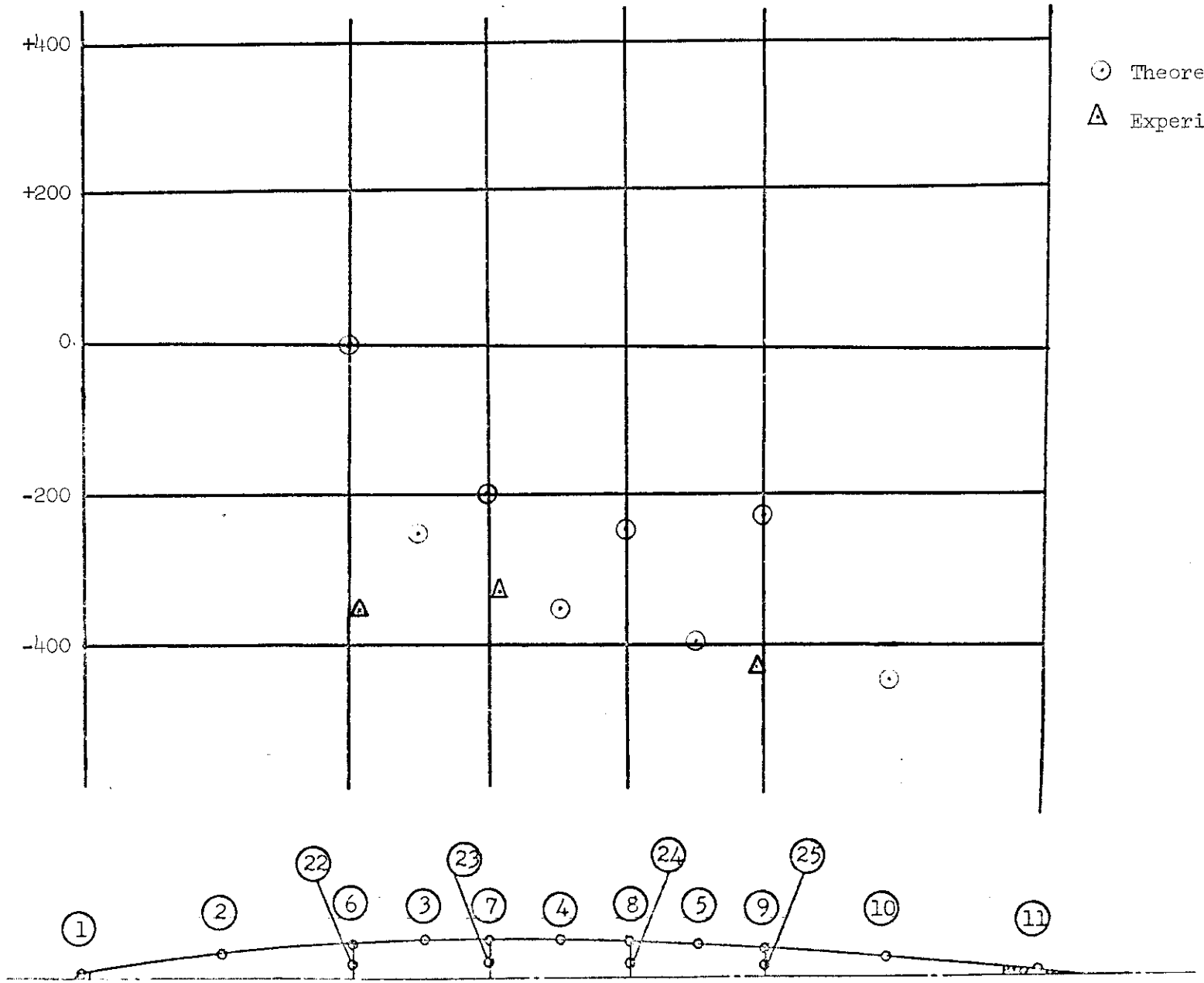

Figure B-3a. - Sta. 91 - 250° symmetrical - upper skin

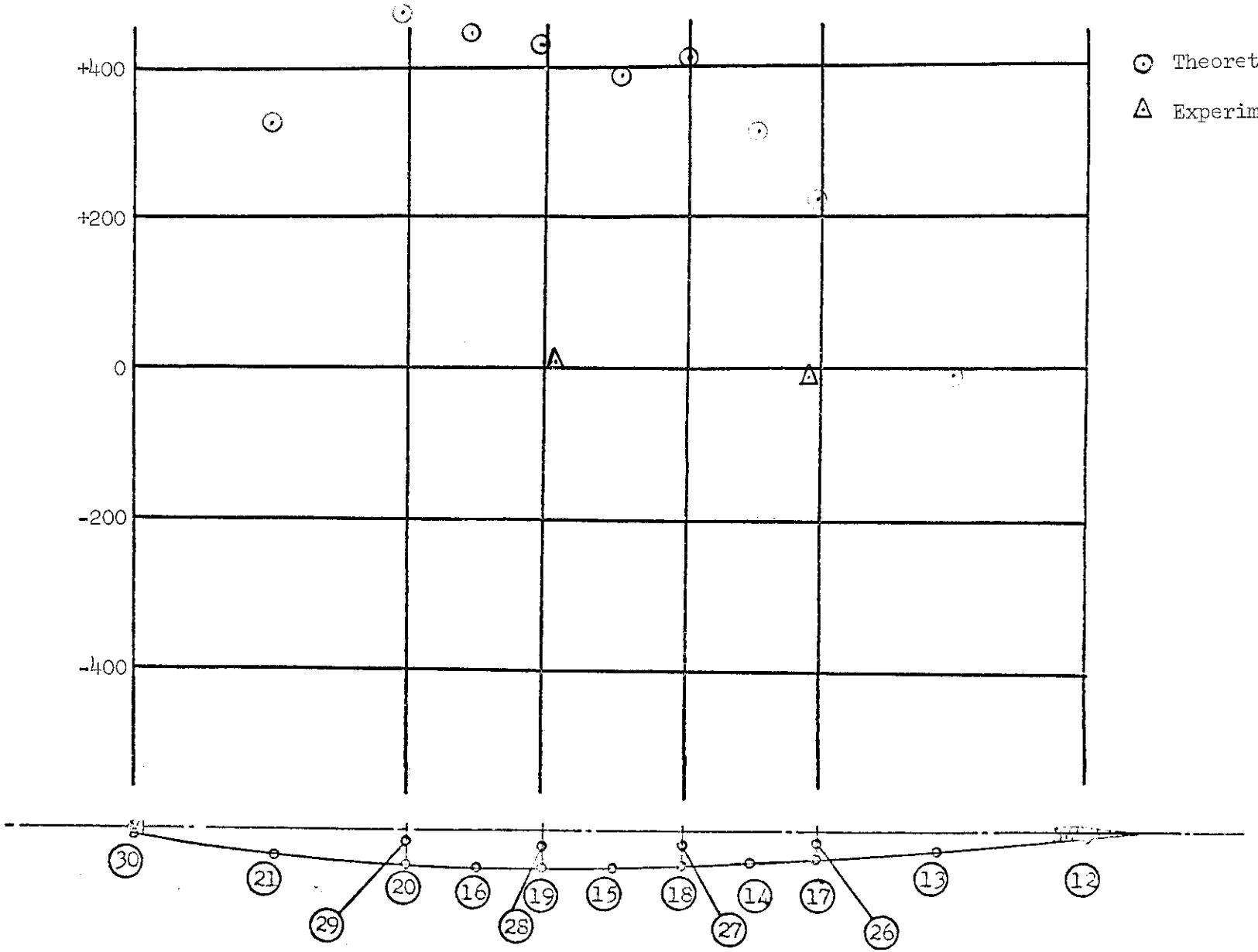

Figure B-3b. - Sta. 91 - 250° symmetrical - lower skin

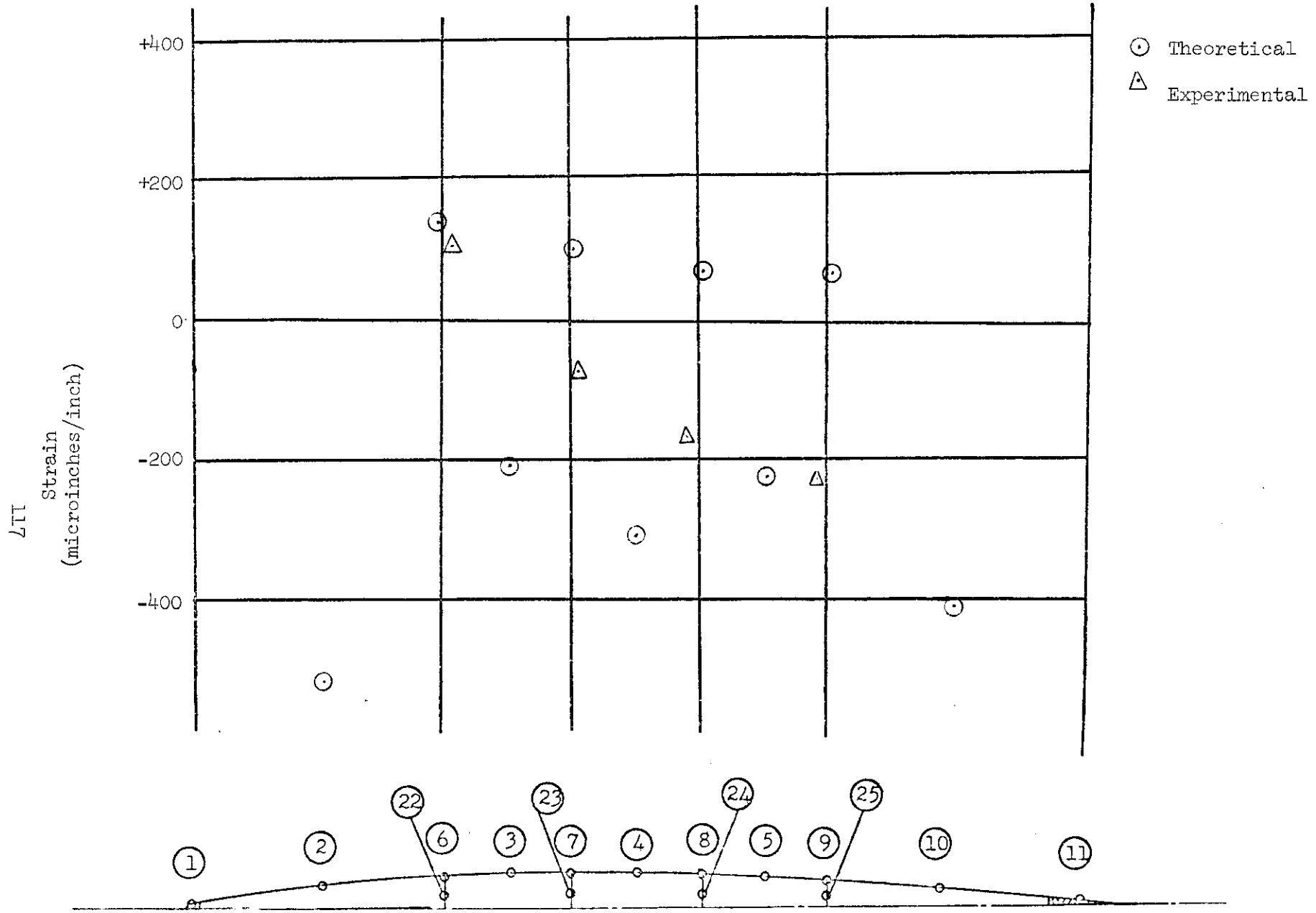

Figure B-4a. - Sta. 91 - 250° unsymmetrical - upper skin

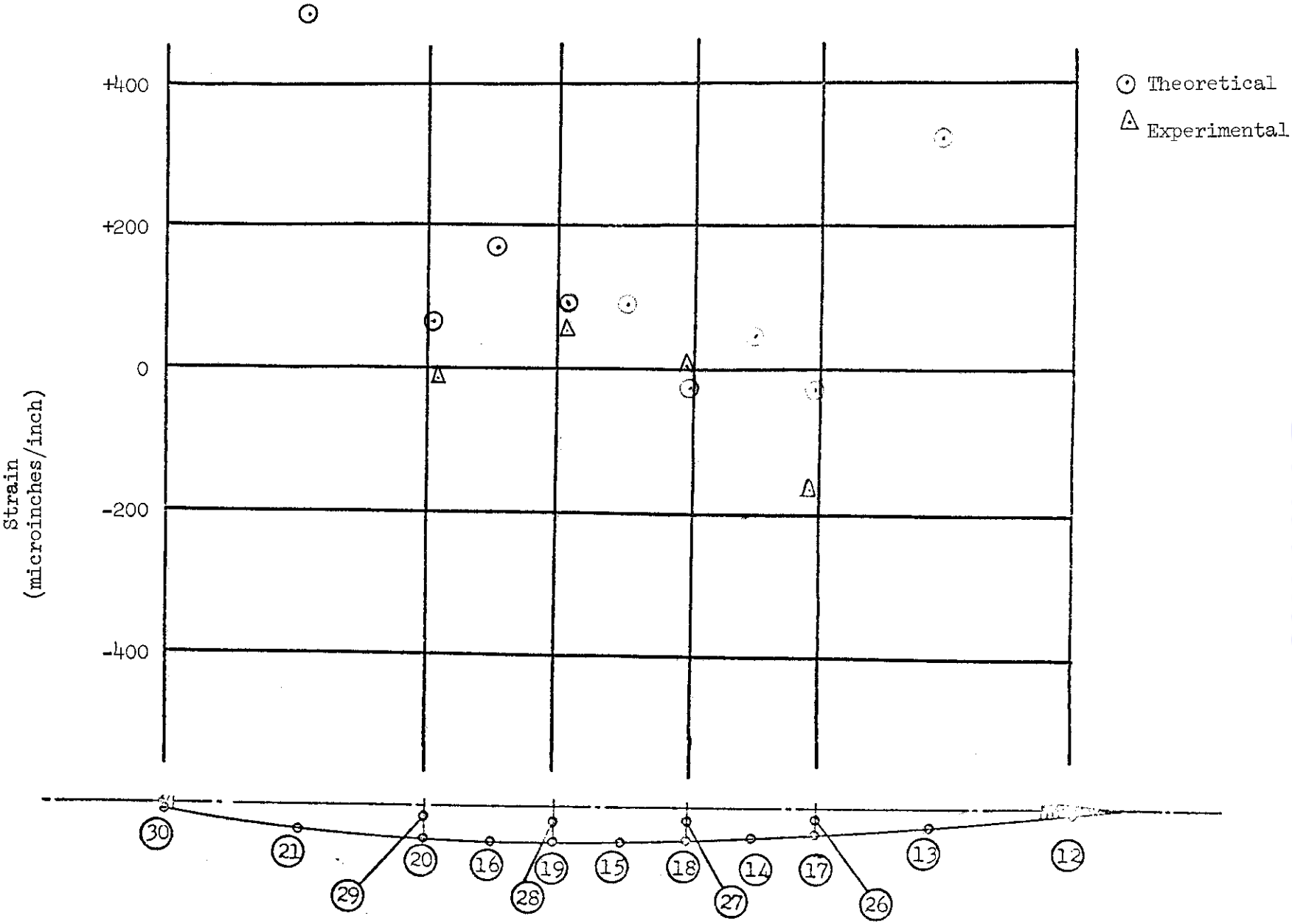

Figure B-4b. - Sta. 91 - 250° unsymmetrical - lower skin

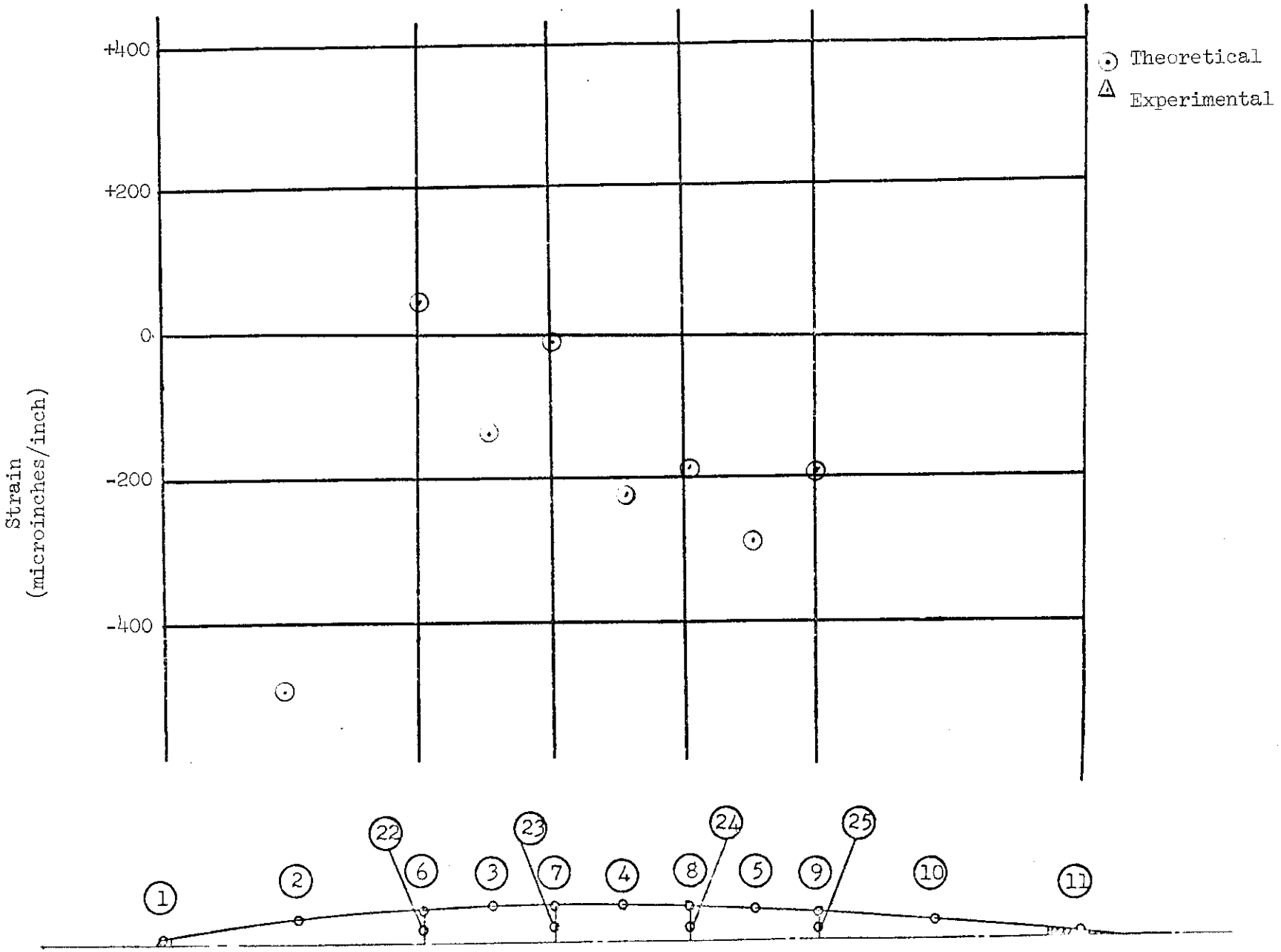

Figure B-5a. - Sta. 91 - 425° symmetrical - upper skin

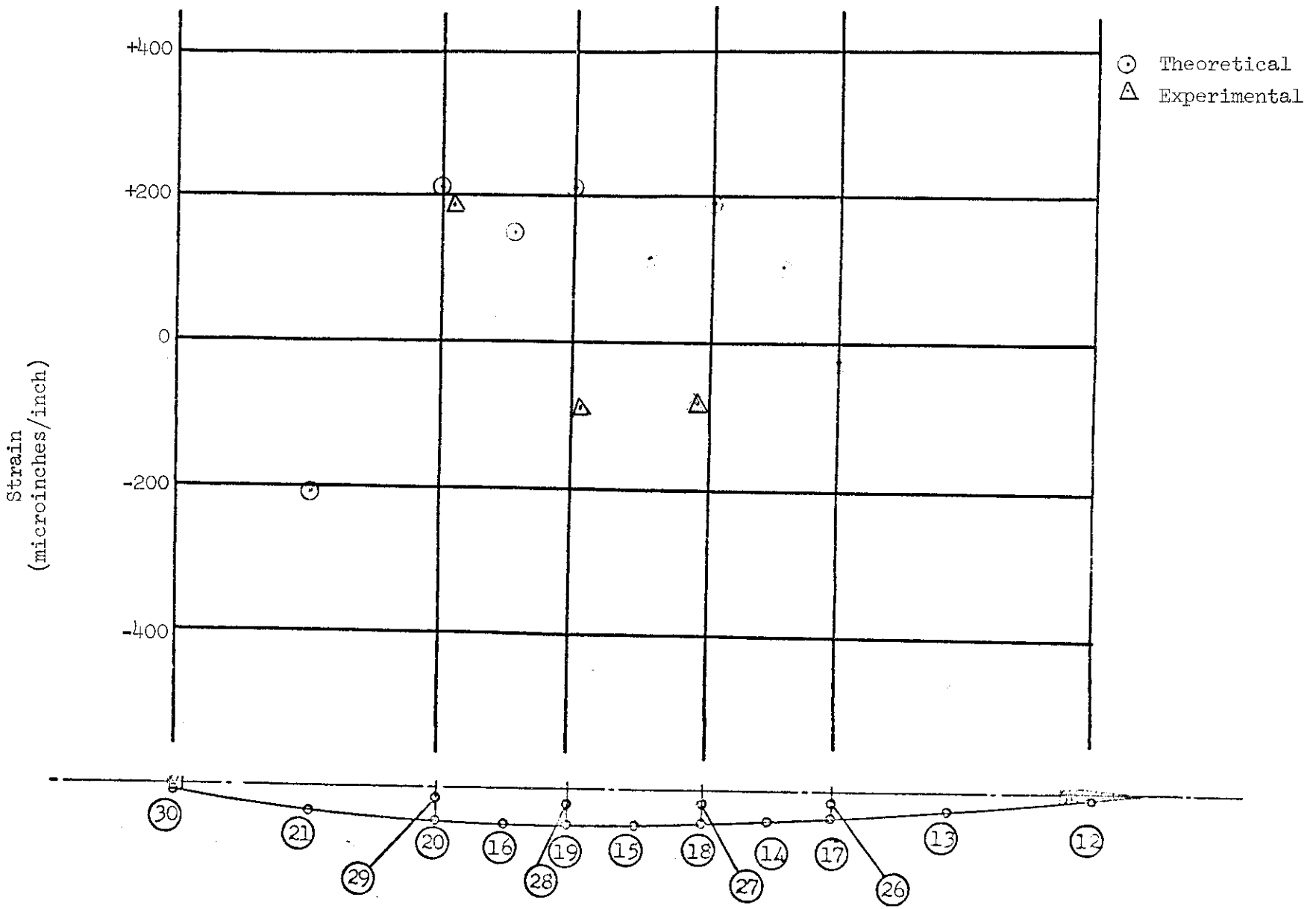

Figure B-5b. - Sta. 91 - 425° symmetrical - lower skin

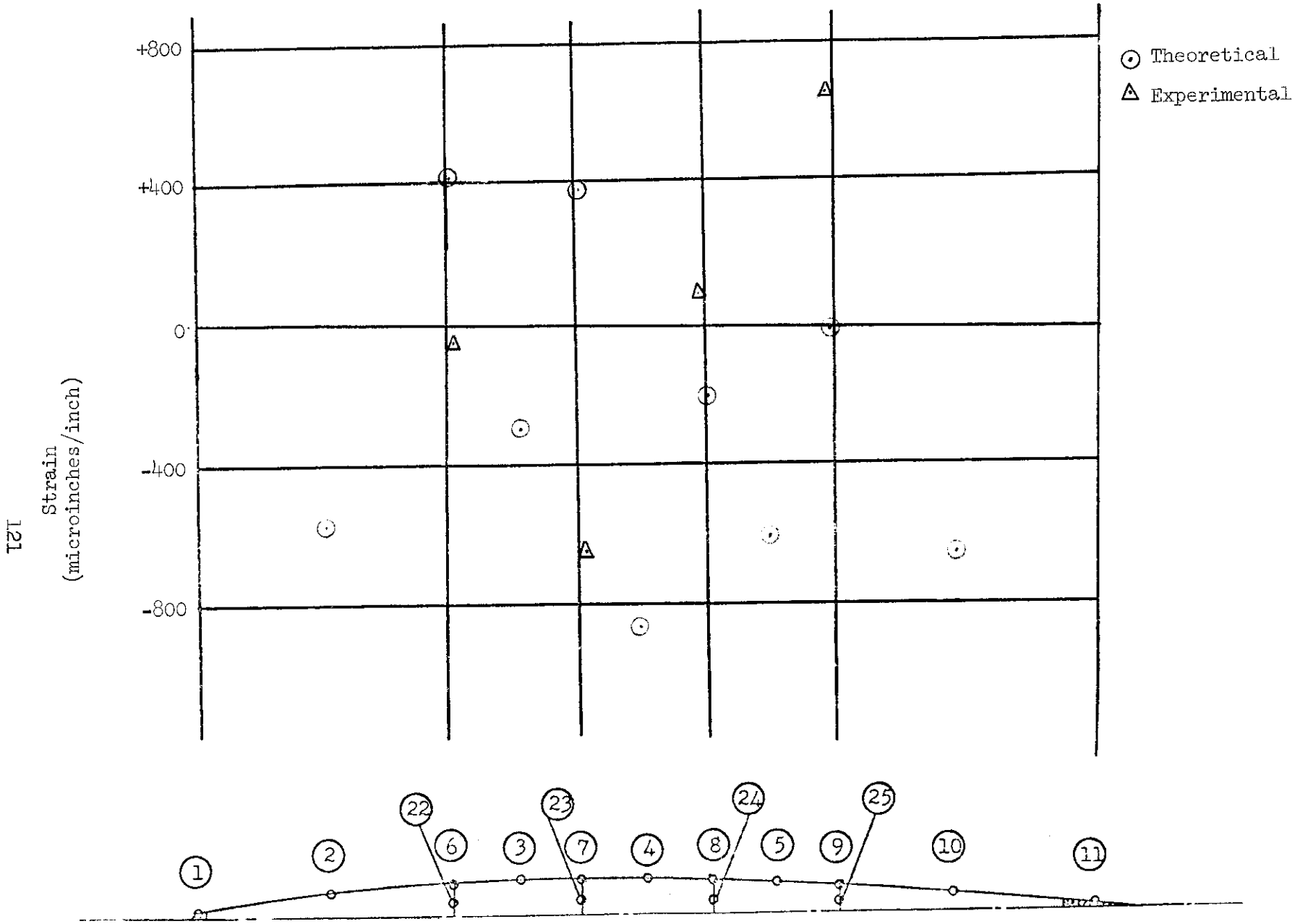

Figure B-6a. - Sta. 91 - 425° unsymmetrical - upper skin

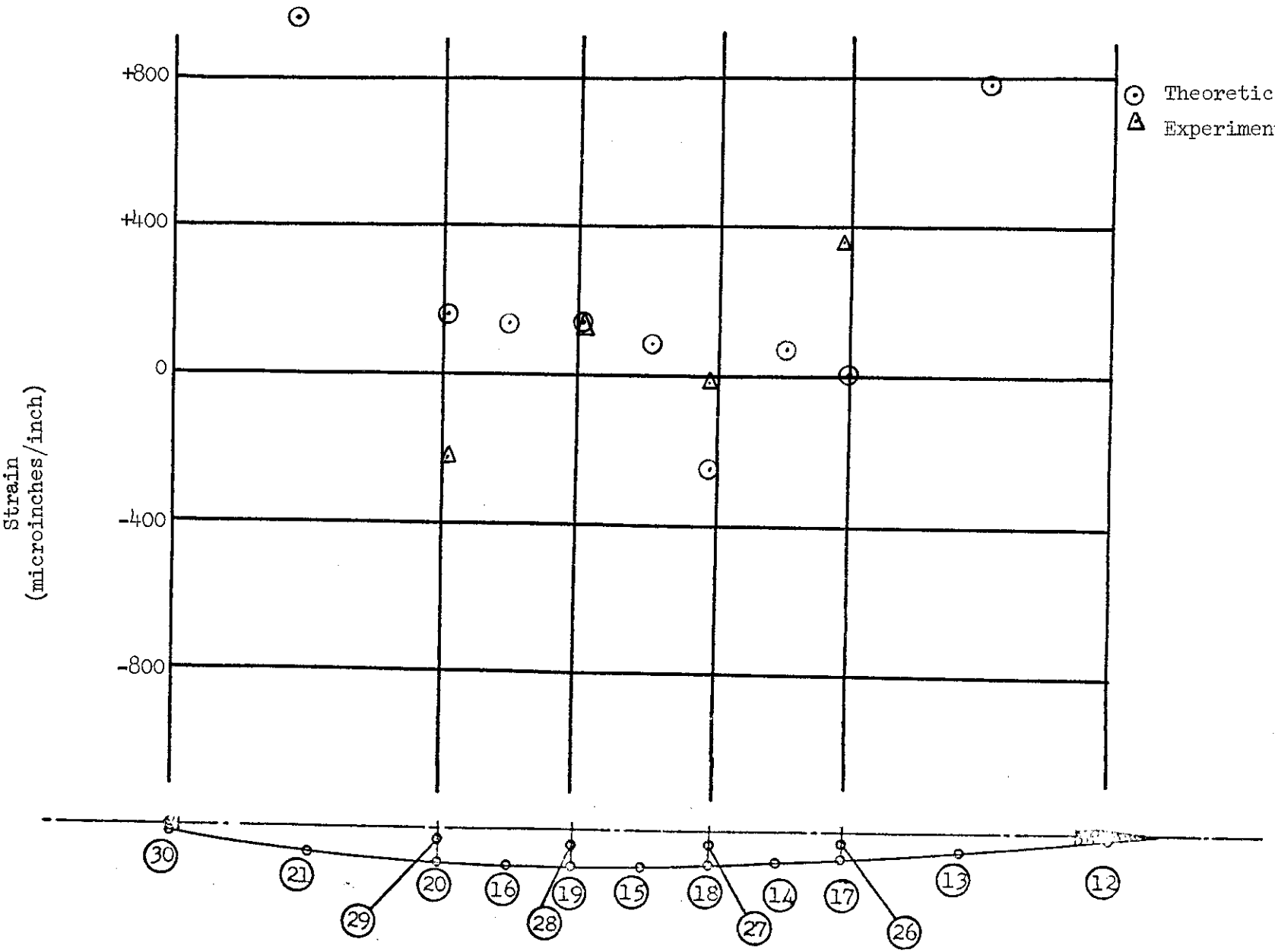

Figure B-6b. - Sta. 91 - 425° unsymmetrical lower skin

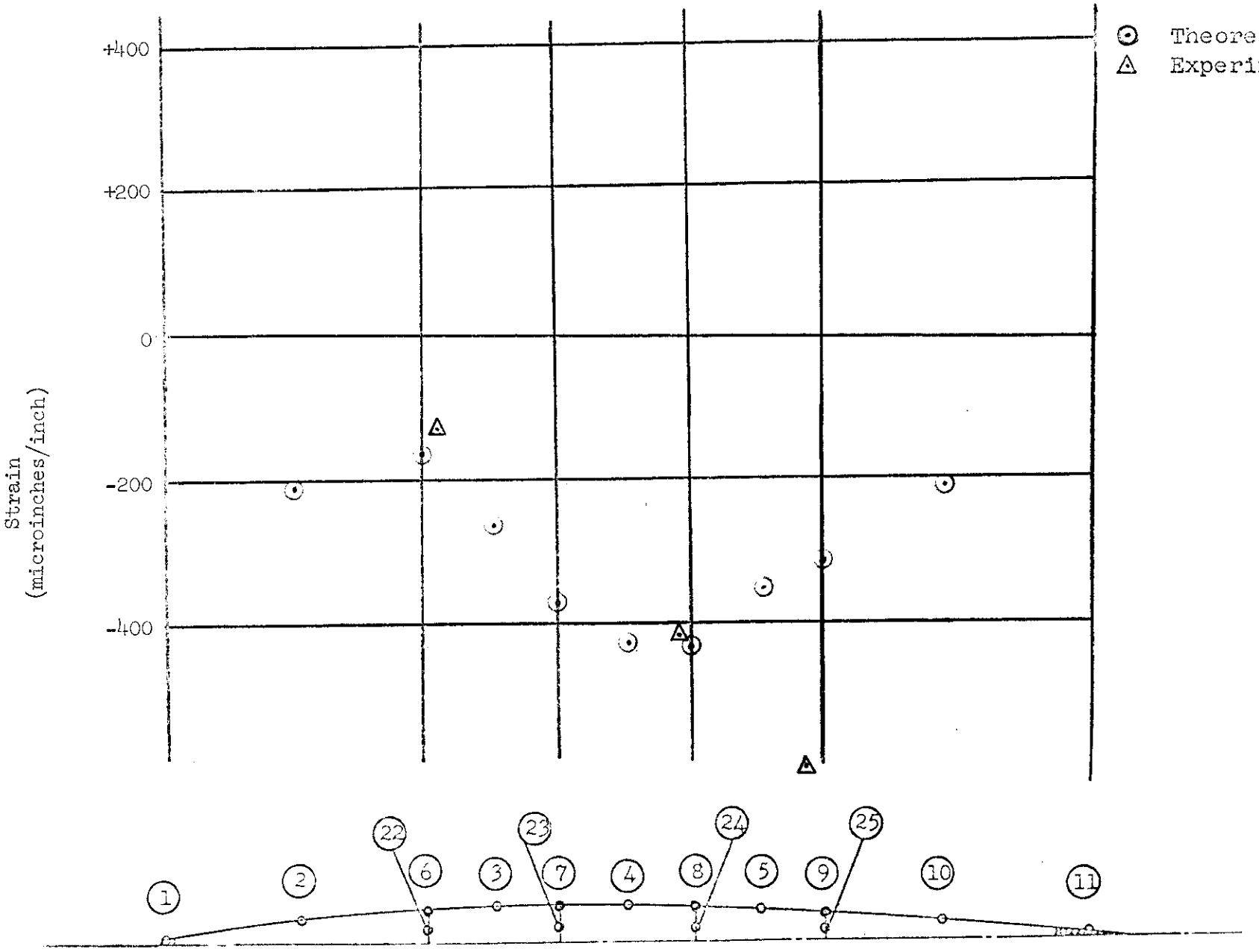

Figure B-7a. - Sta. 102 - 250° symmetrical - upper skin

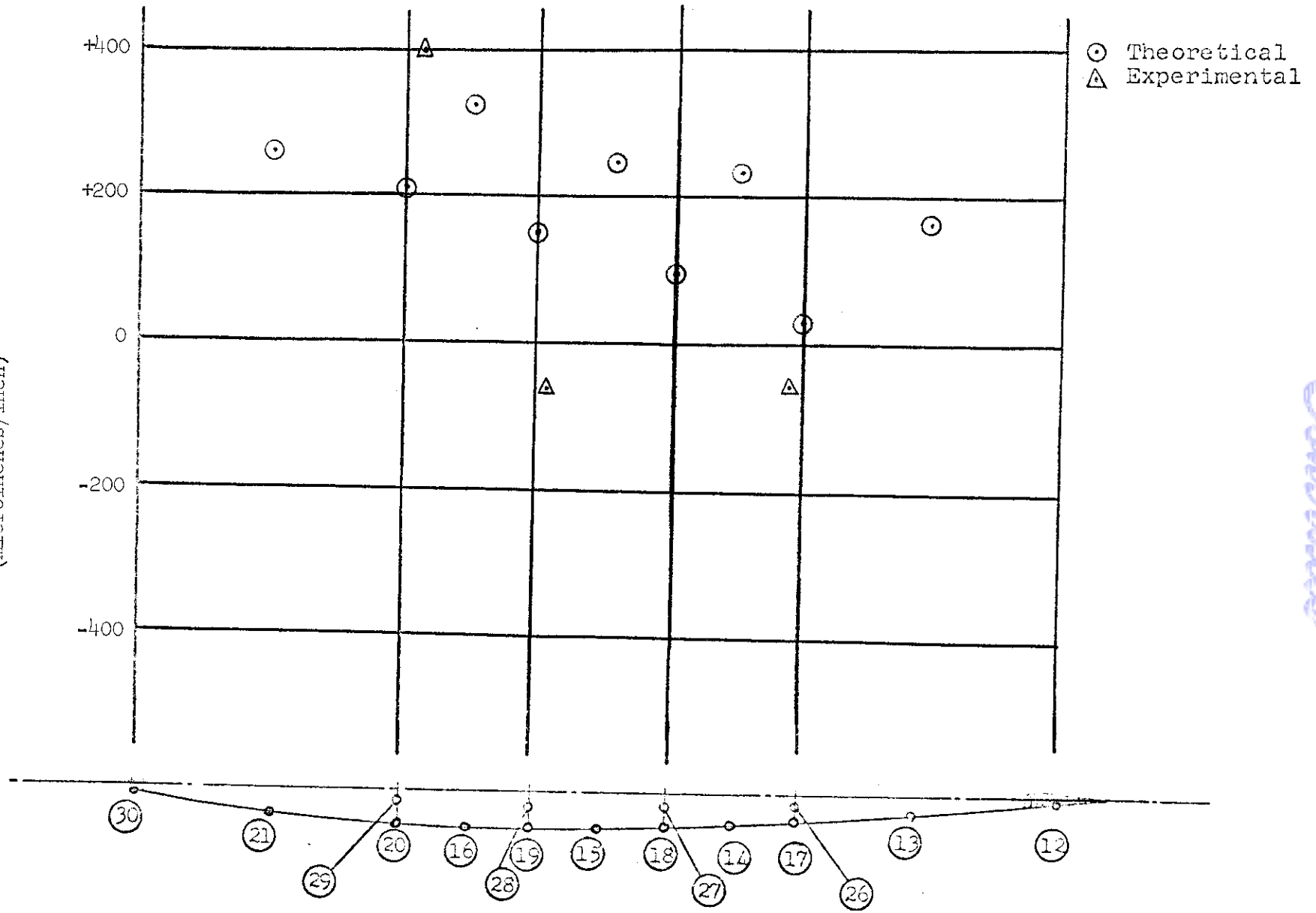

Figure B-7b. - Sta. 102 - 250° symmetrical - lower skin

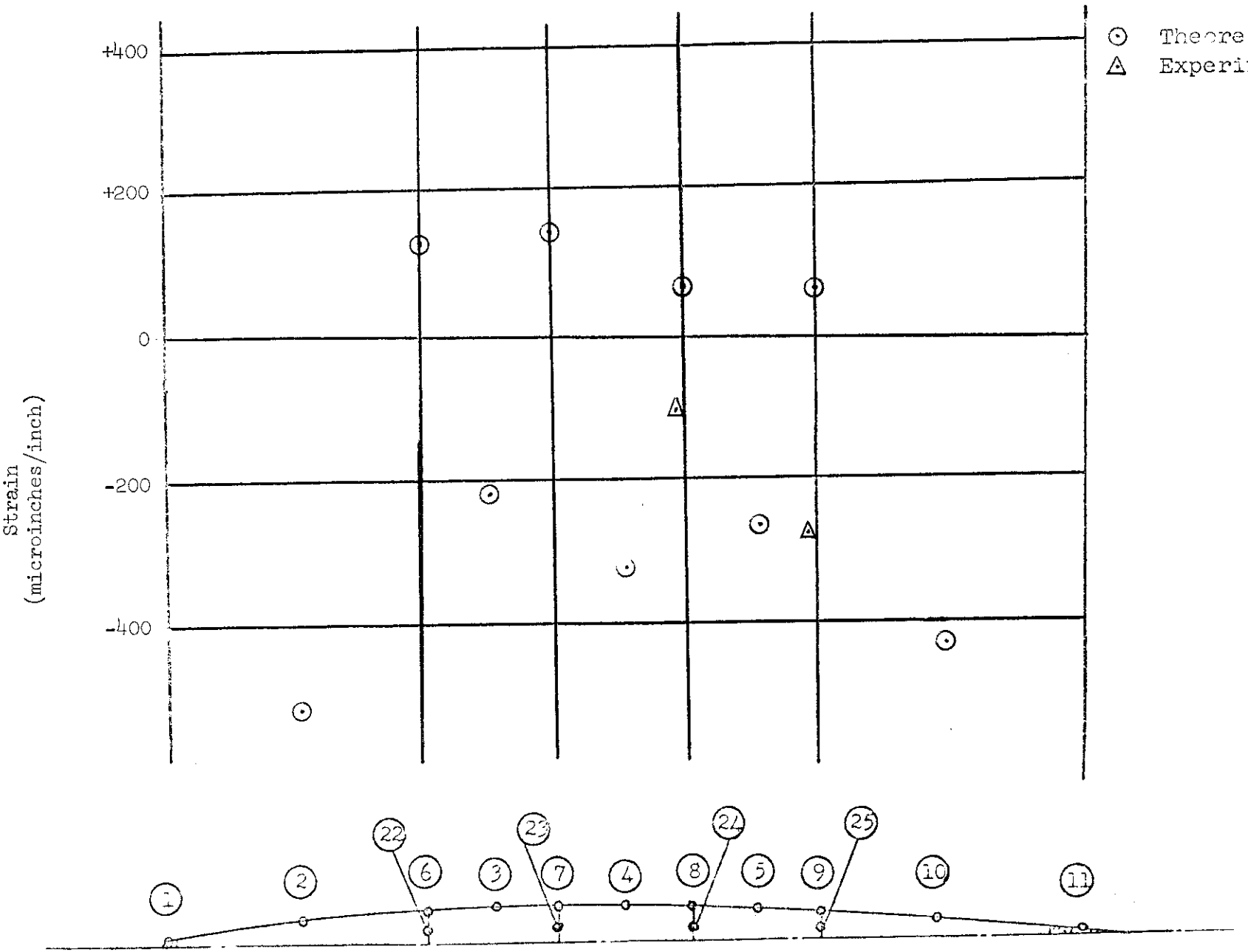

Figure B-8a. - Sta. 102 - 250° unsymmetrical - upper skin

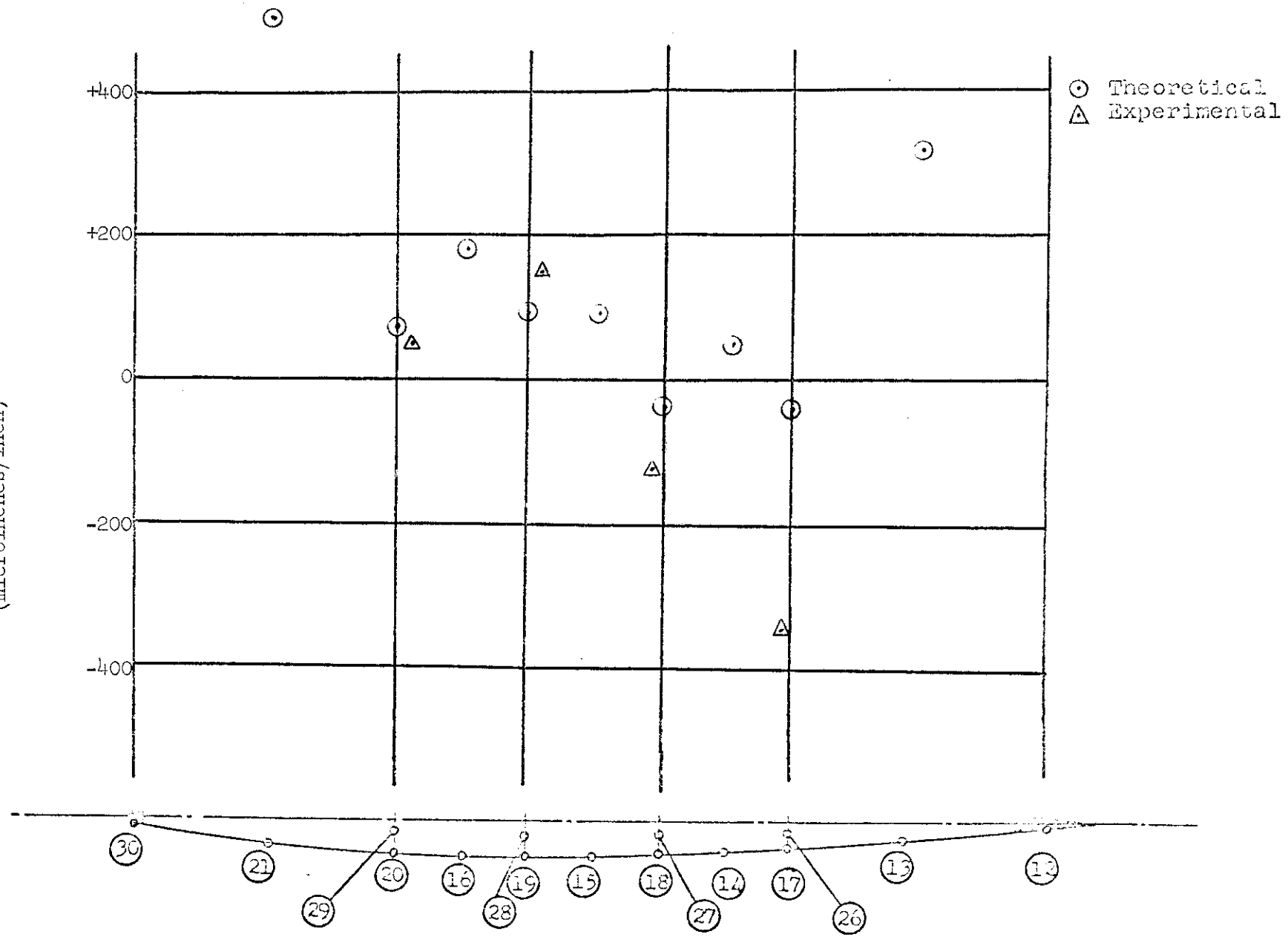

Figure B-8b. - Sta. 102 - 250° unsymmetrical - lower skin

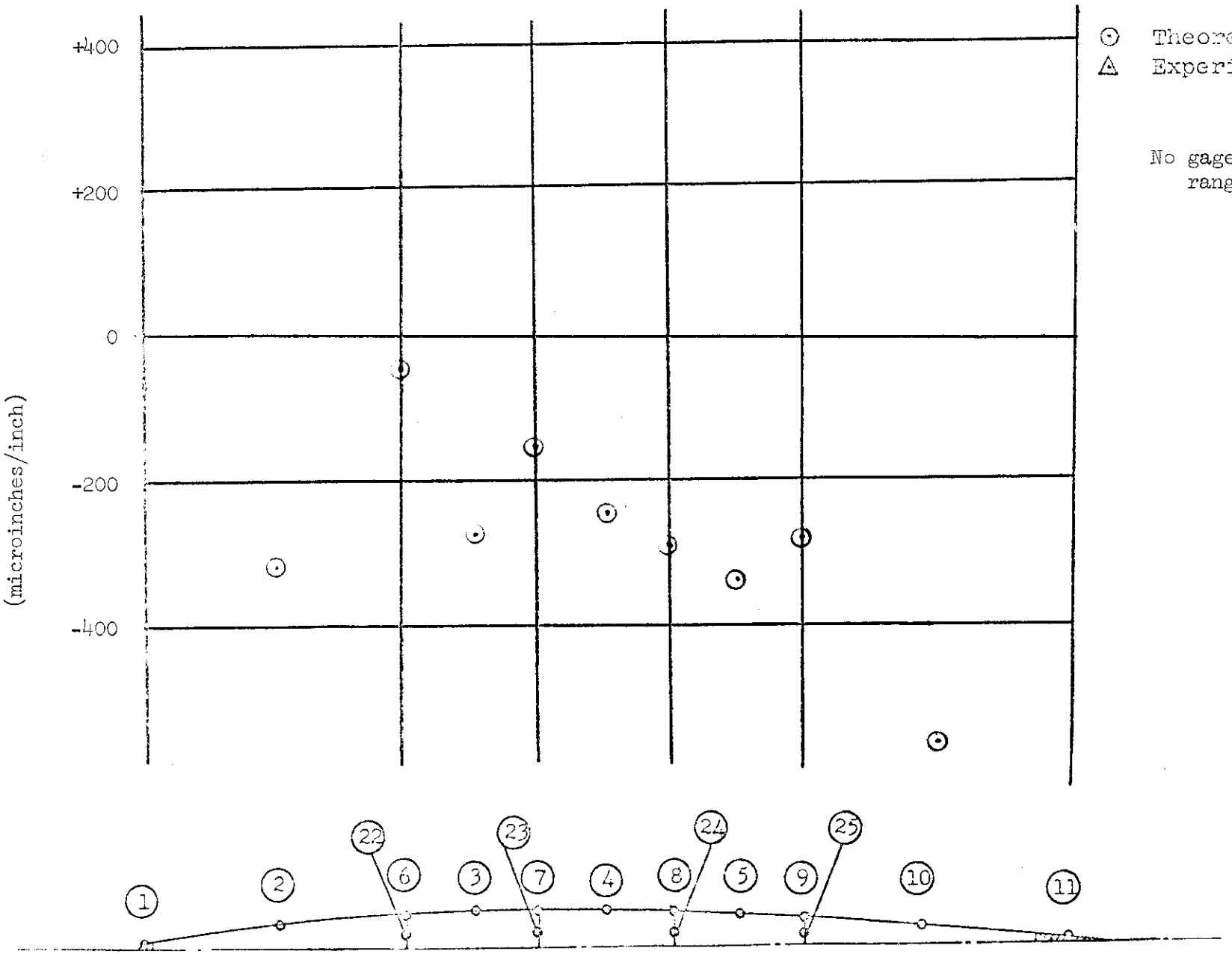

Figure B-9a. - Sta. 102 - 425° symmetrical - upper skin

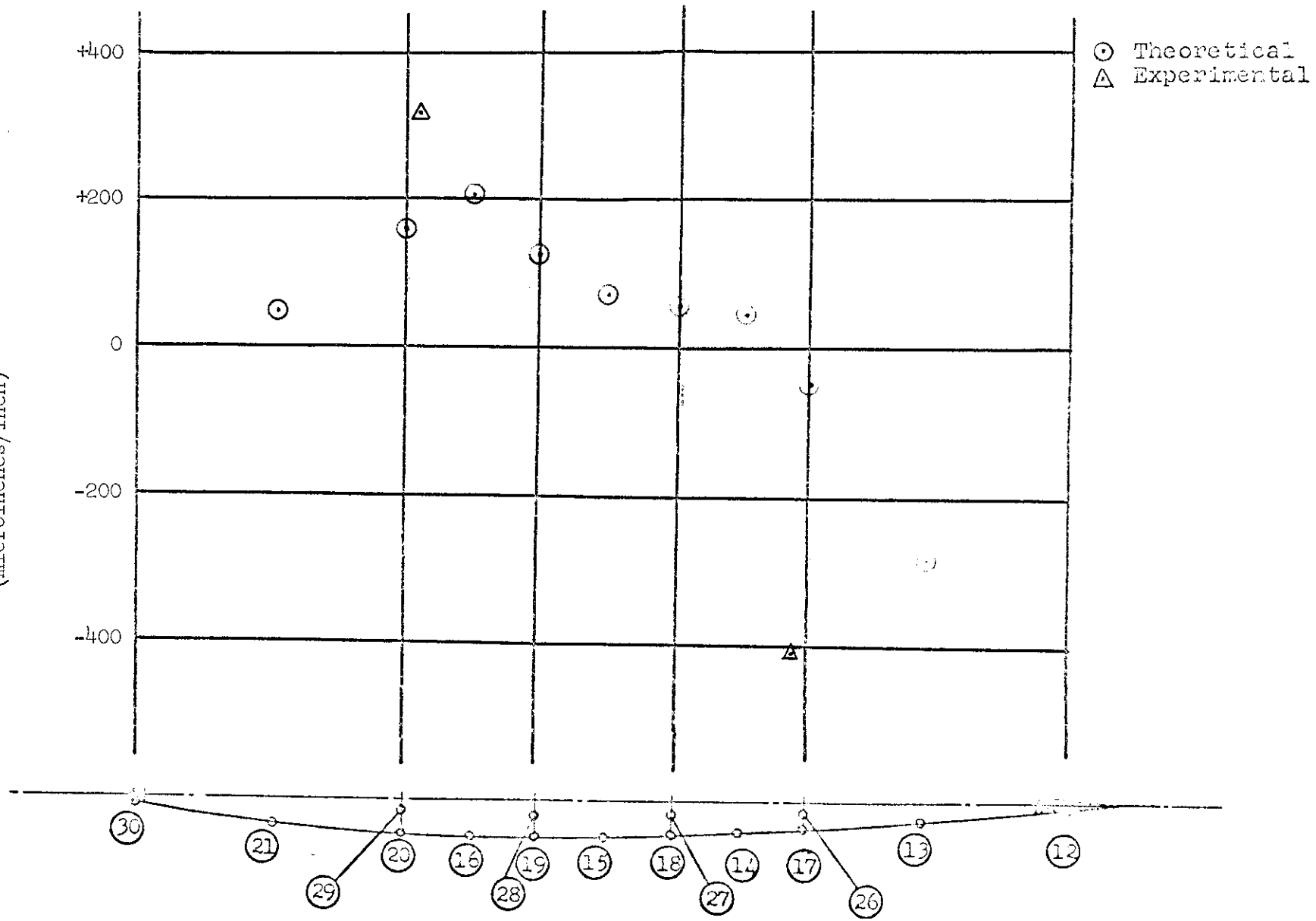

Figure B-9b. - Sta. 102 - 425° symmetrical - lower skin

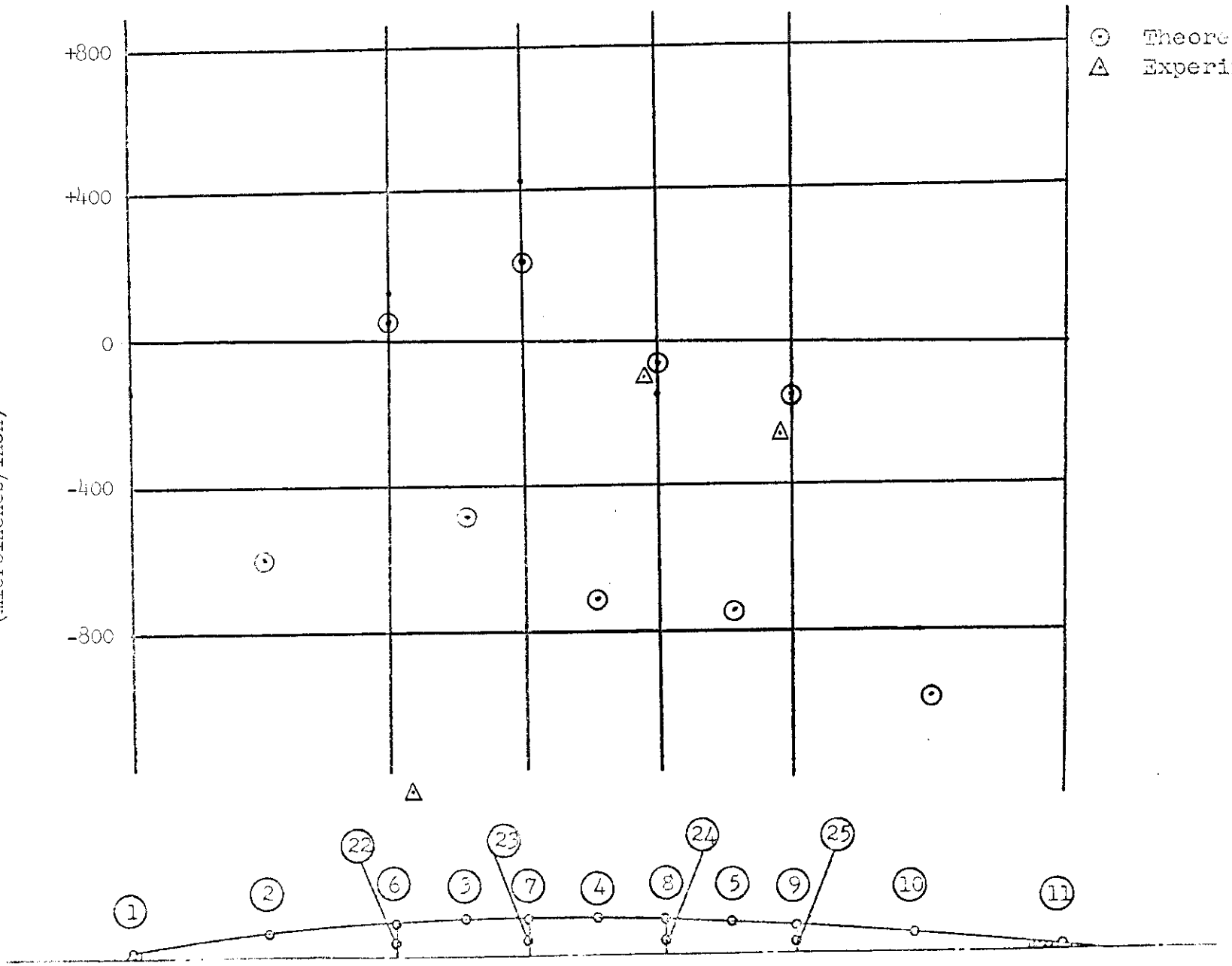

Figure B-10a. - Sta. 102 - 425° unsymmetrical - upper skin

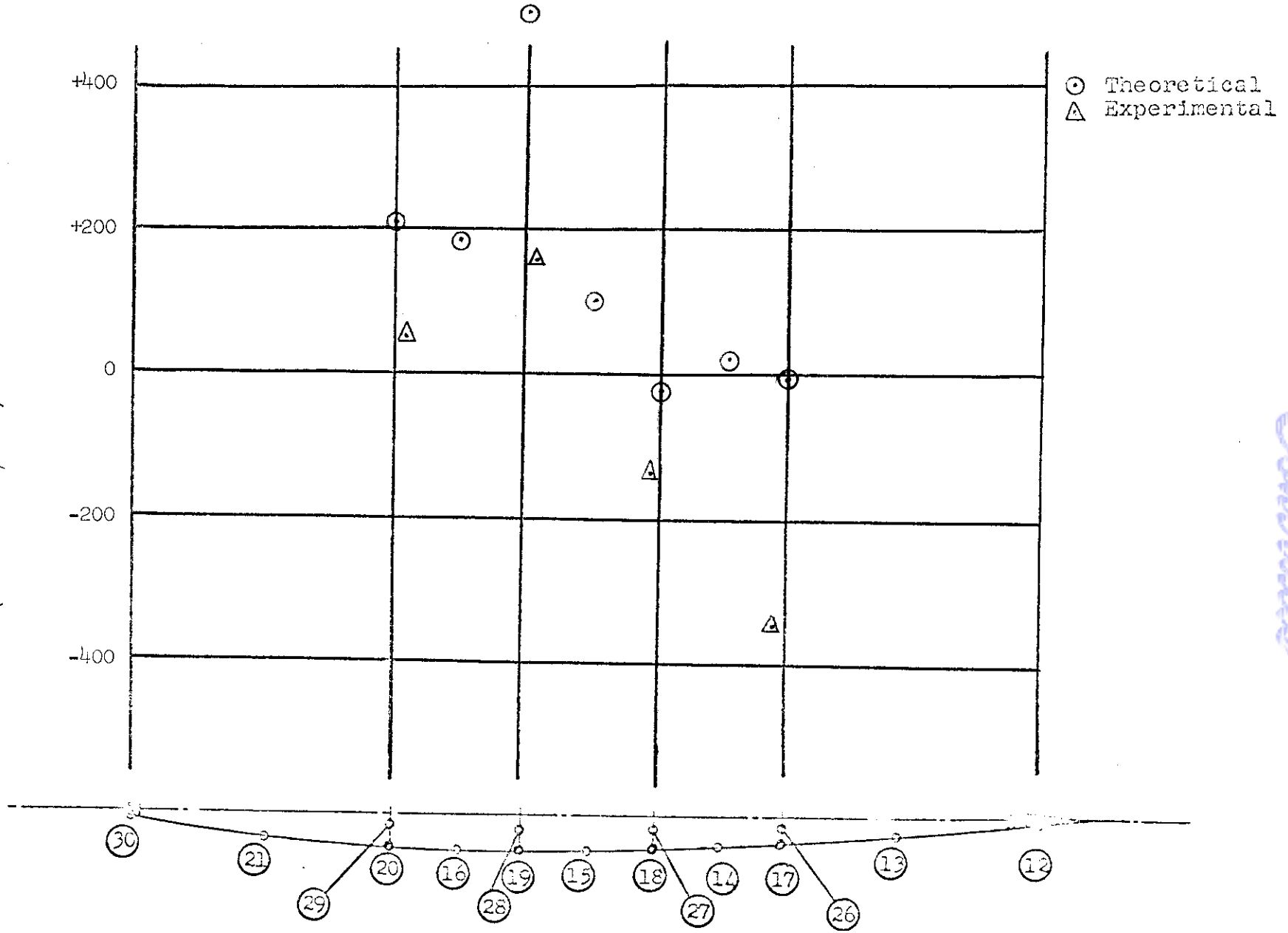

Figure B-10b. - Sta. 102 - 425° unsymmetrical - lower skin

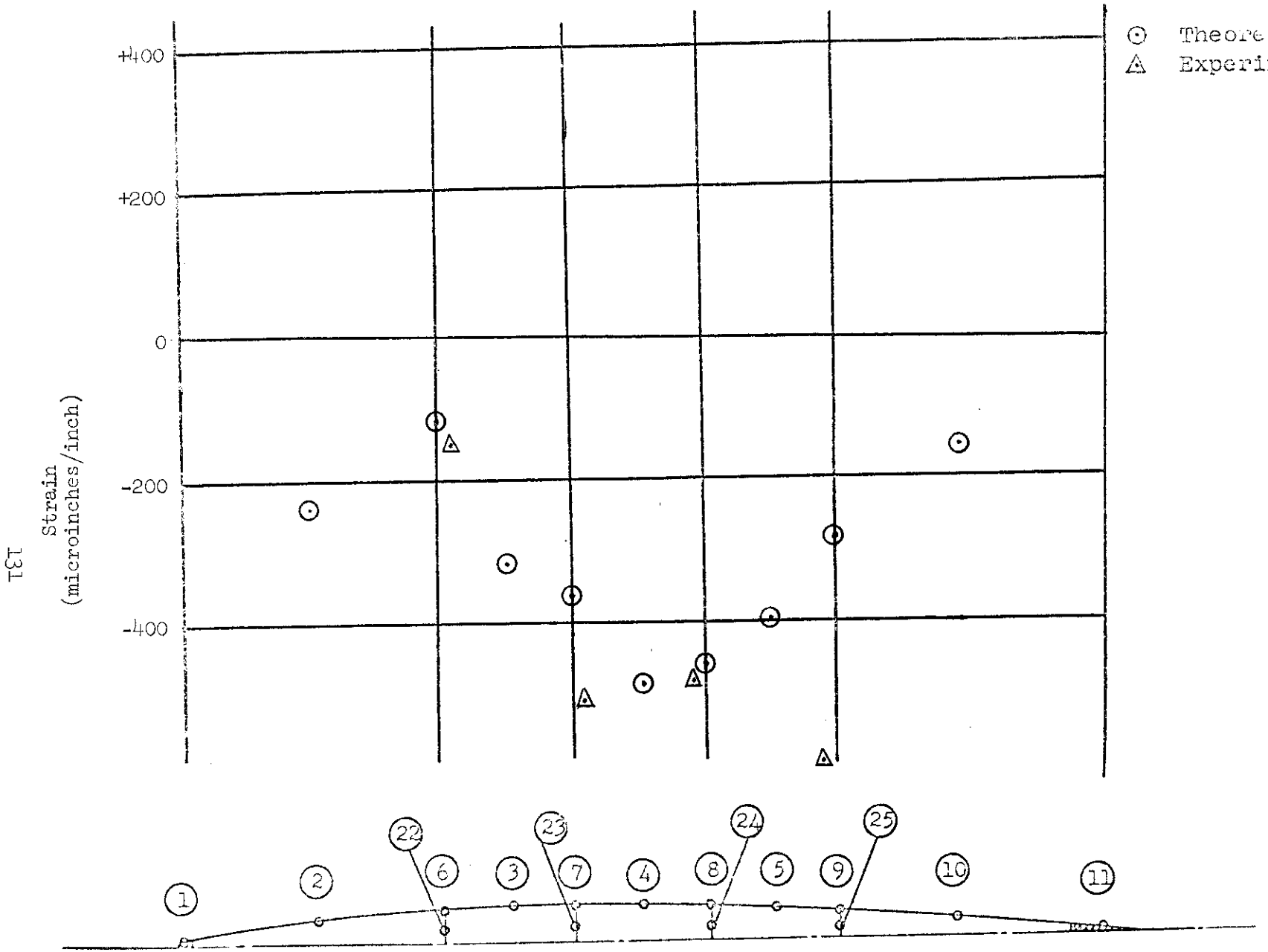

Figure B-11a. - Sta. 113 - 250° symmetrical - upper skin

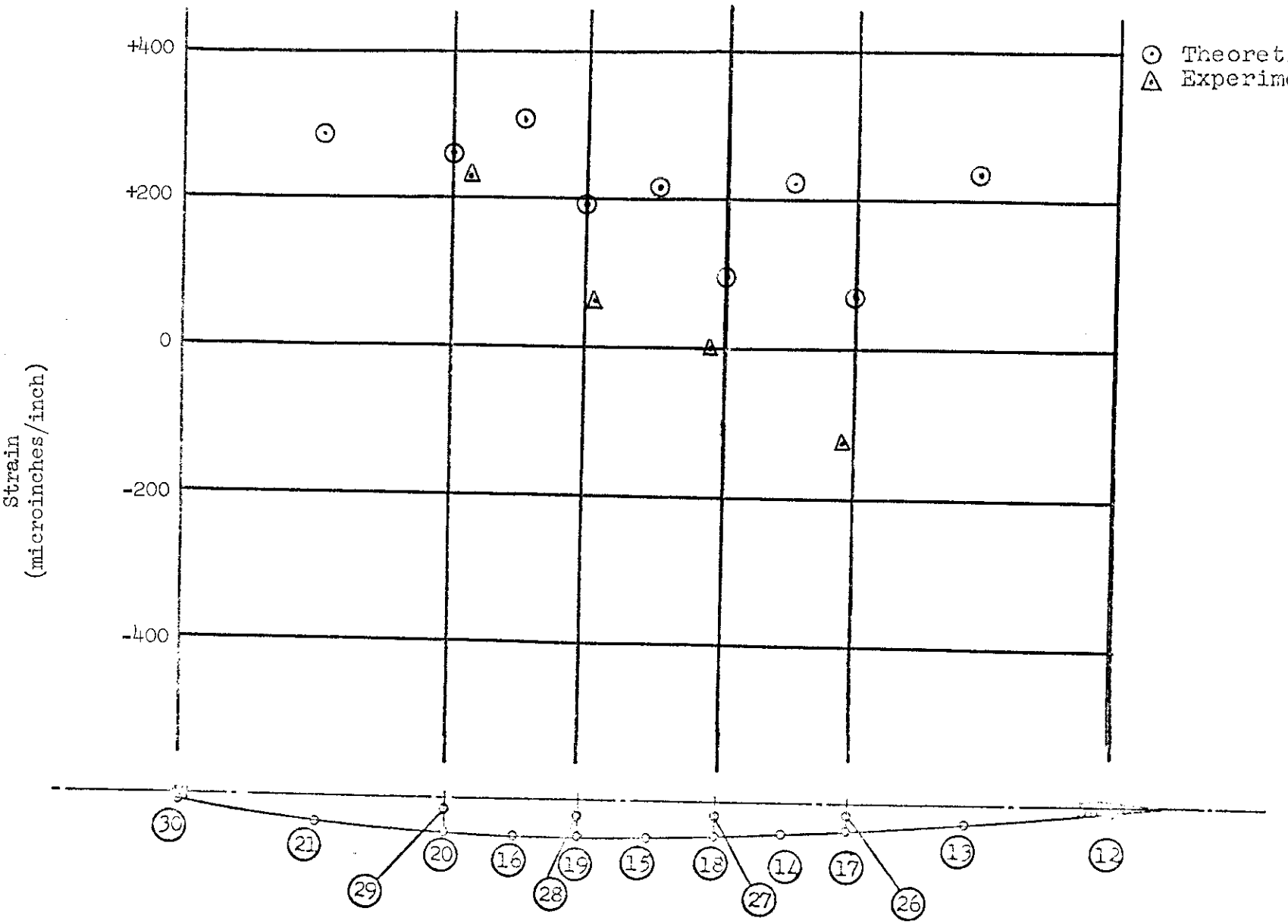

Figure B-11b. - Sta. 113 - 250° symmetrical - lower skin

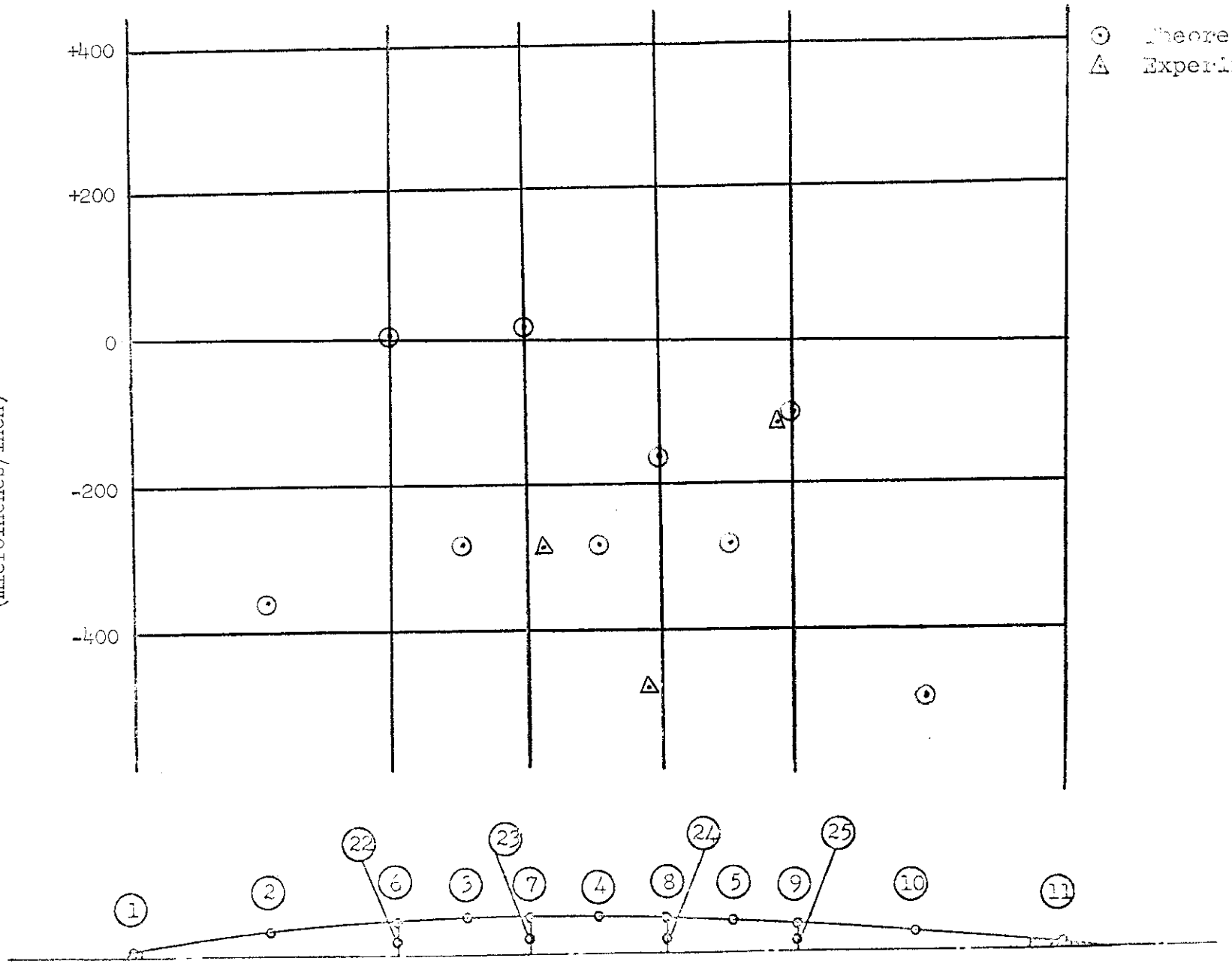

Figure B-12a. - Sta. 113 - 250° unsymmetrical - upper skin

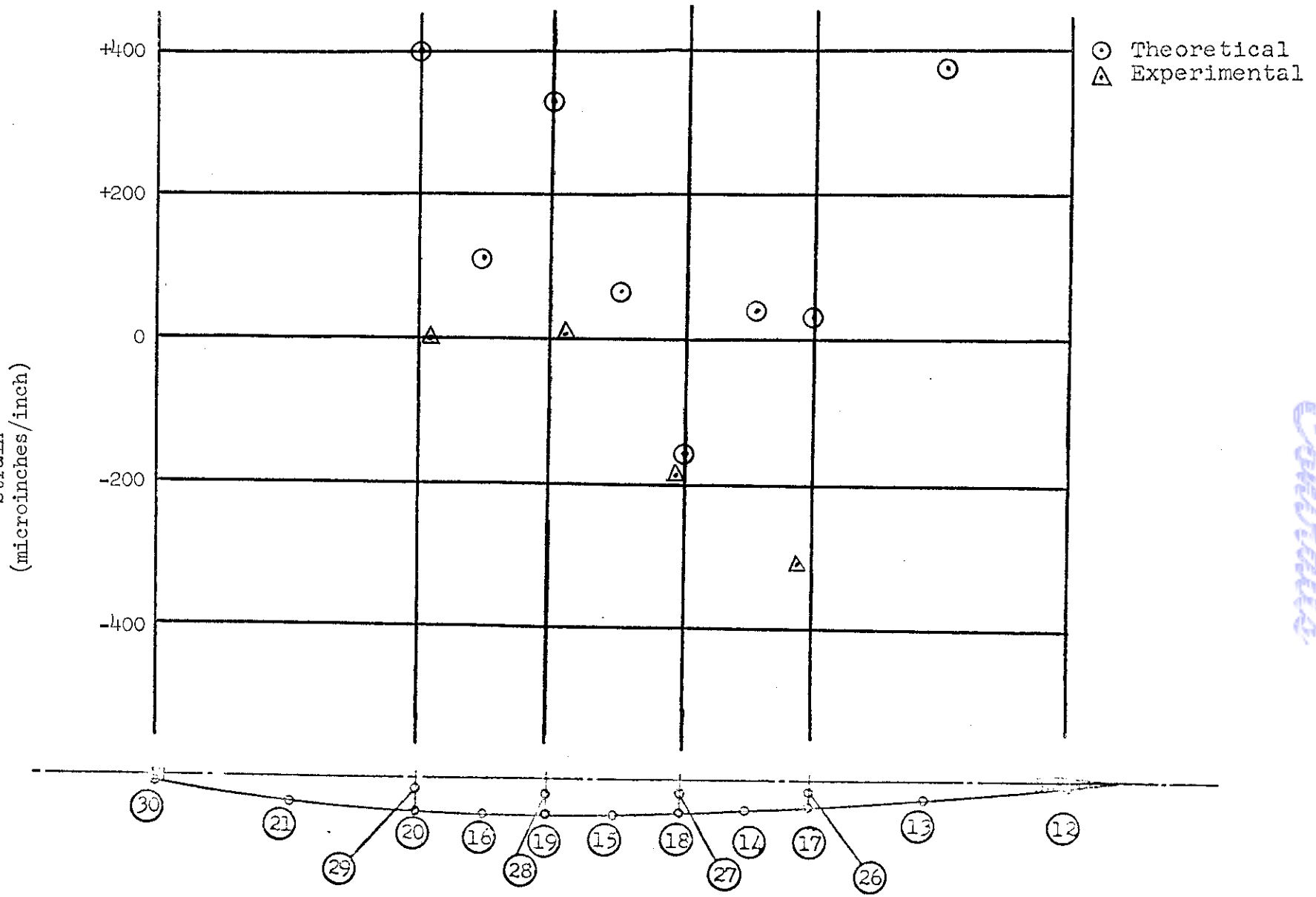

Figure B-12b. - Sta. 113 - 250° unsymmetrical - lower skin

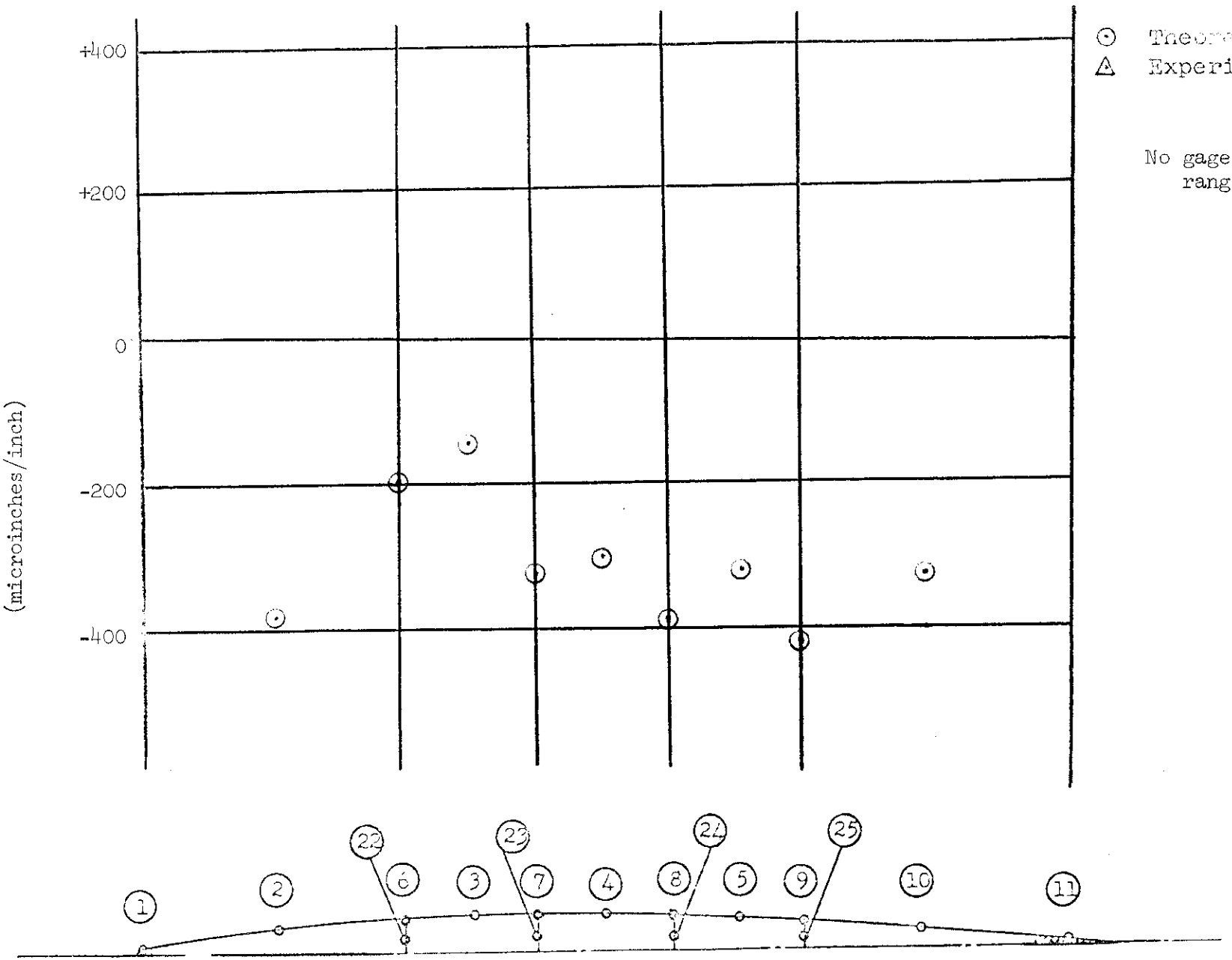

Figure B-13a. - Sta. 113 - 425° symmetrical - upper skin

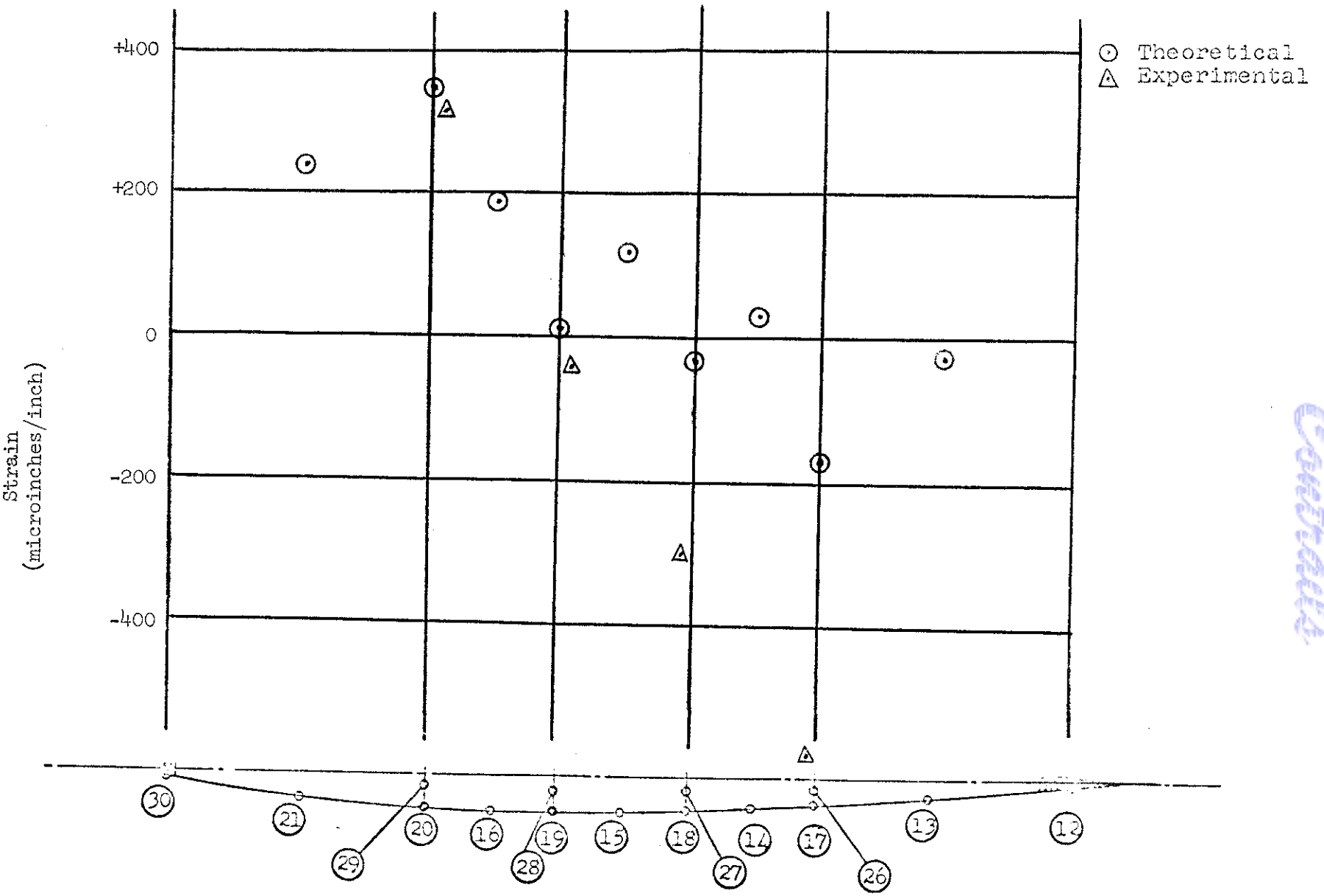

Figure B-13b. - Sta. 113 - 425° symmetrical - lower skin

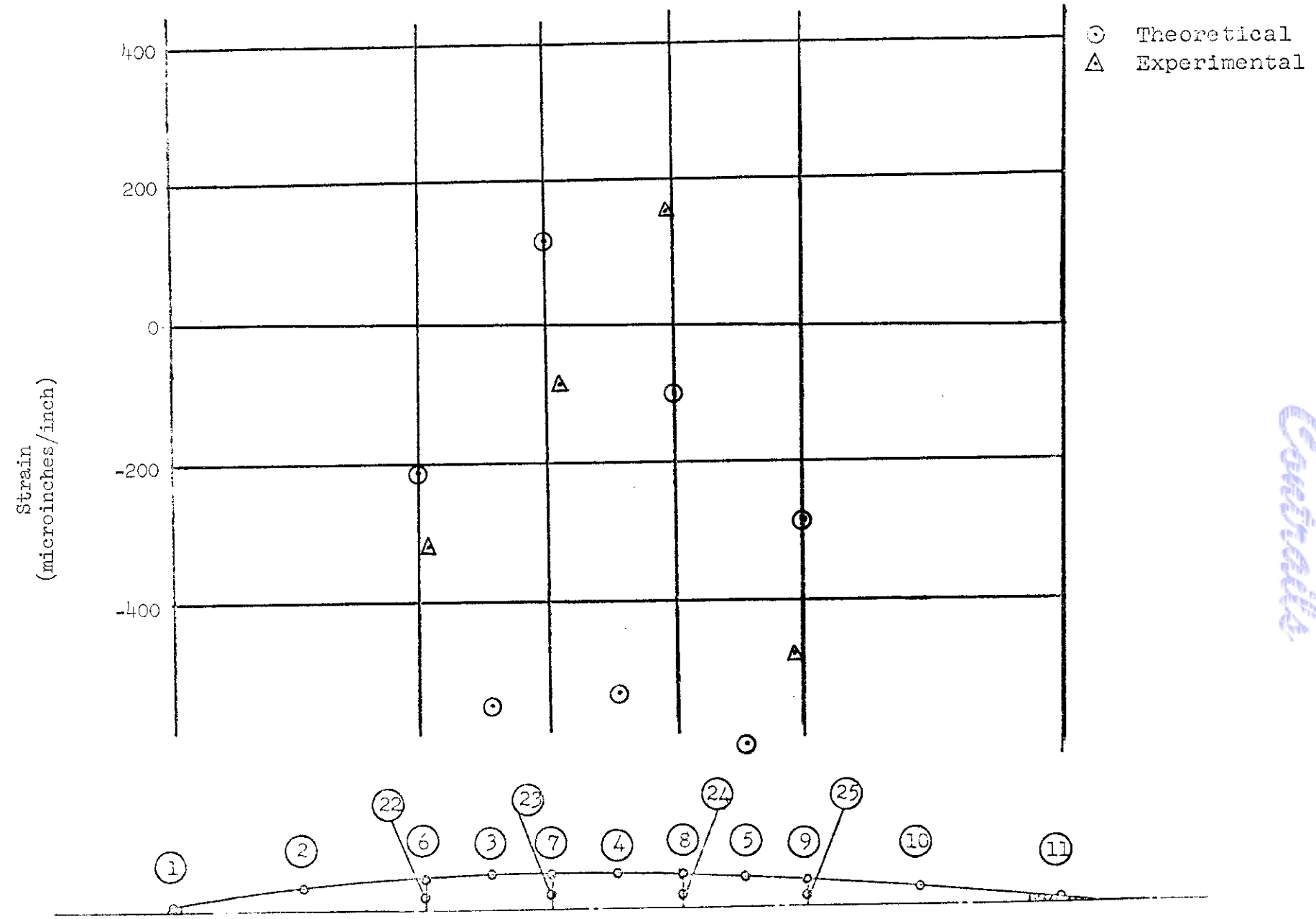

Figure B-14a. - Sta. 113 - 425° unsymmetrical - upper skin

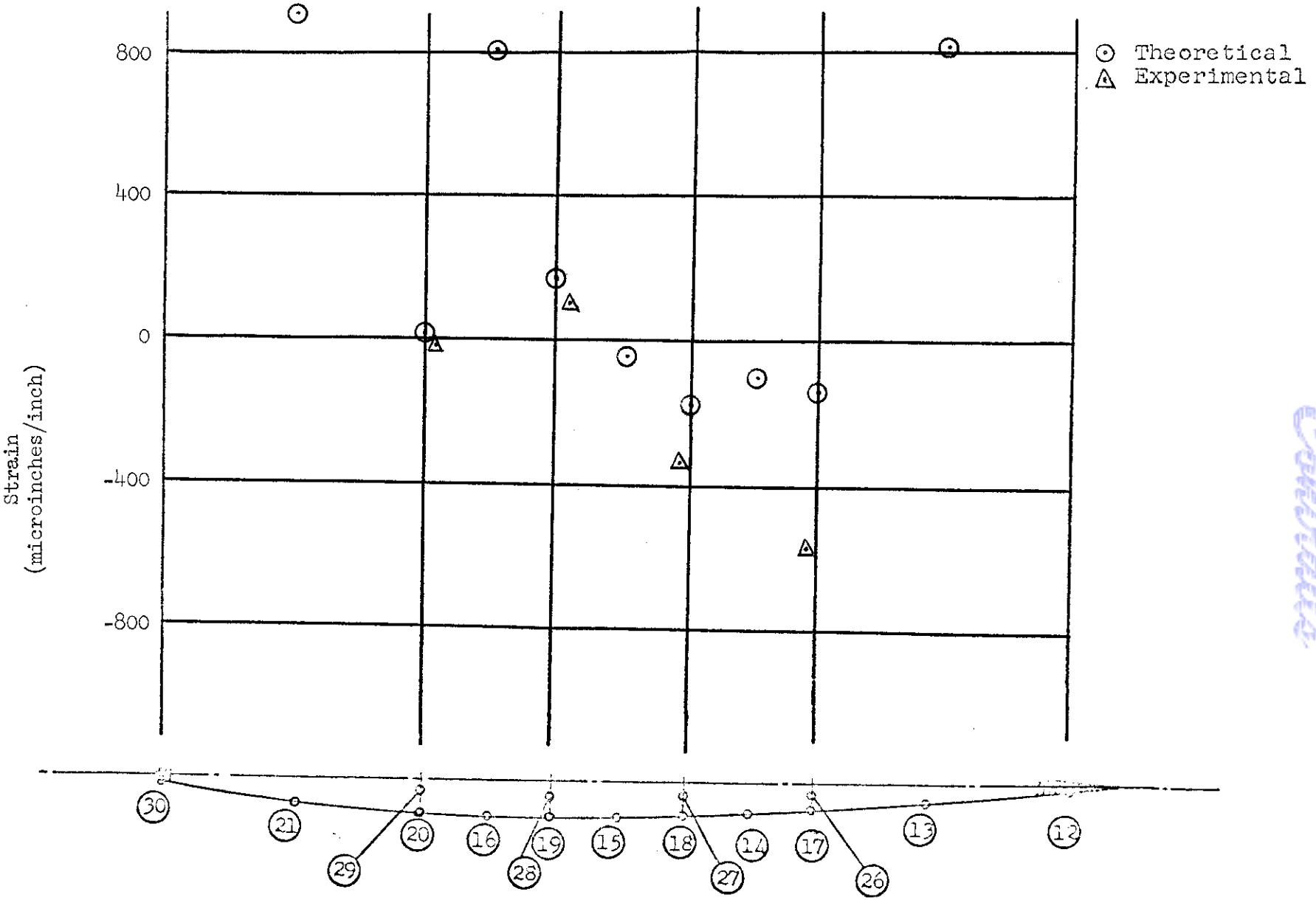

Figure B-14b. - Sta. 113 - 425° unsymmetrical - lower skin

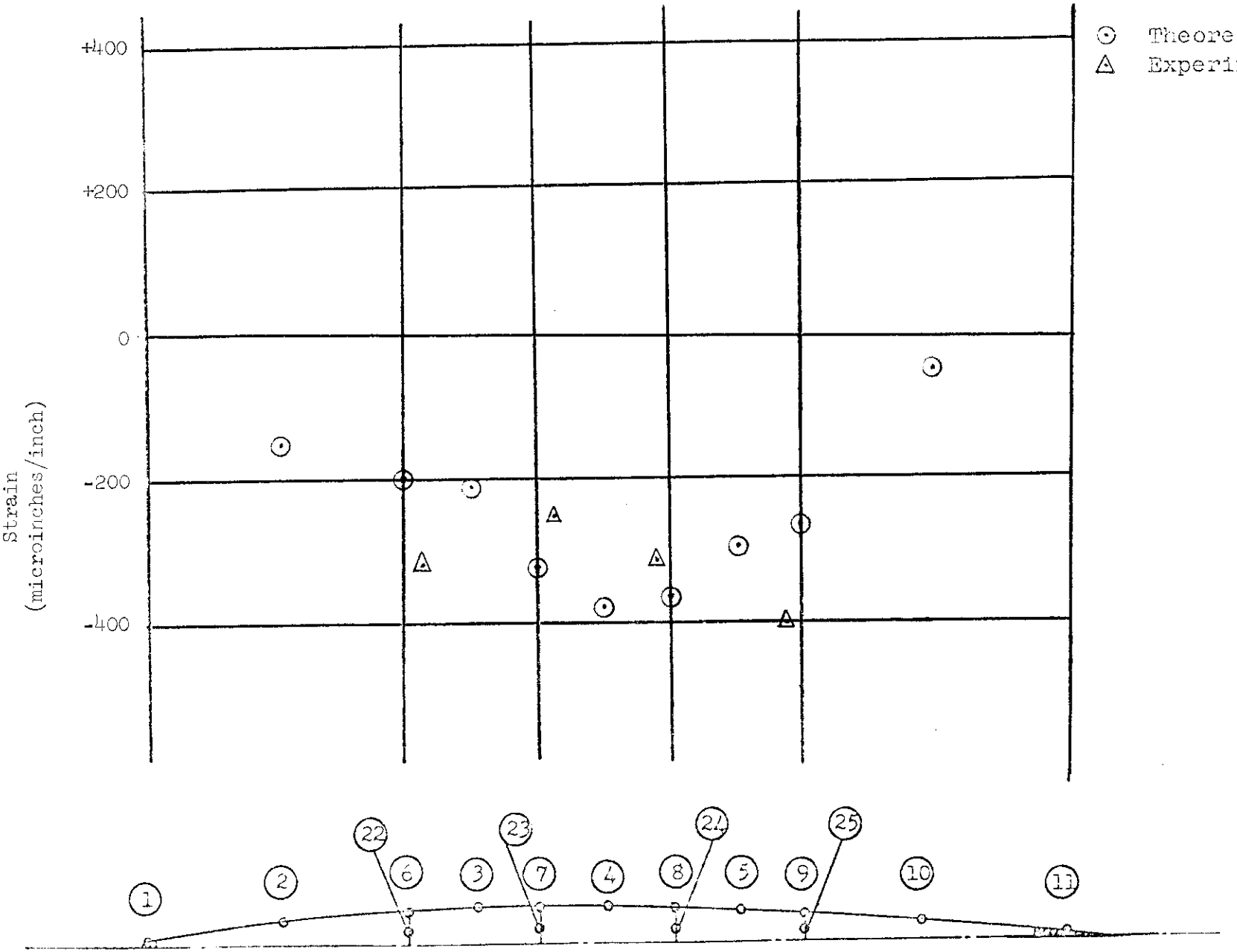

Figure B-15a. - Sta. 124 - 250° symmetrical - upper skin

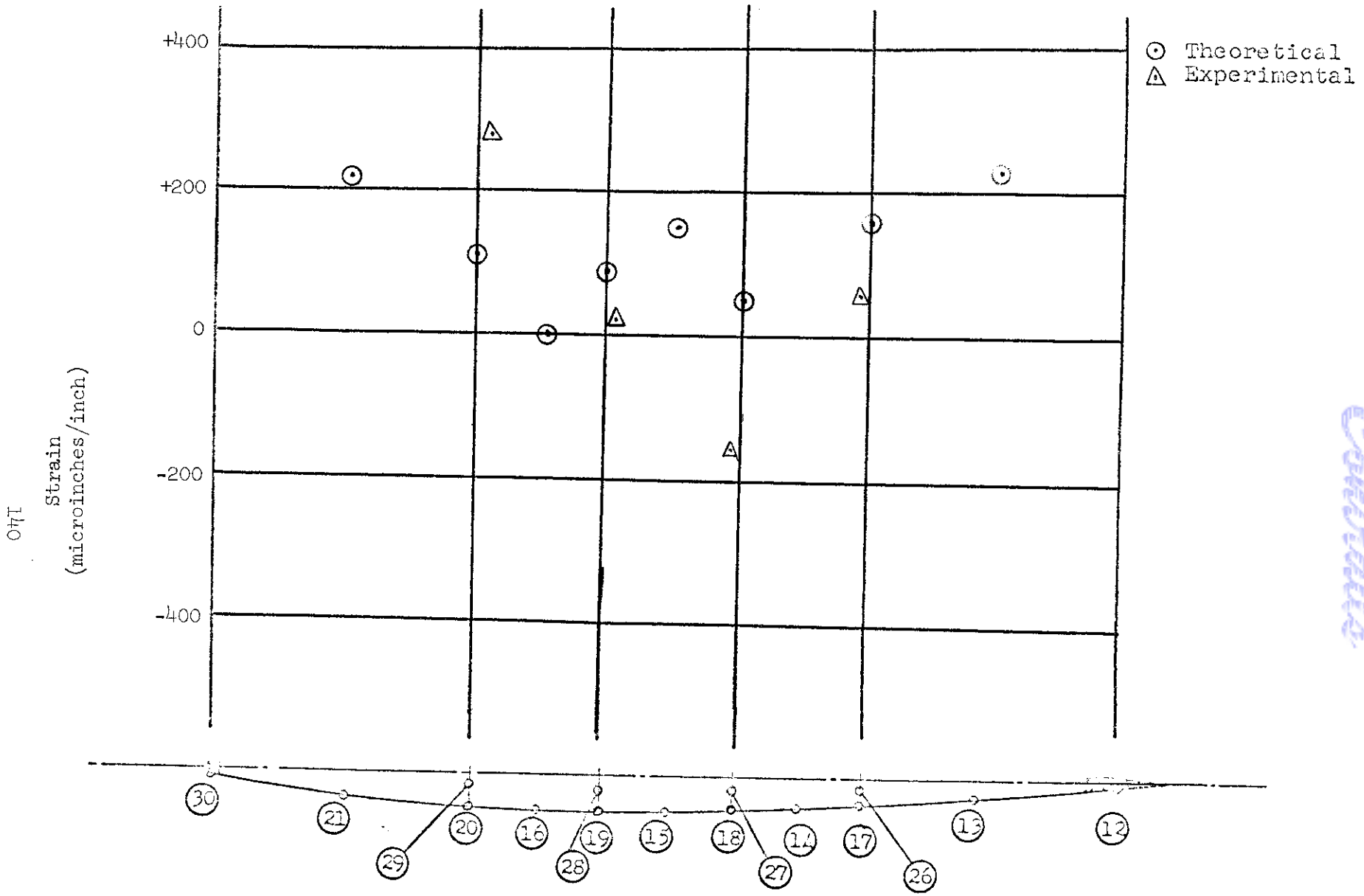

Figure B-15b. - Sta. 124 - 250° symmetrical - lower skin

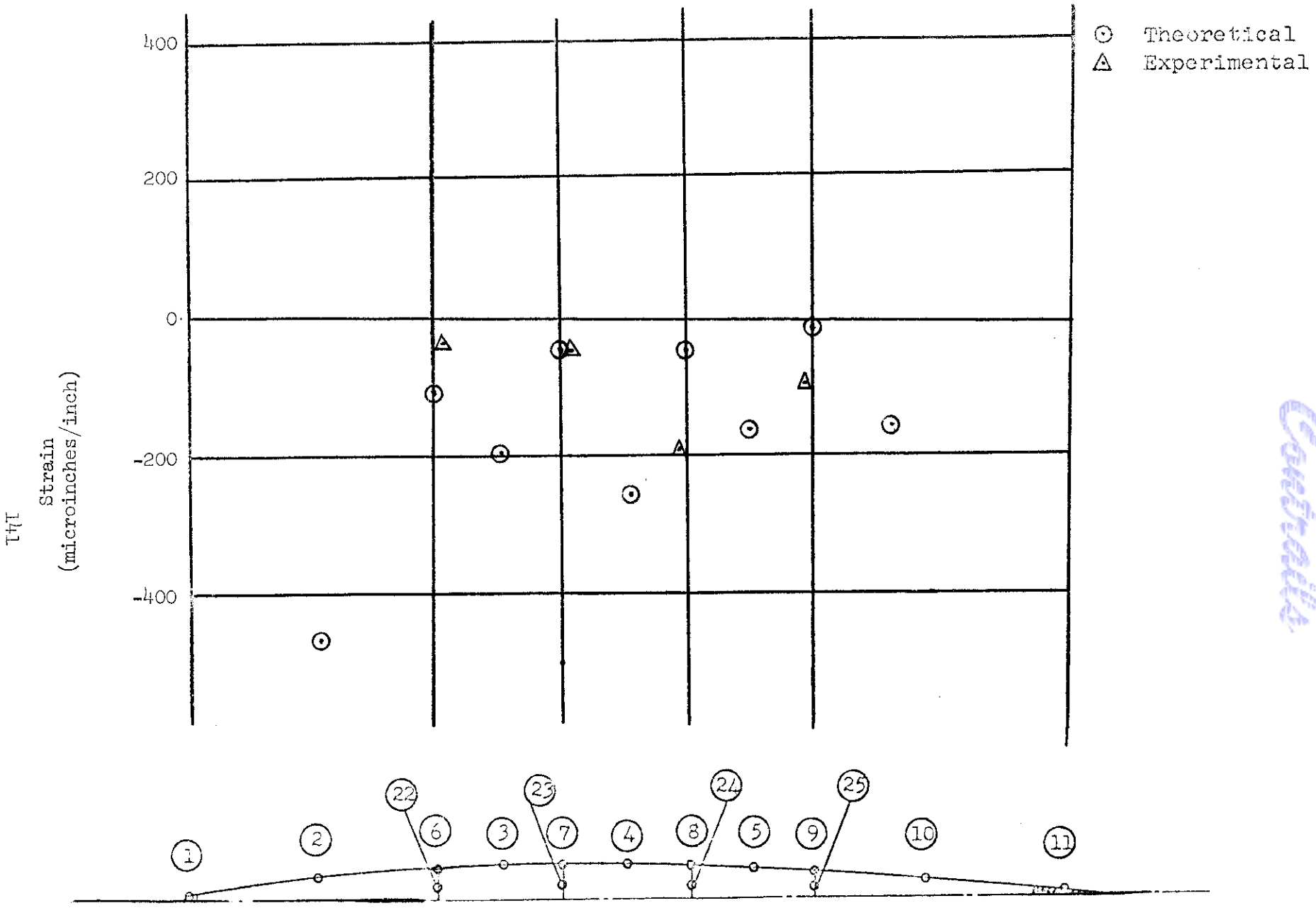

Figure B-16a. - Sta. 124 - 250° unsymmetrical - upper skin

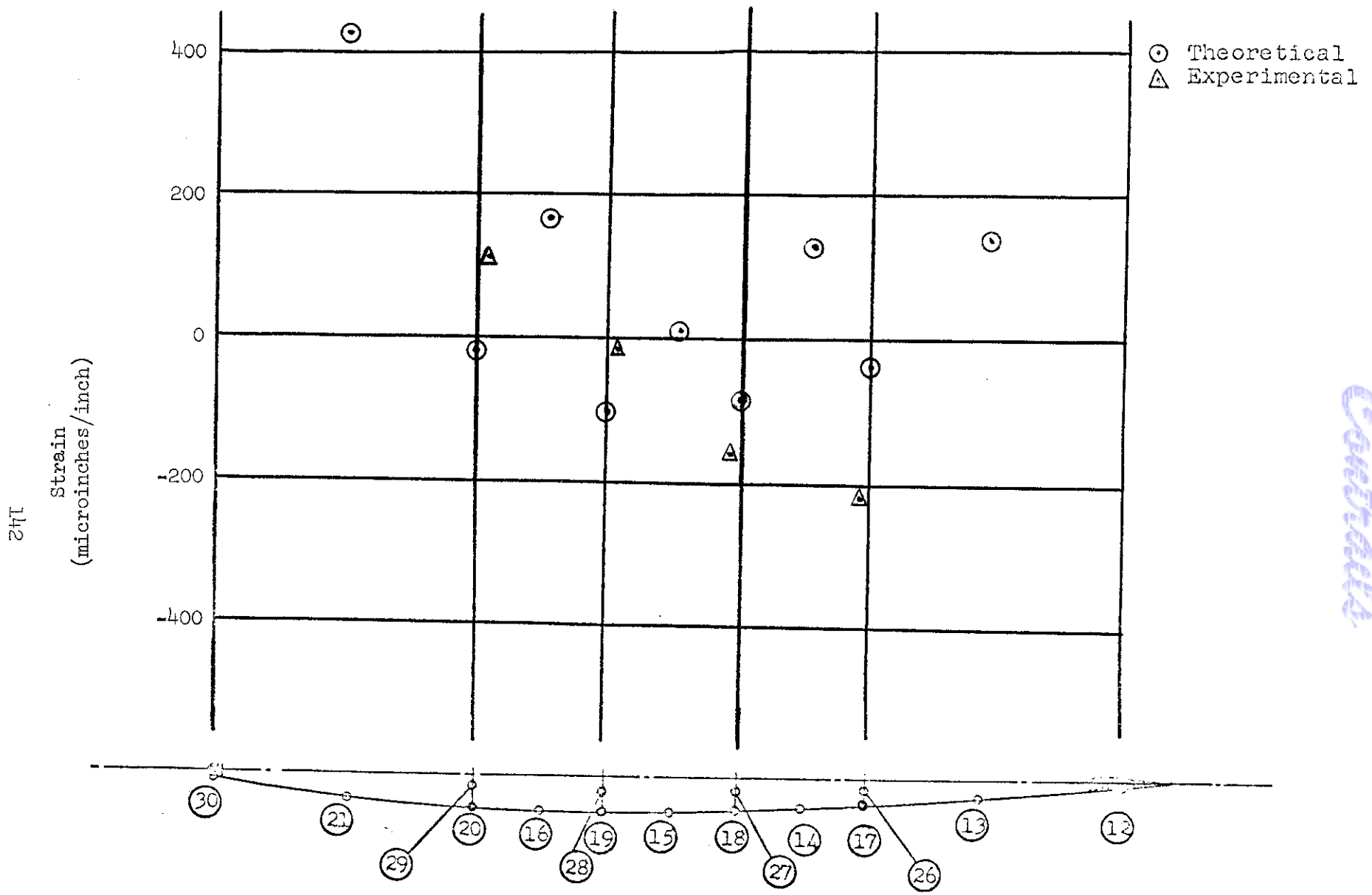

Figure B-16b. - Sta. 124 - 250° unsymmetrical - lower skin

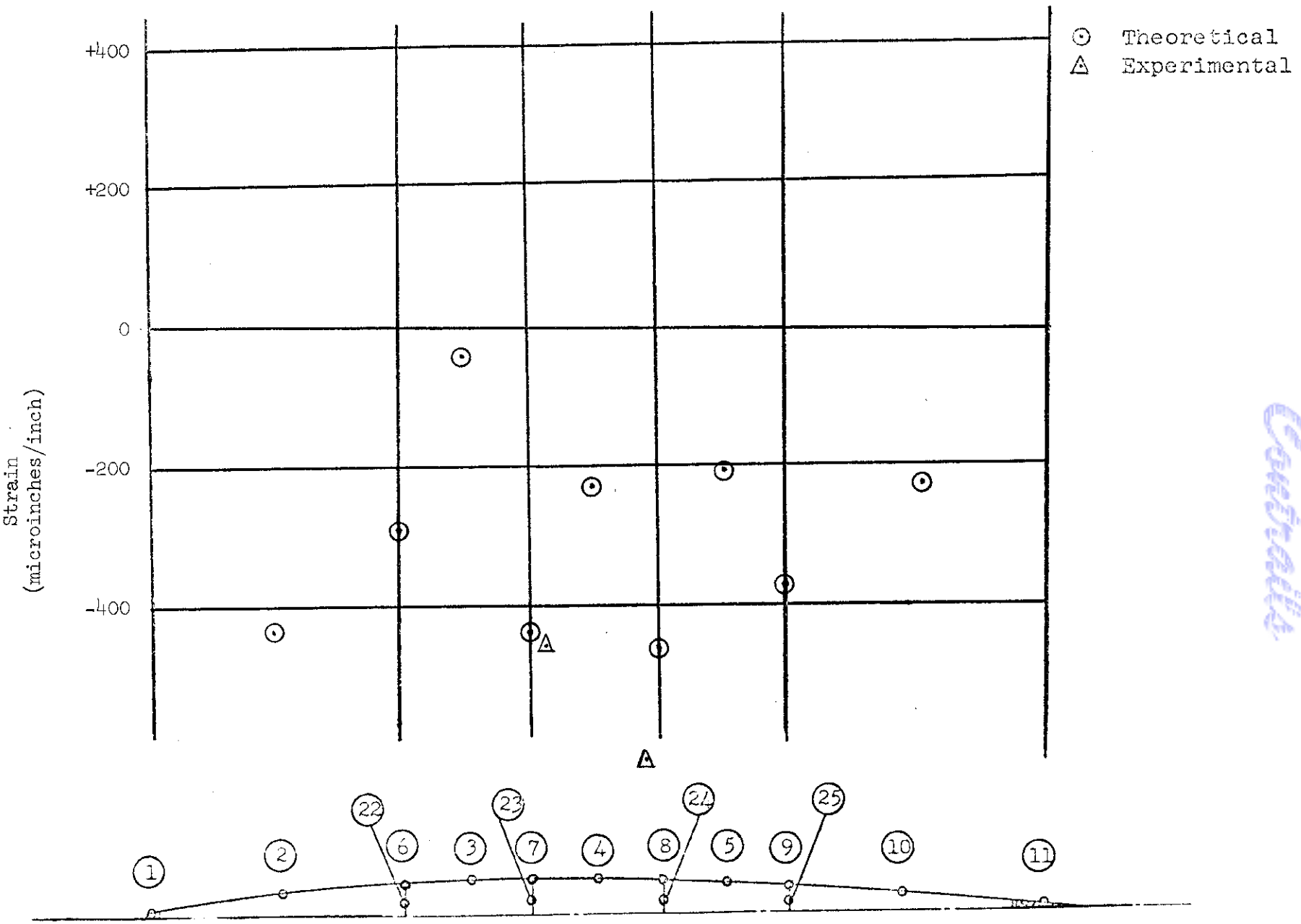

Figure B-17a. - Sta. 124 - 425° symmetrical - upper skin

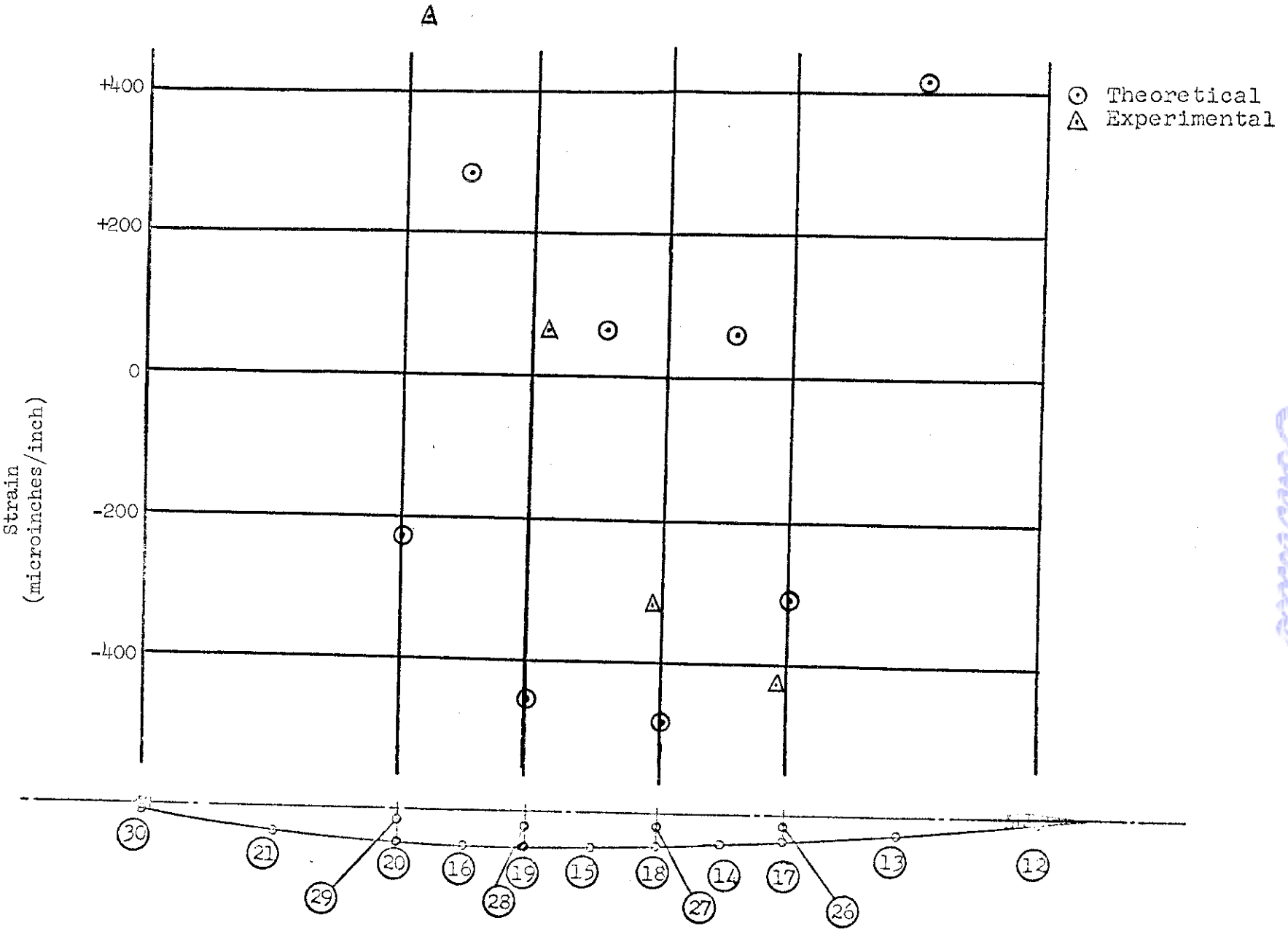

Figure B-17b. - Sta. 124 - 425° Symmetrical - lower skin

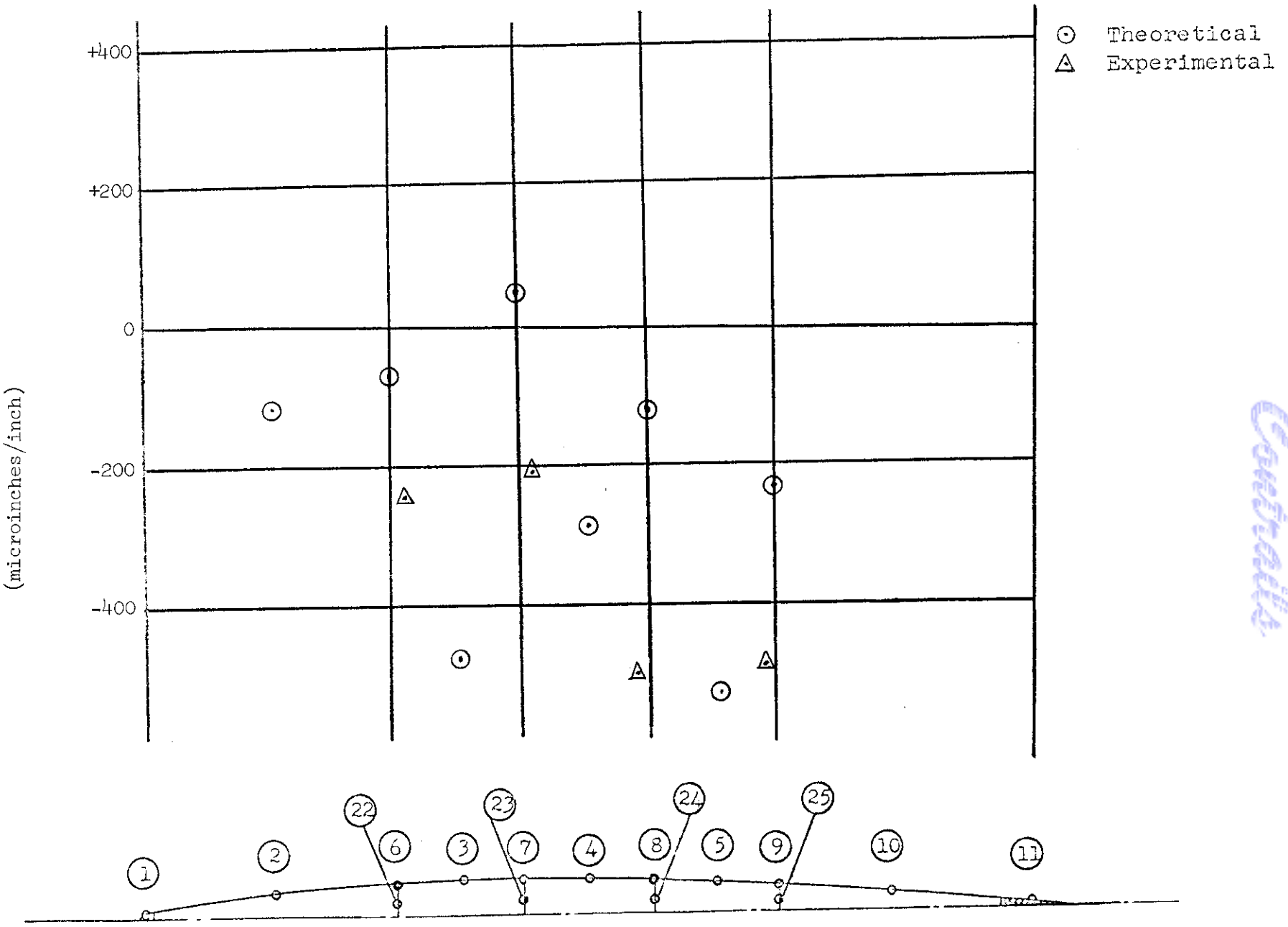

Figure B-18a. - Sta. 124 - 425° unsymmetrical - upper skin

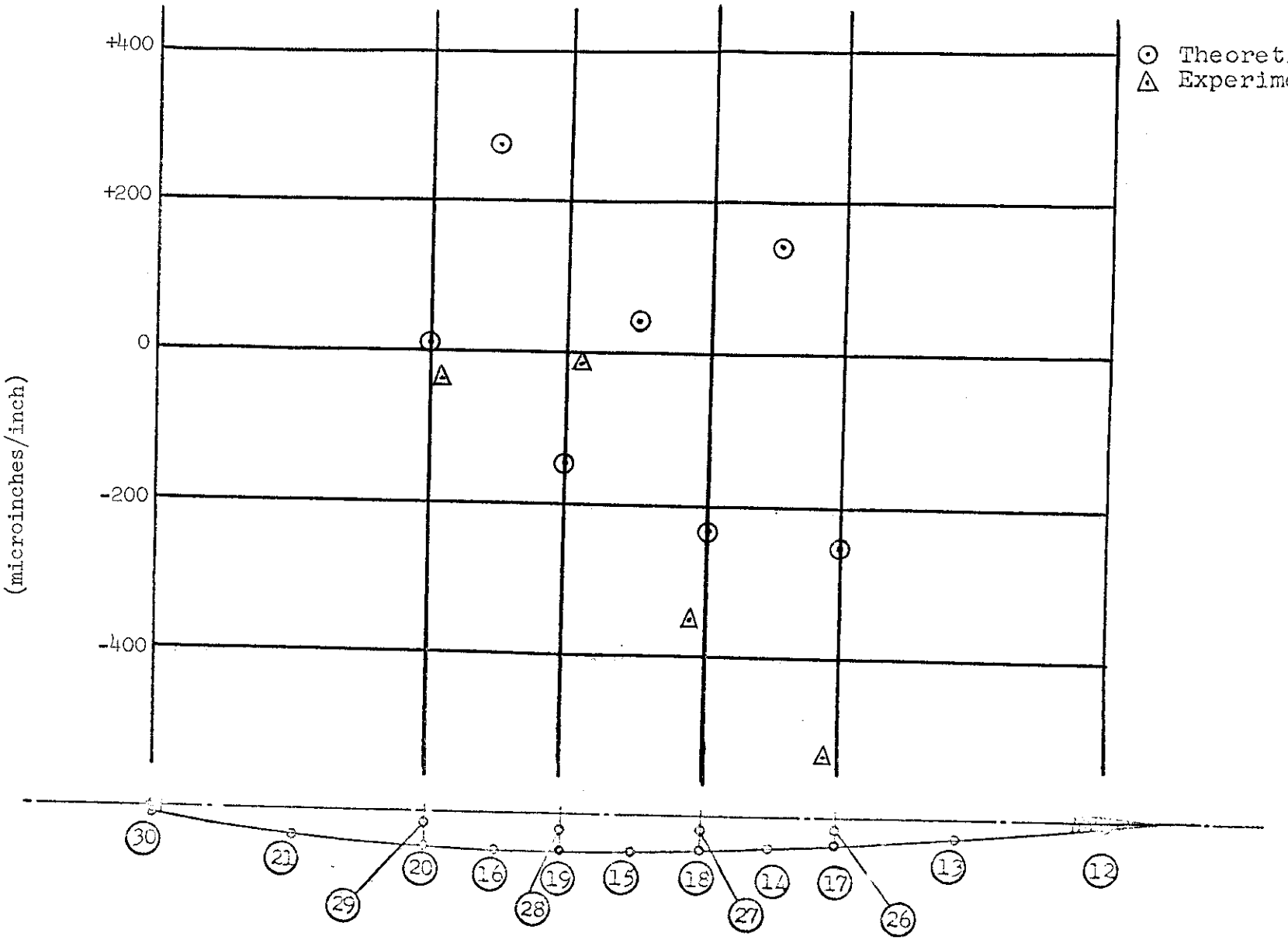

Figure B-18b. - Sta. 124 - 425° unsymmetrical - lower skin

UNCLASSIFIED
Security Classification

DOCUMENT CONTROL DATA - R&D

(Security classification of title, body of abstract and indexing annotation must be entered when the overall report is classified)

1. ORIGINATING ACTIVITY (Corporate author)
The Ohio State University Research Foundation
1314 Kinnear Rd.
Columbus, Ohio 43212

2a. REPORT SECURITY CLASSIFICATION
Unclassified

2b. GROUP
N/A

3. REPORT TITLE
IDENTIFICATION OF SELECTED EXPERIMENTAL DATA ON THERMAL STRESSES

4. DESCRIPTIVE NOTES (Type of report and inclusive dates)
Final Report - May 15, 1966 through September 14, 1967

5. AUTHOR(S) (Last name, first name, initial)
Gatewood, B. E. and O'Connor, James S.

6. REPORT DATE	7a. TOTAL NO. OF PAGES	7b. NO. OF REFS
September 1967	155	

8a. CONTRACT OR GRANT NO.	9a. ORIGINATOR'S REPORT NUMBER(S)
AF33(615)-5074 b. PROJECT NO. 1467 c. Task No. 146702 d.	Final Report 9b. OTHER REPORT NO(S) (Any other numbers that may be assigned this report) AFFDL-TR-67-100

10. AVAILABILITY/LIMITATION NOTICES This document is subject to special export controls and each transmittal to foreign governments or foreign nationals may be made only with prior approval of the Theoretical Mechanics Branch, Structures Division, Air Force Flight Dynamics Laboratory, Wright-Patterson AFB, Ohio 45433

11. SUPPLEMENTARY NOTES	12. SPONSORING MILITARY ACTIVITY
	Air Force Flight Dynamics Laboratory (FDTR) Research and Technology Division Wright-Patterson Air Force Base, Ohio 45433

13. ABSTRACT

This report identifies experimental data on thermal stresses contained in selected reports in the literature. For each selected report, a summary of selected tests, geometry of test specimens, restraints, material properties, temperature distributions, experimented strain and deflection data, and comparisons to theory are given or are identified as to location by figure number or table number in the original published report. Also, the bibliographical listing and evaluation of test data on thermal stress testing given in Technical Report AFFDL-TR-66-67, "Development of Experimental Testing Programs to Verify Thermal Stress Analysis," is brought up to date in an appendix to the present report.

This abstract is subject to special export controls and each transmittal to foreign governments or foreign nationals may be made only with prior approval of the Theoretical Mechanics Branch, Structures Division, Air Force Flight Dynamics Laboratory, Wright-Patterson Air Force Base, Ohio 45433.

DD FORM 1 JAN 64 1473

UNCLASSIFIED
Security Classification

14. KEY WORDS	LINK A		LINK B		LINK C	
	ROLE	WT	ROLE	WT	ROLE	WT
Thermal Stress Test Data Experimental						

INSTRUCTIONS

1. ORIGINATING ACTIVITY: Enter the name and address of the contractor, subcontractor, grantee, Department of Defense activity or other organization *(corporate author)* issuing the report.

2a. REPORT SECURITY CLASSIFICATION: Enter the overall security classification of the report. Indicate whether "Restricted Data" is included. Marking is to be in accordance with appropriate security regulations.

2b. GROUP: Automatic downgrading is specified in DoD Directive 5200.10 and Armed Forces Industrial Manual. Enter the group number. Also, when applicable, show that optional markings have been used for Group 3 and Group 4 as authorized.

3. REPORT TITLE: Enter the complete report title in all capital letters. Titles in all cases should be unclassified. If a meaningful title cannot be selected without classification, show title classification in all capitals in parenthesis immediately following the title.

4. DESCRIPTIVE NOTES: If appropriate, enter the type of report, e.g., interim, progress, summary, annual, or final. Give the inclusive dates when a specific reporting period is covered.

5. AUTHOR(S): Enter the name(s) of author(s) as shown on or in the report. Enter last name, first name, middle initial. If military, show rank and branch of service. The name of the principal author is an absolute minimum requirement.

6. REPORT DATE: Enter the date of the report as day, month, year; or month, year. If more than one date appears on the report, use date of publication.

7a. TOTAL NUMBER OF PAGES: The total page count should follow normal pagination procedures, i.e., enter the number of pages containing information.

7b. NUMBER OF REFERENCES: Enter the total number of references cited in the report.

8a. CONTRACT OR GRANT NUMBER: If appropriate, enter the applicable number of the contract or grant under which the report was written.

8b, 8c, & 8d. PROJECT NUMBER: Enter the appropriate military department identification, such as project number, subproject number, system numbers, task number, etc.

9a. ORIGINATOR'S REPORT NUMBER(S): Enter the official report number by which the document will be identified and controlled by the originating activity. This number must be unique to this report.

9b. OTHER REPORT NUMBER(S): If the report has been assigned any other report numbers *(either by the originator or by the sponsor)*, also enter this number(s).

10. AVAILABILITY/LIMITATION NOTICES: Enter any limitations on further dissemination of the report, other than those imposed by security classification, using standard statements such as:

(1) "Qualified requesters may obtain copies of this report from DDC."

(2) "Foreign announcement and dissemination of this report by DDC is not authorized."

(3) "U. S. Government agencies may obtain copies of this report directly from DDC. Other qualified DDC users shall request through

_____."

(4) "U. S. military agencies may obtain copies of this report directly from DDC. Other qualified users shall request through

_____."

(5) "All distribution of this report is controlled. Qualified DDC users shall request through

_____."

If the report has been furnished to the Office of Technical Services, Department of Commerce, for sale to the public, indicate this fact and enter the price, if known.

11. SUPPLEMENTARY NOTES: Use for additional explanatory notes.

12. SPONSORING MILITARY ACTIVITY: Enter the name of the departmental project office or laboratory sponsoring *(paying for)* the research and development. Include address.

13. ABSTRACT: Enter an abstract giving a brief and factual summary of the document indicative of the report, even though it may also appear elsewhere in the body of the technical report. If additional space is required, a continuation sheet shall be attached.

It is highly desirable that the abstract of classified reports be unclassified. Each paragraph of the abstract shall end with an indication of the military security classification of the information in the paragraph, represented as *(TS), (S), (C), or (U)*.

There is no limitation on the length of the abstract. However, the suggested length is from 150 to 225 words.

14. KEY WORDS: Key words are technically meaningful terms or short phrases that characterize a report and may be used as index entries for cataloging the report. Key words must be selected so that no security classification is required. Identifiers, such as equipment model designation, trade name, military project code name, geographic location, may be used as key words but will be followed by an indication of technical context. The assignment of links, rules, and weights is optional.